Hearing Research 279 (2011) 51–59

Contents lists available at ScienceDirect

Hearing Research

journal homepage: www.elsevier.com/locate/heares

Short-term synaptic plasticity in the auditory brain stem by using in-vivo-like stimulation parameters

Achim Klug*

Department of Physiology and Biophysics, University of Colorado Denver, PO Box 6511, MS 8307, Aurora, CO 80045, USA

ARTICLE INFO

Article history:
Received 20 December 2010
Received in revised form
29 April 2011
Accepted 5 May 2011
Available online 26 May 2011

ABSTRACT

Reduced systems such as brain slices offer a powerful approach to study the physiology of auditory neurons in great detail. However, when studying auditory nuclei in reduced systems such as brain slices, especially highly active auditory brain stem nuclei, one has to be aware that the unphysiological lack of activity in the reduced system compared to the in-vivo situation has a number of important effects on the neurons under investigation, and thus on the data that are measured. Most importantly, the lack of chronic activity in the slice preparation has important effects on the properties of short-term plasticity of the synapses. The main purpose of this article is to discuss how spontaneous activity in auditory neurons, or the lack thereof, can affect the data measured.

1. Chemical synaptic transmission is a slow and demanding process

Chemical synaptic transmission is a process that is inherently expensive, both in terms of energy use and the use of molecules. Synaptic vesicles are filled with transmitter molecules, which are packaged in patches of cell membrane, and into which many different and specific proteins are inserted to endow the vesicle with its particular functionality (Jahn and Scheller, 2006; Jahn et al., 1990; Lang and Jahn, 2008; Südhof et al., 1993). Similarly, after the release event the molecules have to be recycled, regenerated, and resorted, which also consumes energy and time (Dittman and Ryan, 2009; LoGiudice and Matthews, 2007; Smith et al., 2008). Because of the many biochemical and biophysical processes involved in chemical synaptic transmission, this process cannot function at an infinitely fast time scale. As a result, synapses dynamically change during periods of intense and repetitive activity, and these dynamic changes have important consequences on a neural system's processing of ascending information streams (Kandaswamy et al., 2010; Klyachko and Stevens, 2006).

2. Synaptic facilitation affects the processing of complex activity

The presynaptic side of a chemical synapse contains a certain number of synaptic vesicles filled with neurotransmitter. During a presynaptic action potential, voltage gated calcium channels open and calcium triggers the fusion of one ore more vesicles with the presynaptic terminal membrane (Bollmann et al., 2000; Borst and Sakmann, 1996; Burnashev and Rozov, 2005; Katz and Miledi, 1965; Sakaba and Neher, 2001b; Schneggenburger and Neher, 2000, 2005). After the fusion event, calcium that entered the presynaptic terminal in response to the depolarization is still present in the terminal. In order to restore the synapse to its recovered state, calcium needs to be buffered and expelled from the presynaptic terminal (Burnashev and Rozov, 2005). A number of proteins are performing the buffering process, and active calcium transport as well a calcium sodium antiporter are in charge of finally removing calcium from the presynaptic terminal (Burnashev and Rozov, 2005; Neher and Sakaba, 2008). This process functions at a relatively fast time scale, such that after tens of milliseconds calcium levels inside the presynaptic terminal have returned to normal. Multiple action potentials arriving at the presynaptic terminal within a short time period —as it is typical for many auditory neurons— will cause an elevation of calcium level in the terminal, with the result that vesicle release is facilitated. If everything else were equal, these higher calcium levels will cause more synaptic vesicles to fuse than during the first event, and thus repetitive synaptic events will produce higher synaptic currents. Recovery from synaptic facilitation occurs with an exponential time scale over a time period of tens of milliseconds to about 100 ms (Burnashev and Rozov, 2005). Successive action potentials arriving at the terminal after this time period will produce synaptic currents that are much less, or not influenced by facilitation. Successive action potentials arriving within this 100 ms window will be affected by facilitation to varying degrees which depend on the

* Tel.: +1 303 724 4621; fax: +1 303 724 4501.
E-mail address: Achim.klug@ucdenver.edu.

0378-5955/$ – see front matter © 2011 Elsevier B.V. All rights reserved.
doi:10.1016/j.heares.2011.05.011

length of the inter event interval. Note that even though the recovery from synaptic facilitation occurs at a relatively fast time scale of <100 ms, this time period corresponds to firing frequencies of only 10 Hz – a very low firing frequency by standards of most auditory neurons. Therefore, most if not all processing of auditory information should be influenced by synaptic facilitation.

3. Synaptic depression affects the state of the synapse in an opposite direction as facilitation

A second, opposite, effect plays a very important role in controlling synaptic current amplitudes: synaptic depression. Synaptic depression is caused by a depletion of the synaptic vesicle releasable pool (Betz, 1970; Liley and North, 1953; Schneggenburger et al., 1999, 2002; Trussell, 1999; Von Gersdorff and Borst, 2002). Naturally, the presynaptic terminal can only contain a limited number of vesicles, the synaptic vesicle pool. Only a portion of these vesicles takes part in the release process, termed the synaptic vesicle releasable pool. Every synaptic event will release a certain number of vesicles, and thus will deplete the releasable pool (Schneggenburger et al., 2002). Vesicles are recycled as they are getting used, but this process is time-consuming and takes several seconds. Thus, a second synaptic event occurring within that time period can only draw upon a limited number of vesicles. If everything else were equal, synaptic depression will cause the amplitude of a second synaptic event to be smaller than the first (Schneggenburger et al., 2002; Trussell, 1999; Von Gersdorff and Borst, 2002). Producing new vesicles and filing them with transmitter is a more time-consuming process than buffering calcium, and thus recovery from synaptic depression is a considerably slower process than the recovery from synaptic facilitation (Schneggenburger et al., 2002; Wilkinson and Lin, 2004; Wu and Borst, 1999). Depending on the type of synapse, the state of depression, and activity levels during the recovery process, the making of new vesicles can take up to several seconds. Therefore, even neurons firing at very low frequencies of 1 Hz or less are commonly affected by synaptic depression.

4. Other important mechanisms of short-term plasticity

Trains of action potentials or repeated neural activity can have a number of other effects on the state of the synapse: for example, postsynaptic receptors can desensitize in the presence of high concentrations of the receptor molecule (= receptor desensitization; Neher and Sakaba, 2001a,b; Trussell and Fischbach, 1989; Trussell et al., 1988; Wong et al., 2003); presynaptic calcium channels can inactivate during repeated activity, allowing less calcium to flow into the presynaptic terminal (= calcium channel inactivation; Cheng and Augustine, 2008; Forsythe et al., 1998). Interestingly, when lower stimulation frequencies are used, calcium currents may also facilitate due to the repeated activity (Müller et al., 2008; Tsujimoto et al., 2002), thus leading to enhanced vesicle release. Therefore, just these two opposing mechanisms of calcium current plasticity may account for a large degree of short-term synaptic plasticity (Cheng and Augustine, 2008).

All synaptic vesicles do not have the same probability of being released in response to a presynaptic action potential (de Lange et al., 2003; Rizzoli and Betz, 2005; Trommershäuser et al., 2003). Calcium has been shown to enhance transmission after periods of high activity (= post-tetanic potentiation; Habets and Borst, 2005, 2006; Korogod et al., 2005; Lee et al., 2008; Xue and Wu, 2010). Finally, activation of postsynaptic metabotropic glutamate receptors reduces presynaptic release through an endocannabinoid-mediated pathway (Kushmerick et al., 2004). The mechanisms discussed above all have relatively short onset as well as short recovery times and thus are commonly described as mechanisms of short-term synaptic plasticity. Short-term plasticity includes mechanisms that appear and recover on a relatively short time scale of milliseconds to seconds, possibly tens of seconds at most. Synaptic plasticity at even longer time scales, such as LTP or LTD is not discussed here.

The mechanisms described above are just a few examples of many that govern short-term changes in the state of a synapse during periods of repeated activity. Some of these mechanisms act to enhance synaptic currents during periods of repetitive activity, while others act to reduce them. The various effects recover with their own respective time courses, such that during periods of repetitive and complex neural activity with varying inter-spike intervals, synaptic currents are controlled by these various mechanisms with dynamically changing contributions. During periods of repetitive activity, synapses dynamically change in many different ways, and understanding these dynamic changes can be challenging.

5. Short-term plasticity vs. spontaneous activity in the auditory system

Mechanisms of short-term plasticity affect the processing of complex and ongoing sound evoked activity trains. The auditory system is known to be a highly active neural system where neurons in the various auditory centers, especially brain stem centers, can fire with very high frequencies (Brownell, 1975; Brugge and Geisler, 1978; Goldberg and Brownell, 1973; Irvine, 1992; Joris et al., 1994; Kadner et al., 2006; Kiang, 1965; Klug et al., 2006; Kopp-Scheinpflug et al., 2003; Schwarz and Puil, 1997; Smith et al., 1998; Sommer et al., 1993; Spirou et al., 1990, 2005; Wang et al., 2010; Yost et al., 2008). Sound received by the ears is translated into trains of multiple action potentials, such that short-term plasticity can be observed at the synapses even when auditory neurons respond to brief and simple sound stimuli. During exposure to prolonged sound activity, as it is typical for most acoustic environments, auditory neurons fire with ongoing and sometimes complex activity, and thus it is not surprising that short-term plasticity plays a major effect in modulating a synapse's response to the various action potentials of the activity train (MacLeod et al., 2007).

Much less appreciated is the fact that, at least in the lower auditory system, short-term plasticity is at work even during the complete absence of sound. The reason is that auditory neurons, especially brain stem neurons, fire spontaneously at frequencies that can range from around 1 Hz to well over 100 Hz (Geisler et al., 1985; Hudspeth, 1997; Kiang, 1965; Liberman, 1978; Roberts et al., 1988). The major source for this spontaneous activity in the mature auditory system is most likely the tip-link channels at the stereocilia of inner hair cells (Hudspeth, 1989; Hudspeth and Gillespie, 1994; Roberts et al., 1988). The tip-link channels in the hair cell stereocilia have a certain open probability even in the absence of sound, thus leading to influx of calcium and potassium into the hair cell and in turn chronic transmitter release at the hair cell to auditory nerve synapse (Evans and Kros, 2006; Fuchs, 2008; Heil et al., 2007; Hudspeth, 1989). Thus, the sound independent release of transmitter leads to spontaneous firing in auditory nerve fibers. This spontaneous activity is then passed on to the various ascending parallel pathways, and subsequently spreads to many auditory centers where it still can be observed several synapses away from the nerve.

Due to the specific open probabilities of the tip-link channels, auditory neurons are chronically active and fire action potentials even in complete acoustic silence. Moreover, these spontaneous activity levels, which can vary from very low frequencies to about 100 Hz, are suitable to recruit synaptic depression, synaptic

facilitation, and other mechanisms of short-term plasticity in auditory brain stem neurons. In other words, even in absolute acoustic silence, the mechanisms of synaptic facilitation and synaptic depression —and almost certainly other mechanisms as well— are active and actively influencing neurotransmission dynamics. During periods of sound presentation, these mechanisms must play an even more important role (Klyachko and Stevens, 2006; Wang and Manis, 2008; Wang et al., 2010).

6. The in-vitro problem and its consequences

Studies of synaptic transmission are typically performed in reduced systems such as brain slices, in combination with electrophysiological recording methods such as intracellular or patch clamp recordings. Reasons why most investigators choose reduced preparations such as brain slices for such experiments include that these preparations offer great access to the neurons and synapses under investigation, such that specific single neurons or cell types can easily be located and investigated. Reduced systems allow for very detailed measurements of intracellular currents in neurons, down those produced by single channels. They allow for complete pharmacological control over both the extracellular and intracellular environment of the neurons, and allow for very controlled electrical stimulation of single cells. Most of these manipulations would be very difficult if not impossible to do with intact preparations where an electrode is advanced into a brain and an investigator has generally much less control over the question which neuron will be encountered by the electrode. Also, it is very difficult to control the neuron's environment pharmacologically with in-vivo recordings, such that pharmacological agents required to isolate e.g. single currents cannot be used or can only be used in a very limited fashion.

It is therefore fair to say that the invention of reduced systems and the development of electrophysiological methods to record subcellular currents and manipulate a neuron's environment in any way desired has greatly advanced our understanding of neural processing in general, and synaptic function in particular. This is also true for the auditory system, where our understanding of e.g. the creation of specific firing patterns among auditory brain stem neurons, or our understanding of synaptic transmission between auditory nuclei was only made possible by the introduction of such methods. However, one problem of these reduced systems is that the neurons under investigation are contained in a small isolated piece of tissue that is disconnected from many of its inputs and is not functioning in the context of an intact brain. Importantly, during the preparation of the slices of auditory nuclei, the brain is disconnected from the auditory nerve, and the spontaneous activity of auditory nerve fibers is lost. Once tissue is sectioned and the connections to the nerve are severed, auditory neurons are experiencing a non-physiological lack of activity. During electrophysiological recordings from the tissue, prolonged pauses between stimulus presentations are customary, especially when synapses are tested. As a result, auditory neurons in brain slice experiments experience much lower activity levels than they did in the intact brain. It is easy to imagine that this lack of activity has a number of consequences on synaptic physiology. Most importantly, synaptic vesicles are not getting consumed at the typical rate, and presynaptic calcium levels are likely to fall below the concentrations that are typically present in naturally active synapses. The majority of electrophysiological studies in the auditory system using brain slices did not account for this lack of activity. In many cases, for example those in which membrane properties, action potential firing etc. are studied, this will most likely not matter. Also, for studies that focus on the pure mechanisms of synaptic transmission, this will most likely not matter as well. However, studies that aim at investigating the role of auditory synapses during sound processing, this discrepancy might have a large impact. To date, two auditory brain stem synapses have been tested both under conditions in which the background activity was present and was lacking, and for both synapses fundamental differences between the context of chronic activity and prolonged silence have been found (Hermann et al., 2009, 2007; Lorteije et al., 2009; Müller et al., 2010; Wang and Manis, 2008; Wang et al., 2010). One of the two synaptic station tested was the calyx of Held, a giant synapse that connects globular bushy cells in the cochlear nucleus to principal neuron in the medial nucleus of the trapezoid body (MNTB). Hermann et al. (2007) investigated the question how key properties of synaptic transmission might be different at the calyx between silent conditions and conditions that imitate those of the intact brain closer. The calyx of Held has become one of the most important models for studies in synaptic transmission over the last few years, and due to this fact, transmission at this station is understood in great detail (Barnes-Davies and Forsythe, 1995; Schneggenburger and Forsythe, 2006; Von Gersdorff and Borst, 2002). We know that the presynaptic terminal of the calyx of Held has several active zones and releases a great number of vesicles upon each presynaptic stimulation. EPSPs measured at the postsynaptic cell are large and fast, and due to the large size of the EPSCs measured in standard brain slice experiments, it has always been assumed that the calyx of Held to MNTB synapse is a very failsafe synaptic station (meaning that every incoming action potential is reliably related to an outgoing action potential; Taschenberger and Von Gersdorff, 2000, 2002; Trussell, 2002). The perceived reliability of the synapse led to a view in the literature that suggested the MNTB is a pure relay nucleus that converts incoming glutamatergic excitation into outgoing glycinergic inhibition, which is required for a number of computational processes by higher-order nuclei, including sound localization (Brand et al., 2002; Caird and Klinke, 1983; Goldberg and Brown, 1968, 1969; Moore and Caspary, 1983; Spangler et al., 1985).

Does this view change when the same synapse is studied under conditions in which the chronic background activity is considered? How can a context of chronic background activity be effectively tested in a reduced preparation such as a brain slice? The approach of Hermann et al. (2007) was to record both the firing frequency and statistical distribution of spontaneous activity from the MNTB in-vivo, and then they design ongoing stimulus trains that imitate the measured spontaneous activity. MNTB neurons were found to fire with spontaneous rates ranging from about 1 Hz to well over 100 Hz, and the statistical distribution was near Poisson-distributed. Based on these data, the group designed stimulus trains that lasted for many minutes and consisted of thousands of Poisson-distributed events at representative mean frequencies. Afferent inputs to calyces of Held were stimulated with this activity pattern for several minutes in an attempt to bring the synapses into a similar state of activity as they presumably would be in the intact brain. After such a 'conditioning' phase, the synapses are presumably in a state that imitates a situation in which an animal is not receiving any sound input, and its auditory neurons are driven by spontaneous activity only (i.e. the animal is sitting, for example, in a sound proof room). The imitation of chronic spontaneous activity had a number of important effects on synaptic transmission in the calyx of Held.

Most obviously, synaptic amplitudes were depressed to different degrees, dependent on the frequency of the background activity used, and were as small as about 1/4 of the amplitudes measured in resting slices. In other words, the very large synaptic amplitudes typically measured under standard (i.e. resting) brain slice methods and reported in the literature might be a consequence of the artificial lack of activity in standard brain slice preparations, and EPSCs produced by the calyx of Held might be

much smaller in the intact brain than previously reported (Hermann et al., 2007). Apparently, the lack of release events at the presynapse increases the number of synaptic vesicles in the presynaptic pool to levels that do not occur typically in the intact brain. Pool depletion studies have shown that the synaptic vesicle releasable pool in the calyx of Held can contain several thousand vesicles, assuming the absence of release events for at least several seconds (Meyer et al., 2001; Sakaba and Neher, 2001b; Satzler et al., 2002; Schneggenburger and Neher, 2000; Sun and Wu, 2001). However such a situation is not likely to occur in the intact auditory system, even in neurons with a very low spontaneous activity. Chronic spontaneous activity at any frequency will trigger constant release events and thus puts the presynaptic terminal in a state of chronic depression. Again, this state of chronic depression is not dependent on any sound input, but rather is already present in a situation of complete acoustic silence. Thus, the first conclusion is that auditory synapses, especially those in the brain stem that operate under conditions of chronic synaptic depression, typically exhibit synaptic currents are likely to be considerably smaller than measured in standard brain slice experiments in which the natural spontaneous activity is lacking.

7. Synaptic plasticity during ongoing activity

What happens if stimulus trains simulating sound activity are presented? Hermann et al. (2007) introduced such activity into the trains of Poisson-distributed background activity. This was done by embedding high-frequency stimulus trains (imitated auditory signals) into low frequency stimulus trains (imitated background activity). For example, a brief pure-frequency tone (tone burst), a commonly used sound stimulus for in-vivo recordings, would recruit a burst of action potentials at frequencies between 50 and 500 Hz. Thus, a situation which imitates an experimenter playing a tone burst would best be translated into an in-vitro experiment where a short high-frequency stimulus train is seamlessly embedded in a low frequency Poisson-distributed background train of activity. Testing high-frequency trains in the calyx of Held without background activity produces EPSC trains which depress progressively with the number of events in the train. When trains of e.g. 10 or 20 pulses are tested against a background of silence, the observed depression is substantial. For example a 300 Hz train depresses from synaptic amplitudes of typically around 10 nA in response to the first event to about 2 nA in response to the 20th event in the train, i.e. by about 80% (Fig. 1A, black trace & Fig. 1C and D, first group of bars; Hermann et al., 2007; Taschenberger and Von Gersdorff, 2000, 2002).

When the same 300 Hz train was tested embedded in the background of spontaneous activity, the relative depression observed during the same 20 pulse, 300 Hz train was much less than what was observed in the background of silence (Fig. 1B). With the inclusion of spontaneous activity, the EPSC amplitude in response to the first stimulus was depressed compared to a non-active control, and was further depressed over the course of the high-frequency train. However, when comparing the EPSC amplitudes in response to the first and last stimulus of each train, much less relative depression was observed to occur during the 300 Hz in the case where it was embedded in background activity vs. under control conditions (compare events in EPSC train in Fig. 1A and 1B and Fig. 1C and D, last group of bars).

One important consequence of the altered EPSC amplitudes is the observation that not every EPSC leads reliably to a postsynaptic action potential. Failsafeness, or a reliable 1:1 transmission is, according to many studies, one of the hallmarks of the calyx of Held to MNTB synapse – which is why this station is often called a 'relay' nucleus (Mc Laughlin et al., 2008; Taschenberger and Von Gersdorff, 2000, 2002; Wu and Kelly, 1993). The failsafe property of the synapse is based on the observation that each presynaptic action potential will elicit a substantial EPSC that is several fold higher than required to reach threshold for the postsynaptic neuron (Taschenberger and Von Gersdorff, 2000). When EPSCs are measured under conditions of ongoing and chronic background activity, they are still substantial and super threshold in many cases. However, a significant number of

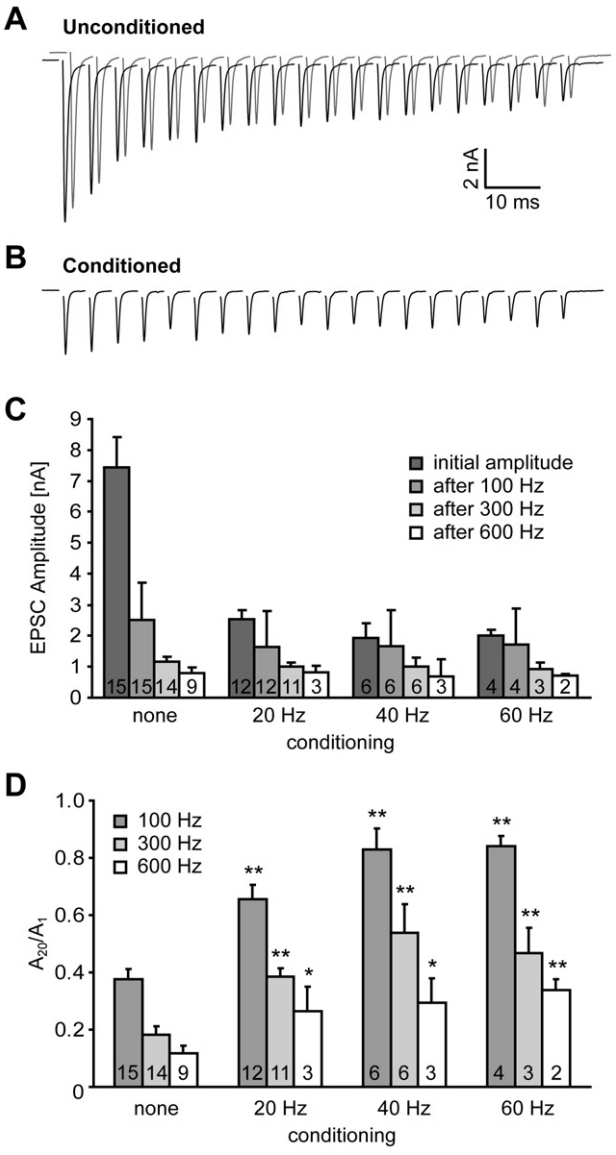

Fig. 1. (A and B) Responses of one neuron to the same 300 Hz/20 pulse stimulus train before conditioning with spontaneous activity (A, black line), while the 300 Hz train was embedded in 60 Hz spontaneous activity (B), and about 5 min after the 'spontaneous' activity was ended (A, gray line). (C) Absolute EPSC amplitudes with various conditioning and test frequencies. Trains of 100 Hz, 300 Hz, and 600 Hz were tested with 20 stimuli in the trains in each case. The dark bars 'initial amplitude' refer to the EPSC amplitude of the first event of a train (similar for 100 Hz, 300 Hz, and 600 Hz stimulus trains), while the bars labeled 'after 100/300/600 Hz' refer to the amplitude of the 20th event in the train of the respective frequency. Numbers in the bars indicate sample size. (D) Ratios of synaptic current amplitudes in response to the last stimulus over the current of the synaptic response to the first stimulus of the 20 pulse trains. Low ratios indicate substantial relative depression during the 20 pulse stimulus trains, while high ratios indicate low relative synaptic depression. Numbers in the bars indicate sample size. An asterisk next to a bar indicates a significantly different mean compared to the respective control (= unconditioned) condition, which is shown be the same color bar in the group 'none' (student's *t*-test). From Hermann et al. 2007. Used with permission.

failures can be observed during periods of high frequency and long-lasting activity (Hermann et al., 2007).

8. Recovery from synaptic depression is faster in active synapses

Recovery from synaptic depression, i.e. the recycling of synaptic vesicles, is a critically important step for maintaining transmission during prolonged periods of activity in a synapse. Naturally, this process is relatively slow since it involves retrieval of membrane patches from the presynaptic membrane, synthesis of vesicles, synthesis of transmitter molecules, filling of the vesicles with the transmitter, adding the new vesicle to a pool of releasable vesicles, and having it go through the various steps of docking and priming before it can be released in response to a presynaptic action potential (Groemer and Klingauf, 2007; Smith et al., 2008). A number of studies have measured the time constant with which the presynaptic terminal produces new vesicles and gets them ready for release. There are mainly two common methods to perform these measurements: the first one involves flushing the synaptic pool by depolarizing the presynaptic terminal for prolonged periods of time, for example via voltage clamp of the presynaptic terminal and imposing a depolarizing voltage command for a prolonged time period. The second method involves depleting the vesicle releasable pool as much as possible by triggering many successive action potentials at a high frequency. Both of these manipulations will cause a large amount of calcium to flow into the presynaptic terminal and thus will cause most if not all vesicles in the readily releasable pool to be released. Following this depletion step, test stimuli at certain points in time after the flush event are given to test the number of newly produced vesicles during that rest period. Such experiments testing how the refilling of the synaptic vesicle releasable pool at the calyx of Held progresses have determined a time constant of about 2–4 s. Thus, a period of inactivity of about 4–8 s will refill the pool to about 95% of its initial value, and approximately restore initial EPSC amplitude responses (Bollmann et al., 2000; von Gersdorff et al., 1997; Wu and Borst, 1999). However, a period of inactivity lasting several seconds does not occur very frequently in the life of auditory brain stem neurons, if ever. Therefore it is surprising that the vesicle releasable pool of an auditory synapse such as the calyx of Held should take up to 8 s to refill – implying that the system would be at least partially unresponsive to incoming events during that time period.

In-vivo recordings from the MNTB of rodents show that MNTB neurons can follow high firing frequencies for prolonged periods of time and subsequently recover at a time course of tens of milliseconds, not seconds (Hermann et al., 2007). Experiments showing recovery of firing have been performed in both MNTB and other auditory brain stem nuclei and involve the presentation of a long tone burst while recording from a single neuron in-vivo, then allowing the cell to recover for various amounts of time and then presenting a second, identical tone burst. During the presentation of the initial tone, cells respond with a certain firing rate and pattern. In the case of the MNTB, responses declined throughout the tone stimulus, partially due to depression at the calyx of Held and partially due to other mechanisms acting at other components of the ascending pathway. During the inter-tone interval (the rest period), vesicle releasable pool recovery as well recovery of other components occurred, and the progress of the various recovery processes was tested by presenting the second identical stimulus to the neuron. The goal was to test how long of an inter-stimulus interval was needed to achieve complete recovery of the pathway. Complete recovery would be indicated by identical responses to the first and second tone. In the experiment involving MNTB, it was found that an inter-stimulus interval of about 80 ms was sufficient to obtain complete recovery of the afferent pathway including the calyx of Held (Hermann et al., 2007). By contrast, recall that in-vitro experiments determined that vesicle pool refilling at the calyx of Held takes about 100 times as long, i.e. about 4–8 s.

Are the two experimental approaches even comparable? The in-vitro experiments test the refilling of a vesicle releasable pool, i.e. the production of new vesicles at the presynaptic terminal (the calyx of Held), while the in-vivo experiment tests the recovery of firing rates of MNTB postsynaptic neurons. Naturally, the latter experiment tests the recovery of not only one presynaptic terminal but the recovery of the entire afferent chain from auditory nerve to cochlear nucleus to MNTB. However, note that such an experiment measures the recovery of the slowest component in the afferent chain. If vesicle pool recovery at the calyx of Held took longer than 80 ms (or if any other component of the afferent chain recovered slower than within 80 ms), recovery of firing could not be observed within that time period. Thus, while the in-vivo and in-vitro experiments test different physiological components, it can be concluded that the upper limit for vesicle releasable pool recovery at the calyx of Held must be around 80 ms.

How can the discrepancy in vesicle pool recovery between the in-vivo situation (80 ms or less) and the in-vitro situation (4–8 s) be reconciled? There are several reasons. First, active synapses with an elevated level of calcium in the presynaptic terminal recover at a faster time scale than silent synapses. The recovery time constant in these active synapses is on the order of tens or hundreds of milliseconds, not seconds (Hosoi et al., 2007; Neher and Sakaba, 2008; Sakaba and Neher, 2001a; Wang and Kaczmarek, 1998). The reason for this faster recovery is that elevated calcium levels in the presynaptic terminal enhance the recruitment of new vesicles to the vesicle releasable pool (Neher and Sakaba, 2008; Wang and Kaczmarek, 1998). In the active brain, especially the active auditory system, where neurons usually fire at relatively high levels, calcium levels are likely to be chronically elevated. As a result, this faster time constant probably plays a much more important role in recovery from depression than the slower time constant that can be observed in rested slices. Still, the in-vivo recordings show recovery of firing at the MNTB on time scales even shorter than that. This discrepancy can be reconciled with the notion that, in chronically active neurons, the vesicle releasable pool never fills up to levels that are considered ‘a full pool’ by in-vitro measurements performed in non-active brain slices. The reason is that filling the pool to these levels requires inactivity for several seconds, which rarely happens in the auditory brain stem. When more typical activity levels are considered, the vesicle releasable pool is only about 1/3 to ¼ of the size of these measurements (Hermann et al., 2007) and thus, time periods required to fill the pool to these (artificially) high levels are not representative for a typical in-vivo situation. Additionally, high levels of activity do not completely empty the pool as done in the described pool-flushing experiments, but rather depress it to certain levels above ‘empty’. Therefore, the dynamic changes in synaptic pool filling levels are much smaller under in-vivo conditions than can be experimentally enforced in brain slices. When dynamic changes in vesicle pool states typical for the active brain are looked at, and corresponding time courses are applied to these changes, similar recovery times from synaptic depression are seen as can be observed in-vivo for the recovery of firing.

9. Other mechanisms of short-term plasticity affect the processing of information streams in the active brain

Besides synaptic depression and facilitation, many other mechanisms of short-term plasticity participate in controlling the amplitude of a signal transferred across a synapse (see above). In

order to understand short-term plasticity, we need to understand the relative importance of each of these mechanisms and its quantitative contribution to the plasticity. One problem is that all of these mechanisms have been investigated at inactive auditory synapses, so their role in controlling transmission during ongoing and complex activity is unclear. However, modeling studies addressing this question have been done both under inactive and active conditions. The idea behind these modeling studies is to create a mathematical model that can capture and reproduce the dynamics of the observed short-term plasticity well, i.e. calculate EPSC amplitudes in response to arbitrarily complex stimulus trains with sufficient accuracy. Any mathematical model that can capture the dynamic changes of EPSC amplitudes in response to arbitrarily complex stimulus trains accurately through the modeling of certain synaptic parameters presumably describes and quantifies these parameters sufficiently well. These models do not only take into account the synaptic effects themselves, but also quantify their relative contribution in reproducing the observed synaptic amplitude changes. Modeling studies are typically performed by taking an observed dataset, in this case a set of recorded EPSC amplitudes in response to a certain stimulus train, and then finding the model which most accurately captures this dataset.

A number of modeling studies have done such an approach. For example, at the calyx of Held, Hennig et al. (2008) have modeled short-term plasticity. They have recorded EPSC amplitudes in response to stimulus trains of different frequencies, and subsequently developed a model which can accurately reproduce the observed EPSC amplitudes. The found that, in order to accurately describe short-term plasticity at the rested calyx, their model needed to include several parameters, namely depression and facilitation, inactivation of calcium channels, inhibition of calcium channels by metabotropic glutamate receptors, AMPA receptor desensitization, and two modes of vesicle recruitment. These results suggest that all these mechanisms make a measureable contribution to short-term plasticity, and thus, omitting them from the model would substantially compromise the accuracy of the predictions. Similar, other groups have also found that a number of parameters are required to include into the model to obtain accurate predictions, although the exact number and type of the parameters varies to some degree between studies (Hosoi et al., 2007; Weis et al., 1999).

Surprisingly, when the same modeling approach was taken to model EPSC amplitudes in response to stimulus trains under conditions of chronic activity, a much simpler model achieved great accuracy and great predictability of the EPSC amplitudes. Specifically, the simplest model which only accounts for the dynamics of synaptic depression already achieves a roughly 95% accuracy (Hermann et al., 2009). In other words, putting synapses in a state of prolonged and chronic activity appears to simplify the dynamics of EPSC amplitude short-term plasticity. This suggests that many of the synaptic short-term plasticity effects that have been demonstrated physiologically and that are required for accurate descriptions of EPSC dynamics in rested tissue may not participate in the shaping of EPSC responses during trains of ongoing activity. Moreover, the inclusion of additional mechanisms such as receptor desensitization, recovery from depression with two different time constants, or facilitation did not contribute to the overall predictive power of the model (Hermann et al., 2009).

We can only speculate about the reasons for this surprising result. Is it really possible that synaptic transmission becomes "simpler" during ongoing synaptic activity such that it can be quantified with simpler models? The answer to this question is unclear. However, note that many cellular and synaptic processes are calcium dependent. Presumably, a synapse that is artificially inactive for prolonged periods of time is depleted of calcium. Once such a synapse is stimulated, calcium enters the presynaptic terminal – and might trigger many different calcium-dependent mechanisms that turn on at their own respective time scales. By contrast, a synapse that has been chronically active for a prolonged period of time might have experienced prolonged influx of calcium into the presynaptic terminal, and thus might be in a steady-state between calcium influx and calcium elimination. Further studies are needed to address this very interesting and important question, and determine how the various mechanisms of short-term plasticity change with chronic activity.

10. Extracellular calcium concentration changes depression characteristics

All experiments described above were performed under conditions in which the extracellular calcium concentration of the slice preparations was kept at 2 mM, the same concentration used in the vast majority of brain slice experiments. Many investigators choose this concentration for historic reasons. Another reason why many investigators choose this particular concentration is the fact that natural cerebrospinal fluid has been shown to contain about 1.2–1.5 mM of free calcium (Jones et al., 1992; Jones and Keep, 1988). When artificial cerebrospinal fluid is used to replace the natural cerebrospinal fluid during the slice experiments, some of the calcium mixed into the solution binds with other ions and molecules present in the solution, such that a higher concentration of calcium has to be added to the solution than free calcium is desired. Presumably, the standardly used 2 mM calcium concentration compares relatively well in terms of free calcium to the natural cerebrospinal fluid. The extracellular calcium concentration in most auditory nuclei is not known, but it seems reasonable to assume that it would be similar as in other brain regions, as cerebrospinal fluid is secreted in the ventricles and diffuses across the brain, before it is taken up.

However, if the extracellular calcium concentration chosen in the experiments described above were higher than in the extracellular environment of the intact brain, most of the properties described in the same experiments would have yielded inaccurate results. The reason is that a higher calcium concentration would lead to more calcium entering the presynaptic terminal during transmission events, and subsequently the number of synaptic vesicles released in response to stimulations would have been overestimated. Moreover, the synaptic vesicle releasable pool would deplete faster in such experiments than under control conditions and thus the amount of synaptic depression would be overestimated. Due to this exaggerated depression, many results regarding synaptic amplitudes during ongoing trains of activity, as well as the failsafeness of auditory synapses would have to be revisited. Therefore, it is critical to determine the extracellular calcium concentration in auditory nuclei correctly, and use this correct calcium concentration for the artificial cerebrospinal fluid in brain size experiments. How can the correct extracellular calcium concentration of auditory neurons be determined? There are a number of methods available, but unfortunately none of them are technically very simple. Lorteije et al. (2009) have chosen a very elegant approach to determine extracellular calcium concentrations in the medial nucleus of the trapezoid body physiologically. They performed in-vivo patch clamp recordings from MNTB principal neurons while stimulating the animal's ears with sounds of various types and durations. They recorded calyx produced EPSC trains from MNTB neurons in response to sound stimulation, and analyzed these EPSC trains for the depression behavior of the afferent synapses, the calyces of Held. Subsequently, they prepared brain slices from animals of the same species and age group, patch clamped MNTB neurons in those slices and recorded calyceal EPSC

trains recruited by electrical stimulation of afferent inputs. They measured depression behavior in synapses in a similar way as done during the in-vivo experiments. Then they tested synaptic depression in response to these trains under different calcium concentrations, asking the question, which calcium concentration would lead to the best match between in-vivo and in-vitro depression behavior of the same synapses. The surprising answer was that an extracellular calcium concentration of 1.2 mM (corresponding to an even lower concentration of free calcium) best matched the depression observed in-vivo. Based on this result, it indeed appears that most experiments described above used a non-physiological calcium concentration that probably caused an exaggeration of synaptic depression – with consequences on a number of the described parameters.

Therefore, determining and using the correct extracellular calcium concentration for the brain slice experiment at hand will have to be the next design improvement of any brain slice experiment that aims at the understanding of how neural circuits process information. One interesting question resulting from the data described here is why the calcium concentration in the MNTB would be lower than in most other brain areas. A local depletion of extracellular calcium due to the high levels of activity of very large synapses, which take up a lot of calcium, might be the most likely reason. Borst and Sakmann (1999) have shown that during periods of repeated activity, the calcium concentration in the synaptic cleft of the calyx of Held can drop considerably, most likely due to the exceptional size of the presynapse (Borst and Sakmann, 1999). This work was done in 8–10 day old rats, i.e. before hearing onset in the animals. A number of parameters change at the calyx of Held during the first two weeks of postnatal development, and it is unclear if this local calcium depletion also occurs in post-hearing animals. If it does, and if calcium also gets depleted in the MNTB of the intact brain, then it appears that the extracellular calcium concentration dynamically fluctuates with activity levels. During periods of high auditory activity, extracellular calcium concentrations might drop and recover during subsequent periods of relative silence. Such dynamic changes would add an entirely new component to short-term synaptic plasticity, but obviously pose major problems for brain slice experiments attempting to emulate conditions of the intact brain as closely as possible. More detailed studies are needed to determine calcium concentrations present in the extracellular space of auditory nuclei, and to determine potential dynamic changes of this concentration with activity levels.

11. Studying the interaction of several highly active inputs in brain slices

A different area in which the use of naturally present spontaneous activity can change our view of information processing is in cases where excitation and inhibition are integrated with each other. Again, most brain slice experiments that test the interaction of excitation and inhibition test the two types of inputs under conditions in which naturally present background activity is not used. EPSC amplitudes measured under such silent conditions are compared to IPSC amplitudes measured under similar silent conditions, in an attempt to compare the relative strength of the two types of inputs, and ultimately to assess the computational result of their integration. However, in cases in which one of the two inputs, or both, are spontaneously active in the intact brain, such a comparison becomes difficult, since the strength of the involved inputs that is compared in such experiments is not necessarily the strength with which they interact under in-vivo conditions. If one of the inputs, for example the excitation, is spontaneously active in the intact brain, then it is likely that the strength of this excitatory input is overestimated in the brain slice experiment – since EPSCs produced by that input are likely to be smaller in-vivo than measured in such an experiment. If the inhibition is assessed correctly in the same experiment (since it is not spontaneously active), the relative strength of excitation vs. inhibition will be assessed differently in such an experiment than it would be present in the intact brain. As a result, the role that inhibition would have in this system in suppressing spikes might be much larger than found in such an experiment, and might ultimately be misinterpreted altogether.

A scenario that is more typical for the auditory system is a situation in which both the excitatory and inhibitory inputs to a neuron are spontaneously active. Most auditory brain stem nuclei receive both excitatory and inhibitory inputs of auditory origin and thus both types of inputs are likely to be spontaneously active in-vivo. In such cases, the important question is to which degree the two types of inputs depress during in-vivo like activity levels. Since the two types of synapses are designed fundamentally different, it is unlikely that the degrees of depression would be similar, even if the afferent inputs experienced similar activity levels. Thus, an assessment of the synaptic strength of excitation and inhibition performed in non-active preparations might not only result in inaccurate absolute measurements of EPSC and IPSC amplitudes, but also in inaccurate assessments of the relative strength between the two – and consequently in an inaccurate assessment of the potential computational roles of the inputs. Only once the depression levels under in-vivo conditions have been determined, it will be possible to estimate the effects of the integration of the two correctly.

12. Conclusions

Reduced systems such as brain slices offer a powerful approach to study the physiology of auditory neurons in great detail. The reduced system offers great access to the neurons under investigation and allows for the measurement of physiological parameters that would be very difficult if not impossible to measure in the intact brain. However, when studying auditory nuclei, especially highly active auditory brain stem nuclei in reduced systems, one has to be aware that the lack of activity in the reduced system compared to the in-vivo situation has a number of important effects on the data that are measured. Most importantly, the lack of chronic activity in the slice preparation has a number of consequences on the physiological state of the synapses under investigation. In most extreme cases, measuring physiological parameters of synapses under such conditions can lead to results that are not representative for the functioning of the synapses in the active brain, and ultimately to misinterpretations of the functioning of the neural system under investigation. Reintroducing physiologically relevant spontaneous activity as described above is one important way how discrepancies between reduced systems and intact brains can be addressed. Such an approach might be easier to implement for some brain nuclei than others. In the case of the calyx of Held/MNTB system, almost all excitatory input to postsynaptic neurons originates from one single synapse. In this case it very easy to electrically stimulate the single corresponding afferent axon and perform the recordings. By contrast, other auditory nuclei receive multiple excitatory and inhibitory inputs that may impact the postsynaptic neuron with different latencies and different activity patterns, making it much more difficult to stimulate each input with its respective biologically relevant background activity. Another problem of the approach described above is that spontaneous activity rates vary greatly among auditory neurons, even within the same nucleus. For example, Hermann et al. (2007) found MNTB neurons that fired spontaneously at rates below 1 Hz, but also found neurons that fired at rates of above 100 Hz. When

recording from these neurons in brain slices, it is impossible to determine the original firing rate that a given MNTB neuron used to exhibit in the intact brain. Therefore, neurons can only be conditioned with a standard set of background rates, which in some cases might be very similar to the natural background rate of the neurons, and in other cases might not be.

Nevertheless, the inclusion of even standard trains of background activity is an important step in closing gaps between in-vitro preparations and the intact brain. Together with the use of tissue from more mature animals (Taschenberger and Von Gersdorff, 2000, 2002), the use of physiological temperatures (Kushmerick et al., 2006; Postlethwaite et al., 2007), and the use of physiologically relevant extracellular calcium levels (Borst, 2010; Lorteije et al., 2009), this will ensure that brain slice experiments are as representative for the information processing performed by the intact brain as can possibly be done at this time – and thus help exploit the advantages of the reduced system approach maximally.

References

Barnes-Davies, M., Forsythe, I., 1995. Pre- and postsynaptic glutamate receptors at a giant excitatory synapse in rat auditory brainstem slices. J. Physiol. 488 (Pt 2), 387–406.

Betz, W.J., 1970. Depression of transmitter release at the neuromuscular junction of the frog. J. Physiol. 206, 629–644.

Bollmann, J., Sakmann, B., Borst, J., 2000. Calcium sensitivity of glutamate release in a calyx-type terminal. Science 289, 953–957.

Borst, J., Sakmann, B., 1999. Depletion of calcium in the synaptic cleft of a calyx-type synapse in the rat brainstem. J. Physiol. 521 (Pt 1), 123–133.

Borst, J.G., Sakmann, B., 1996. Calcium influx and transmitter release in a fast CNS synapse. Nature 383, 431–434.

Borst, J.G.G., 2010. The low synaptic release probability in vivo. Trends Neurosci. 33, 259–266.

Brand, A., Behrend, O., Marquardt, T., McAlpine, D., Grothe, B., 2002. Precise inhibition is essential for microsecond interaural time difference coding. Nature 417, 543–547.

Brownell, W., 1975. Organization of the cat trapezoid body and the discharge characteristics of its fibers. Brain Res. 94, 413–433.

Brugge, J., Geisler, C., 1978. Auditory mechanisms of the lower brainstem. Annu. Rev. Neurosci. 1, 363–394.

Burnashev, N., Rozov, A., 2005. Presynaptic Ca2+ dynamics, Ca2+ buffers and synaptic efficacy. Cell Calcium 37, 489–495.

Caird, D., Klinke, R., 1983. Processing of binaural stimuli by cat superior olivary complex neurons. Exp. Brain Res. Exp. Hirnforschung Exp. Cérébrale 52, 385–399.

Cheng, Q., Augustine, G.J., 2008. Calcium channel modulation as an all-purpose mechanism for short-term synaptic plasticity. Neuron 57, 171–172.

de Lange, R.P.J., de Roos, A.D.G., Borst, J.G.G., 2003. Two modes of vesicle recycling in the rat calyx of Held. J. Neurosci. 23, 10164–10173.

Dittman, J., Ryan, T.A., 2009. Molecular circuitry of endocytosis at nerve terminals. Annu. Rev. Cell Dev. Biol. 25, 133–160.

Evans, M.G., Kros, C.J., 2006. The cochlea–new insights into the conversion of sound into electrical signals. J. Physiol. 576, 3–5.

Forsythe, I., Tsujimoto, T., Barnes-Davies, M., Cuttle, M.F., Takahashi, T.T., 1998. Inactivation of presynaptic calcium current contributes to synaptic depression at a fast central synapse. Neuron 20, 797–807.

Fuchs, P., 2008. Why do hair cells have ribbons? Focus on "synaptic ribbon enables temporal precision of hair cell afferent synapse by increasing the number of readily releasable vesicles: a modeling study". J. Neurophysiol. 100, 1695–1696.

Geisler, C.D., Deng, L., Greenberg, S.R., 1985. Thresholds for primary auditory fibers using statistically defined criteria. J. Acoust. Soc. Am. 77, 1102–1109.

Goldberg, J.M., Brown, P.B., 1968. Functional organization of the dog superior olivary complex: an anatomical and electrophysiological study. J. Neurophysiol. 31, 639–656.

Goldberg, J.M., Brown, P.B., 1969. Response of binaural neurons of dog superior olivary complex to dichotic tonal stimuli: some physiological mechanisms of sound localization. J. Neurophysiol. 32, 613–636.

Goldberg, J.M., Brownell, W.E., 1973. Discharge characteristics of neurons in anteroventral and dorsal cochlear nuclei of cat. Brain Res. 64, 35–54.

Groemer, T.W., Klingauf, J., 2007. Synaptic vesicles recycling spontaneously and during activity belong to the same vesicle pool. Nat. Neurosci. 10, 145–147.

Habets, R., Borst, J., 2006. An increase in calcium influx contributes to post-tetanic potentiation at the rat calyx of Held synapse. J. Neurophysiol. 96, 2868–2876.

Habets, R.L.P., Borst, J.G.G., 2005. Post-tetanic potentiation in the rat calyx of Held synapse. J. Physiol. 564, 173–187.

Heil, P., Neubauer, H., Irvine, D., Brown, M., 2007. Spontaneous activity of auditory-nerve fibers: insights into stochastic processes at ribbon synapses. J. Neurosci. 27, 8457–8474.

Hennig, M.H., Postlethwaite, M., Forsythe, I.D., Graham, B.P., 2008. Interactions between multiple sources of short-term plasticity during evoked and spontaneous activity at the rat calyx of Held. J. Physiol 586, 3129–3146.

Hermann, J., Grothe, B., Klug, A., 2009. Modeling short-term synaptic plasticity at the calyx of held using in vivo-like stimulation patterns. J. Neurophysiol. 101, 20–30.

Hermann, J., Pecka, M., Von Gersdorff, H., Grothe, B., Klug, A., 2007. Synaptic transmission at the calyx of held under in vivo like activity levels. J. Neurophysiol. 98, 807–820.

Hosoi, N., Sakaba, T., Neher, E., 2007. Quantitative analysis of calcium-dependent vesicle recruitment and its functional role at the calyx of Held synapse. J. Neurosci. 27, 14286–14298.

Hudspeth, A.J., 1989. How the ear's works work. Nature 341, 397–404.

Hudspeth, A.J., 1997. How hearing happens. Neuron 19, 947–950.

Hudspeth, A.J., Gillespie, P.G., 1994. Pulling springs to tune transduction: adaptation by hair cells. Neuron 12, 1–9.

Irvine, D.R.F., 1992. In: Popper, A.N., Fay, R.R. (Eds.), Physiology of the auditory brainstem, the mammalian auditory pathway: Neurophysiology, vol. 2. Springer Verlag, New York, pp. 153–231.

Jahn, R., Scheller, R.H., 2006. SNAREs–engines for membrane fusion. Nat. Rev. Mol. Cell Biol. 7, 631–643.

Jahn, R., Hell, J., Maycox, P.R., 1990. Synaptic vesicles: key organelles involved in neurotransmission. J. Physiol. (Paris) 84, 128–133.

Jones, H., Keep, R., Butt, A., 1992. The development of ion regulation at the blood-brain barrier. Prog. Brain Res. 91, 123–131.

Jones, H.C., Keep, R.F., 1988. Brain fluid calcium concentration and response to acute hypercalcaemia during development in the rat. J. Physiol. 402, 579–593.

Joris, P., Carney, L., Smith, P., Yin, T., 1994. Enhancement of neural synchronization in the anteroventral cochlear nucleus. I. Responses to tones at the characteristic frequency. J. Neurophysiol. 71, 1022–1036.

Kadner, A., Kulesza, R., Berrebi, A., 2006. Neurons in the medial nucleus of the trapezoid body and superior paraolivary nucleus of the rat may play a role in sound duration coding. J. Neurophysiol. 95, 1499–1508.

Kandaswamy, U., Deng, P.-Y., Stevens, C.F., Klyachko, V.A., 2010. The role of presynaptic dynamics in processing of natural spike trains in hippocampal synapses. J. Neurosci. 30, 15904–15914.

Katz, B., Miledi, R., 1965. The measurement of synaptic delay, and the time course of acetylcholine release at the neuromuscular junction. Proc. R Soc. Lond B. Biol. Sci. 161, 483–495.

Kiang, N. 1965. Discharge patterns of single fibers in the cat's auditory nerve.

Klug, A., Bauer, E., Hanson, J., Pollak, G.D., 2006. Processing of species-specific vocalizations in the auditory brainstem and midbrain of Mexican free tailed bats (*Tadarida brasiliensis*). In: Kanwal, J.S., Ehret, G. (Eds.), Behavior and Neurodynamics for Auditory Communication. Cambridge University Press, Cambridge, pp. 132–155.

Klyachko, V., Stevens, C., 2006. Excitatory and feed-forward inhibitory hippocampal synapses work synergistically as an adaptive filter of natural spike trains. Plos Biol. 4, e207.

Kopp-Scheinpflug, C., Lippe, W.R., Dörrscheidt, G.J., Rübsamen, R., 2003. The medial nucleus of the trapezoid body in the gerbil is more than a relay: comparison of pre- and postsynaptic activity. J. Assoc. Res. Otolaryngol. 4, 1–23.

Korogod, N., Lou, X., Schneggenburger, R., 2005. Presynaptic Ca2+ requirements and developmental regulation of posttetanic potentiation at the calyx of Held. J. Neurosci. 25, 5127–5137.

Kushmerick, C., Renden, R., Von Gersdorff, H., 2006. Physiological temperatures reduce the rate of vesicle pool depletion and short-term depression via an acceleration of vesicle recruitment. J. Neurosci. 26, 1366–1377.

Kushmerick, C., Price, G., Taschenberger, H., Puente, N., Renden, R., Wadiche, J., Duvoisin, R., Grandes, P., Von Gersdorff, H., 2004. Retroinhibition of presynaptic Ca2+ currents by endocannabinoids released via postsynaptic mGluR activation at a calyx synapse. J. Neurosci. 24, 5955–5965.

Lang, T., Jahn, R., 2008. Core proteins of the secretory machinery. Handb Exp. Pharmacol., 107–127.

Lee, J.S., Kim, M.-H., Ho, W.-K., Lee, S.-H., 2008. Presynaptic release probability and readily releasable pool size are regulated by two independent mechanisms during posttetanic potentiation at the calyx of Held synapse. J. Neurosci. 28, 7945–7953.

Liberman, M.C., 1978. Auditory-nerve response from cats raised in a low-noise chamber. J. Acoust. Soc. Am. 63, 442–455.

Liley, A.W., North, K.A., 1953. An electrical investigation of effects of repetitive stimulation on mammalian neuromuscular junction. J. Neurophysiol. 16, 509–527.

LoGiudice, L., Matthews, G., 2007. Endocytosis at ribbon synapses. Traffic 8, 1123–1128.

Lorteije, J.A.M., Rusu, S.I., Kushmerick, C., Borst, J.G.G., 2009. Reliability and precision of the mouse calyx of held synapse. J. Neurosci. 29, 13770–13784.

MacLeod, K.M., Horiuchi, T.K., Carr, C.E., 2007. A role for short-term synaptic facilitation and depression in the processing of intensity information in the auditory brain stem. J. Neurophysiol. 97, 2863–2874.

Mc Laughlin, M., van der Heijden, M., Joris, P.X., 2008. How secure is in vivo synaptic transmission at the calyx of Held? J. Neurosci. 28, 10206–10219.

Meyer, A., Neher, E., Schneggenburger, R., 2001. Estimation of quantal size and number of functional active zones at the calyx of held synapse by nonstationary EPSC variance analysis. J. Neurosci. 21, 7889–7900.

Moore, M.J., Caspary, D.M., 1983. Strychnine blocks binaural inhibition in lateral superior olivary neurons. J. Neurosci. 3, 237–242.

Müller, M., Felmy, F., Schneggenburger, R., 2008. A limited contribution of Ca2+ current facilitation to paired-pulse facilitation of transmitter release at the rat calyx of Held. J. Physiol. 586, 5503–5520.
Müller, M., Goutman, J.D., Kochubey, O., Schneggenburger, R., 2010. Interaction between facilitation and depression at a large CNS synapse reveals mechanisms of short-term plasticity. J. Neurosci. 30, 2007–2016.
Neher, E., Sakaba, T., 2001a. Estimating transmitter release rates from postsynaptic current fluctuations. J. Neurosci. 21, 9638–9654.
Neher, E., Sakaba, T., 2001b. Combining deconvolution and noise analysis for the estimation of transmitter release rates at the calyx of Held. J. Neurosci. 21, 444–461.
Neher, E., Sakaba, T., 2008. Multiple roles of calcium ions in the regulation of neurotransmitter release. Neuron 59, 861–872.
Postlethwaite, M., Hennig, M.H., Steinert, J.R., Graham, B.P., Forsythe, I.D., 2007. Acceleration of AMPA receptor kinetics underlies temperature-dependent changes in synaptic strength at the rat calyx of Held. J. Physiol. 579, 69–84.
Rizzoli, S.O., Betz, W.J., 2005. Synaptic vesicle pools. Nat. Rev. Neurosci. 6, 57–69.
Roberts, W.M., Howard, J., Hudspeth, A.J., 1988. Hair cells: transduction, tuning, and transmission in the inner ear. Annu. Rev. Cell Biol. 4, 63–92.
Sakaba, T., Neher, E., 2001a. Calmodulin mediates rapid recruitment of fast-releasing synaptic vesicles at a calyx-type synapse. Neuron 32, 1119–1131.
Sakaba, T., Neher, E., 2001b. Quantitative relationship between transmitter release and calcium current at the calyx of held synapse. J. Neurosci. 21, 462–476.
Satzler, K., Sohl, L., Bollmann, J., Borst, J., Frotscher, M., Sakmann, B., Lubke, J., 2002. Three-dimensional reconstruction of a calyx of Held and its postsynaptic principal neuron in the medial nucleus of the trapezoid body. J. Neurosci. 22, 10567–10579.
Schneggenburger, R., Neher, E., 2000. Intracellular calcium dependence of transmitter release rates at a fast central synapse. Nature 406, 889–893.
Schneggenburger, R., Neher, E., 2005. Presynaptic calcium and control of vesicle fusion. Curr. Opin. Neurobiol. 15, 266–274.
Schneggenburger, R., Forsythe, I.D., 2006. The calyx of Held. Cell Tissue Res. 326, 311–337.
Schneggenburger, R., Meyer, A., Neher, E., 1999. Released fraction and total size of a pool of immediately available transmitter quanta at a calyx synapse. Neuron 23, 399–409.
Schneggenburger, R., Sakaba, T., Neher, E., 2002. Vesicle pools and short-term synaptic depression: lessons from a large synapse. Trends Neurosci. 25, 206–212.
Schwarz, D., Puil, E., 1997. Firing properties of spherical bushy cells in the anteroventral cochlear nucleus of the gerbil. Hear Res. 114, 127–138.
Smith, P.H., Joris, P.X., Yin, T.C., 1998. Anatomy and physiology of principal cells of the medial nucleus of the trapezoid body (MNTB) of the cat. J. Neurophysiol. 79, 3127–3142.
Smith, S.M., Renden, R., Von Gersdorff, H., 2008. Synaptic vesicle endocytosis: fast and slow modes of membrane retrieval. Trends Neurosci. 31, 559–568.
Sommer, I., Lingenhöhl, K., Friauf, E., 1993. Principal cells of the rat medial nucleus of the trapezoid body: an intracellular in vivo study of their physiology and morphology. Exp. Brain Res. Exp. Hirnforschung Exp. Cérébrale 95, 223–239.
Spangler, K., Warr, W., Henkel, C., 1985. The projections of principal cells of the medial nucleus of the trapezoid body in the cat. J. Comp. Neurol. 238, 249–262.
Spirou, G., Brownell, W., Zidanic, M., 1990. Recordings from cat trapezoid body and HRP labeling of globular bushy cell axons. J. Neurophysiol. 63, 1169–1190.
Spirou, G.A., Rager, J., Manis, P.B., 2005. Convergence of auditory-nerve fiber projections onto globular bushy cells. Neuroscience 136, 843–863.
Südhof, T.C., Petrenko, A.G., Whittaker, V.P., Jahn, R., 1993. Molecular approaches to synaptic vesicle exocytosis. Prog. Brain Res. 98, 235–240.
Sun, J., Wu, L., 2001. Fast kinetics of exocytosis revealed by simultaneous measurements of presynaptic capacitance and postsynaptic currents at a central synapse. Neuron 30, 171–182.
Taschenberger, H., Von Gersdorff, H., 2000. Fine-tuning an auditory synapse for speed and fidelity: developmental changes in presynaptic waveform, EPSC kinetics, and synaptic plasticity. J. Neurosci. 20, 9162–9173.
Taschenberger, H., Leao, R., Rowland, K., Spirou, G., Von Gersdorff, H., 2002. Optimizing synaptic architecture and efficiency for high-frequency transmission. Neuron 36, 1127–1143.
Trommershäuser, J., Schneggenburger, R., Zippelius, A., Neher, E., 2003. Heterogeneous presynaptic release probabilities: functional relevance for short-term plasticity. Biophys. J. 84, 1563–1579.
Trussell, L., 2002. Modulation of transmitter release at giant synapses of the auditory system. Curr. Opin. Neurobiol. 12, 400–404.
Trussell, L.O., 1999. Synaptic mechanisms for coding timing in auditory neurons. Annu. Rev. Physiol. 61, 477–496.
Trussell, L.O., Fischbach, G.D., 1989. Glutamate receptor desensitization and its role in synaptic transmission. Neuron 3, 209–218.
Trussell, L.O., Thio, L.L., Zorumski, C.F., Fischbach, G.D., 1988. Rapid desensitization of glutamate receptors in vertebrate central neurons. Proc. Natl. Acad. Sci. U S A 85, 4562–4566.
Tsujimoto, T., Jeromin, A., Saitoh, N., Roder, J., Takahashi, T., 2002. Neuronal calcium sensor 1 and activity-dependent facilitation of P/Q-type calcium currents at presynaptic nerve terminals. Science 295, 2276–2279.
Von Gersdorff, H., Borst, J., 2002. Short-term plasticity at the calyx of held. Nat. Rev. Neurosci. 3, 53–64.
Von Gersdorff, H., Schneggenburger, R., Weis, S., Neher, E., 1997. Presynaptic depression at a calyx synapse: the small contribution of metabotropic glutamate receptors. J. Neurosci. 17, 8137–8146.
Wang, L.Y., Kaczmarek, L.K., 1998. High-frequency firing helps replenish the readily releasable pool of synaptic vesicles. Nature 394, 384–388.
Wang, Y., Manis, P.B., 2008. Short-term synaptic depression and recovery at the mature mammalian endbulb of Held synapse in mice. J. Neurophysiol. 100, 1255–1264.
Wang, Y., Ren, C., Manis, P.B., 2010. Endbulb synaptic depression within the range of presynaptic spontaneous firing and its impact on the firing reliability of cochlear nucleus bushy neurons. Hear Res. 270, 101–109.
Weis, S., Schneggenburger, R., Neher, E., 1999. Properties of a model of Ca(++)-dependent vesicle pool dynamics and short-term synaptic depression. Biophys. J. 77, 2418–2429.
Wilkinson, R., Lin, M., 2004. Endocytosis and synaptic plasticity: might the tail wag the dog? Trends Neurosci. 27, 171–174.
Wong, A.Y.C., Graham, B.P., Billups, B., Forsythe, I.D., 2003. Distinguishing between presynaptic and postsynaptic mechanisms of short-term depression during action potential trains. J. Neurosci. 23, 4868–4877.
Wu, L., Borst, J., 1999. The reduced release probability of releasable vesicles during recovery from short-term synaptic depression. Neuron 23, 821–832.
Wu, S., Kelly, J., 1993. Response of neurons in the lateral superior olive and medial nucleus of the trapezoid body to repetitive stimulation: intracellular and extracellular recordings from mouse brain slice. Hear Res. 68, 189–201.
Xue, L., Wu, L.-G., 2010. Post-tetanic potentiation is caused by two signaling mechanisms affecting quantal size and quantal content. J. Physiol..
Yost, W., Popper, A., Fay, R., 2008. In: Popper, A.N., Fay, R.R. (Eds.), Auditory Perception of Sound Sources, Springer Handbook of Auditory Research, vol. 29. Springer Verlag, New York.

J Neurophysiol 101: 20–30, 2009.
First published October 29, 2008; doi:10.1152/jn.90243.2008.

Modeling Short-Term Synaptic Plasticity at the Calyx of Held Using In Vivo-Like Stimulation Patterns

Joachim Hermann, Benedikt Grothe, and Achim Klug
Ludwig-Maximilians-University Munich, Munich, Germany

Submitted 6 February 2008; accepted in final form 18 October 2008

Hermann J, Grothe B, Klug A. Modeling short-term synaptic plasticity at the calyx of Held using in vivo-like stimulation patterns. *J Neurophysiol* 101: 20–30, 2009. First published October 29, 2008; doi:10.1152/jn.90243.2008. We measured synaptic responses to complex stimulus trains in the calyx of Held and used the data to test how well several vesicle-release models could capture the observed dynamics. We tested stimulation protocols consisting of Poisson-distributed activity with periodically changing mean frequencies, trains with constant inter spike intervals, and stimulus trains derived from in vivo responses to natural sounds. All stimuli were embedded in chronic background activity attempting to imitate the naturally occurring spontaneous activity in the auditory brain stem. We found that already the most basic model variant produced very good results, exhibiting very high correlation coefficients between the experimental data and the model predictions. None of the more complex model variants, which incorporated receptor desensitization, synaptic facilitation, and double-exponential recovery from depression, showed improved data-prediction matching accuracy. These findings are in contrast to previous modeling work performed in nonchronically active synapses, where the inclusion of additional physiological parameters into the modeling process tended to result in models with higher accuracy. Our findings suggest that the functional state of chronically active calyces may differ from the functional state of silent calyces and that this functional state of chronically active synapses can be described in relatively simple terms.

INTRODUCTION

The short-term dynamics of synaptic transmission under various activity levels have been modeled in a number of synapses (Abbott et al. 1997; Gundlfinger et al. 2007; Markram and Tsodyks 1996; Tsodyks et al. 1998), among them the calyx of Held in the auditory brain stem. Basic features of most of these models are the vesicle release from a readily releasable vesicle pool as well as a pool size-dependent vesicle recovery (Weis et al. 1999). Beyond these basic features, additional effects have been incorporated, for example, calcium-dependent facilitation (Varela et al. 1997) or postsynaptic receptor desensitization (Graham et al. 2004). These physiological effects of short-term plasticity have been demonstrated to shape synaptic transmission at the calyx of Held, thus the inclusion of them into the modeling process are supposed to yield more accurate models with higher predictive power, as was observed by those investigators.

However, the modeling studies mentioned in the preceding text were based on data recorded from in vitro brain slice preparations. In the case of the calyx of Held, these preparations lack the chronic background spontaneous activity that calyces experience in the intact brain (Irvine 1992; Kadner et al. 2006; Kopp-Scheinpflug et al. 2003; Smith et al. 1998; Sommer et al. 1993). This spontaneous activity is a common feature in the nervous system, and one of the hallmarks of neurons in the auditory brain stem. On average, it evokes firing rates of ~25 Hz at the calyx of Held in gerbils. Indeed, calyces in brain slice preparations lacking this chronic activity differ in a number of physiological properties of synaptic transmission, such as baseline synaptic amplitudes, depression during high-frequency stimulation, recovery from depression, or transmission fidelity (Hermann et al. 2007).

The focus of the present study was to find the model variant that would capture transmission at the calyx of Held during typical in vivo activity levels. Rather than including all known parameters of short-term plasticity into the model, our approach was to evaluate different models incorporating different physiological effects and to test how well each one of these variants could predict neural responses to the complex stimulation patterns used in the study. To imitate naturally occurring activity as closely as possible, all presented stimuli were embedded in chronic background activity resembling the spontaneous activity present in the intact brain. The embedded test stimuli incorporated a large amount of statistical complexity and, in some cases, were derived from auditory responses to sound clips. Different variations of the basic model were used to predict the synaptic currents produced by a given calyx of Held to these stimuli, and these predictions were compared with the neuron's actual responses as determined through voltage-clamp recordings from gerbil brain slice preparations.

METHODS

Slice preparation

Coronal slices of brain stem were prepared from Mongolian gerbils (*Meriones uniguiculatus*) aged 15–19 days old. Animals were briefly anesthetized by isoflurane inhalation (Isofluran Curamed, Curamed Pharma) and decapitated. The brain stem was dissected out under ice-cold dissection Ringer [containing (in mM) 125 NaCl, 2.5 KCl, 1 $MgCl_2$, 0.1 $CaCl_2$, 25 glucose, 1.25 NaH_2PO_4, 25 $NaHCO_3$, 0.4 ascorbic acid, 3 myo-inositol, and 2 pyruvic acid; all chemicals from Sigma]. Sections of 180–200 μm were cut with a vibratome (VT100S, Leica). Slices were transferred to an incubation chamber containing extracellular solution [ECS; containing (in mM) 125 NaCl, 2.5 KCl, 1 $MgCl_2$, 2 $CaCl_2$, 25 glucose, 1.25 NaH_2PO_4, 25 $NaHCO_3$, 0.4 ascorbic acid, 3 myo-inositol, and 2 pyruvic acid, all chemicals from Sigma] and bubbled with 5% CO_2-95% O_2. Slices were incubated for 30 min at 37°C, after which the chamber was brought to room temperature. Recordings were obtained within 4–5 h of slicing.

Address for reprint requests and other correspondence: A. Klug, Neurobiology Group—Dept. of Biology II, Grosshaderner Strasse 2, 82152 Martinsried Germany (E-mail: achim.klug@lmu.de).

The costs of publication of this article were defrayed in part by the payment of page charges. The article must therefore be hereby marked "*advertisement*" in accordance with 18 U.S.C. Section 1734 solely to indicate this fact.

Whole cell recordings

All recordings were performed at 36–37°C. After incubation, slices were transferred to a recording chamber and continuously superfused with ECS at 3–4 ml/min through a gravity-fed perfusion system. Medial Nucleus of the trapezoid body (MNTB) neurons were viewed through a Zeiss Axioskop 2 FS microscope equipped with DIC optics and a ×40 water-immersion objective (Zeiss). Whole cell voltage-clamp recordings were made with an EPC 10 double amplifier (HEKA Instruments), the holding potential was −60 mV, Signals were filtered at 10 kHz and subsequently digitized at 50 kHz using Patchmaster Version 2.02 software (HEKA Instruments). Uncompensated series resistance was 9.7 ± 1.1 MΩ (mean ± SE) and was compensated to 1.8 ± 0.3 MΩ with a lag time of 10 μs. Potential changes in series resistance were monitored throughout the recordings and data collection was discontinued whenever uncompensated series resistance changed by >2 MΩ.

Patch pipettes were pulled from 1.5 mm borosilicate glass (Harvard Instruments) using a DMZ Universal Puller (Zeitz Instruments). Pipettes were filled with cesium-methanesulfonate-based solution [containing (in mM) 125 $CsMeSo_3$, 4.5 $MgCl_2$, 9 HEPES, 5 EGTA, 14 tris-phosphocreatine, 4 Na_2-ATP, 0.3 tris-GTP, and 1.5 $CaCl_2$, all chemicals from Sigma].

Strychnine hydrochloride (500 nM; Sigma) was added to the bath to block glycinergic inhibition, and 5 mM QX-314 (Alomone Labs) was added to the pipette fill to eliminate sodium currents.

Stimulation of synaptic inputs

Synaptic currents were elicited by midline stimulation of the calyceal input fiber bundle with a 5 MΩ bipolar stimulation electrode (matrix electrodes with 270 μm distance, Frederic Haer). Stimuli were 100-μs-long square pulses with a constant voltage 10 V above the stimulation threshold (10–40 V) delivered with a STG 2004 computer-controlled four-channel stimulator (Multichannel Systems) and a stimulation isolation unit (Iso-Flex, AMPI). Due to the long stimulation durations (≤10 min), some cells showed stimulation failures, i.e., they did not show an excitatory postsynaptic current (EPSC) after the stimulation artifact. In cases where cells showed >5% failures they were removed from further analysis.

Data analysis and vesicle release model

All data analyses were done with Igor Pro 5.05A (WaveMetrics) and Matlab 6.5 (The Mathworks). Unless stated otherwise, values are always provided with the standard error. To assess the short-term dynamics of synaptic currents, a vesicle release model was implemented and fitted to the experimental data. The model was first described independently by Tsodyks and Markram (1997) and Abbott et al. (1997) and has since been repeatedly used by various investigators. The model can be divided into two parts, the reduction of the pool of available neurotransmitter at the time point of a synaptic event and the recovery of the pool in between release events. The dynamically changing size of the pool is characterized by $I(t)$ which is a measure of the synaptic current produced by all available neurotransmitter vesicles in the pool. The reduction is regarded as an instantaneous event described by

$$I_{\text{after}} = I_{\text{before}} \cdot (1 - P_R) \tag{1}$$

with a constant release probability P_R. The "after" and "before" subscripts refer to the immediate times before and after the arrival of the action potential. The recovery process follows the differential equation:

$$\frac{dI}{dt} = \frac{I_0 - I}{\tau} \tag{2}$$

where I_0 is the synaptic current created by the amount of neurotransmitter vesicles in case of a fully recovered functional vesicle pool, and τ is the recovery time constant. Solving the differential equation and combining it with *Eq. 1* leads to an iterative form that can be used to calculate the amount of vesicles available at the synaptic event n based on values calculated for event $n - 1$ as follows

$$I_n = I_0 - [I_0 - I_{n-1}(1 - P_R)] \cdot \exp\left(\frac{-(t_n - t_{n-1})}{\tau}\right) \tag{3}$$

The synaptic current i_n is produced by a fraction of the available vesicles: $i_n = P_R \cdot I_n$. This value was compared with the experimentally measured EPSC amplitudes. The model has three free parameters, namely P_R, τ, and I_0. To calculate the optimal parameter set, the squared error

$$\frac{1}{N}\sum_{n=1}^{N} \Delta i_n^2 = \frac{1}{N}\sum_{n=1}^{N} (i_n \text{ (experiment)} - i_n \text{ (model)})^2 \tag{4}$$

was minimized using the downhill simplex method (Nelder and Mead 1965).

Model variants

To account for additional influences on short-term dynamics of synaptic currents, three variants of the vesicle release model were implemented. In the first variant, the single-exponential recovery was replaced by a double-exponential time course (Wang and Kaczmarek 1998)

$$\frac{dI}{dt} = \frac{I_0^{\text{fast}} - I}{\tau_{\text{fast}}} + \frac{I_0^{\text{slow}} - I}{\tau_{\text{slow}}} \tag{5}$$

For the second extension, synaptic facilitation was included (Varela et al. 1997). The release probability was raised for every synaptic event by the factor $F \cdot (1 - P_R)$ to restrict the release probability to values smaller than 1. In between events it decayed with the characteristic time constant τ_R back to its minimum value $P_R^{\min}$

$$\frac{dP_R}{dt} = -\frac{P_R^{\min} - P_R}{\tau_R} \tag{6}$$

In the third variant an additional factor $R(t)$ representing receptor desensitization was included (Graham et al. 2004)

$$i_n = P_R \cdot I_n \cdot R(t) \tag{7}$$

$R(t)$ was raised for every synaptic event by the factor $D \cdot (I_n/I_0)$ where D defines the percentage of receptors that desensitize for each synaptic event. Between events, $R(t)$ recovers with a characteristic time constant τ_D

$$\frac{dR}{dt} = -\frac{1 - R}{\tau_D} \tag{8}$$

Because the model variants affect distinct parts of the basic model, the extensions can also be combined. For all three variants and their combinations, the additional free parameters were included into the parameter optimization and the squared error was minimized similar to the simple model.

Model predictions

For stimulation patterns with regular inter pulse intervals, the steady-state amplitude I^* can be calculated as a function of the stimulation frequency, f, and the time constant, τ_A, which describes the exponential time course from any initial amplitude to the steady

state. To calculate these two values, the iterative formula for I_n can be rewritten as

$$I_n = a + b \cdot I_{n-1} \quad (9)$$

with a and b representing the more complex terms from the original equation describing the basic model

$$a = I_0 - I_0 \cdot \exp\left(\frac{-(t_n - t_{n-1})}{\tau}\right) \quad (10)$$

$$b = (1 - P_R) \cdot \exp\left(\frac{-(t_n - t_{n-1})}{\tau}\right) \quad (11)$$

The steady-state amplitude can be calculated by equating the currents at event n and event $n - 1$

$$I^* = \frac{a}{1 - b} = I_0 - \frac{I_0 \cdot P_R}{\exp[1/(f \cdot \tau)] - 1 + P_R} \quad (12)$$

The interpulse interval $t_n - t_{n-1}$ has been replaced with the inverse of the stimulation frequency $1/f$. Multiplying I^* with the release probability P_R gives an estimate for the steady-state EPSC which can be compared with experimental values.

To calculate the time constant τ_A, the deviation from the steady-state J_n is defined as follows

$$J_n = I_n - I^* \quad (13)$$

Now the resulting iterative equation $J_n = b \cdot J_{n-1}$ can be solved in a noniterative way

$$J_n = b^n \cdot J_0 \quad (14)$$

By replacing n with $t/\Delta t$ and J with I, one can obtain an explicit solution of this equation

$$I(t) = I^* + \exp\left(\frac{\ln b}{\Delta t} \cdot t\right) \cdot J_0 \quad (15)$$

The characteristic time constant can now be extracted from the exponent and results in

$$\tau_A = -\frac{\Delta t}{\ln b} = -\frac{\Delta t}{\ln(1 - P_R) - \Delta t/\tau} = \frac{1}{1/\tau - f \cdot \ln(1 - P_R)} \quad (16)$$

RESULTS

The central goal of this study was to model the short-term synaptic dynamics at the calyx of Held in response to highly complex stimulation patterns. Furthermore, we wanted to investigate the synaptic dynamics under conditions mimicking the in vivo situation of chronically active synapses as closely as possible. We therefore embedded our various stimulation protocols in spontaneous background activity mimicking the naturally occurring spontaneous firing of cells in the auditory brain stem. As we have shown previously (Hermann et al. 2007), this activity causes several changes in the properties of synaptic transmission, mainly a significant decrease in synaptic strength and a decrease of synaptic depression in response to high-frequency stimulation. Here we used a Poisson distributed pulse train with a mean frequency of 20 Hz to simulate spontaneous background activity. Neurons were initially stimulated with this background activity for ≥2 min to "condition" the synapses. During this conditioning period, the synapses reached a new steady state with significantly lower synaptic currents (Hermann et al. 2007). We term this condition the "in-vivo-like rested state" of the synapse because we assume that in vivo calyces of Held are in this state in the absence of any sound stimulation. All other stimulations used in the present study were embedded in this background activity, and the change between stimulus and background was gapless, guaranteeing a true embedding of the recorded stimulus. This experimental design attempts to imitate the in vivo situation, in which periods of sound stimulation are embedded in the naturally occurring spontaneous activity. The mean initial synaptic strength of all cells measured as the EPSC in voltage-clamp experiments was 12.2 ± 1.2 nA ($n = 16$). During the 2 min of conditioning with the 20-Hz Poisson train, this value dropped to 4.1 ± 0.6 nA, corresponding to a decrease to 34% of the initial amplitude.

Poisson-distributed test trains

The first set of test stimuli consisted of Poisson distributed trains with varying mean frequencies. The stimulus consisted of 34 segments and had alternating periods of low and high activity levels as depicted in Fig. 1*A*. Each one of these 34 periods had a given mean frequency, which was applied for a brief time period and then changed at the beginning of the next segment of the stimulus train. The distribution of single events within these periods was Poisson with the exception that interpulse intervals <1 ms were not used. The low activity periods had mean frequencies ranging from 5 to 50 Hz, whereas the high activity periods had mean frequencies between 100 and 350 Hz. The entire stimulus was 30 s long and consisted of 1,201 stimulations.

We had two motivations to choose this particular type of stimulation. First, this stimulation protocol is highly complex and is made of many very different sequences of inter pulse intervals. Therefore it is possible to obtain a lot of information about synaptic dynamics with this stimulus. Second, it covers the full range of frequencies experienced by MNTB cells in an intact brain. A normal Poisson train with a fixed mean frequency could, for example, not account for longer periods of low activity reflecting silence and at the same time mimic sound input that would result in high activity. Therefore a pattern with varying mean frequencies reflects naturally occurring auditory activity closer.

For each neuron, experiments were started by conditioning the synapse to background activity for ≥2 min with the 20-Hz Poisson stimulus described in the preceding text. Next, the Poisson test train with varying mean frequencies described here was played to calyces, embedded into the 20-Hz background activity and repeated four times wherever possible. An example of a single voltage-clamp trace of recorded EPSCs is shown in Fig. 1*B*. EPSC amplitudes were extracted and the mean amplitudes were calculated from the four repetitions. The grey area in Fig. 1*C* indicates the maximum and minimum EPSC measured over the four repetitions.

Next, the EPSC amplitudes were modeled using the basic variant of our prediction model. The black line in Fig. 1*C* corresponds to the model prediction. The EPSC amplitudes predicted by the model were fit against the mean amplitudes calculated from the four repetitions. For most events, the prediction falls inside the grey area depicted in Fig. 1*C*,

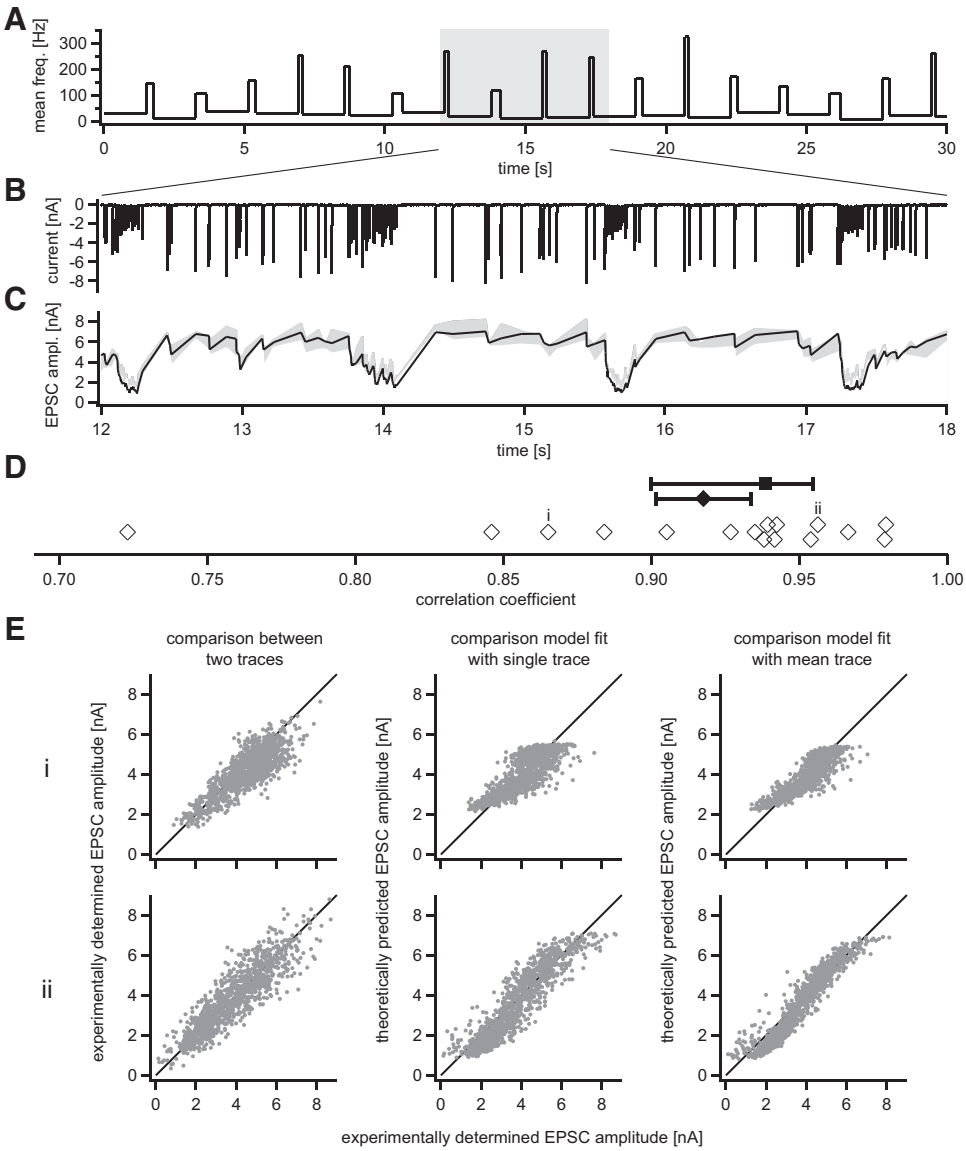

FIG. 1. *A*: time course of the 1st stimulation protocol. The graph represents the mean frequencies of the pulse trains. The single events in each period are Poisson distributed. The low-frequency segments have durations of 2 s each, the high-frequency segments consist of 50 stimulation events each. *B*: clip of a voltage clamp trace of an excitatory postsynaptic current (EPSC) train recorded from a neuron that was stimulated with the train described in *A*. The trace represents 1 single recording. In this and all other figures showing data traces, stimulation artifacts were blanked for clarity. *C*: EPSC amplitudes extracted from the data trace shown above. Presented are data from 4 repetitions of the same stimulus. Gray area indicates the maximum and minimum amplitude recorded among the 4 repetitions. Black line represents the predicted EPSC amplitudes to the same stimulus train calculated by the basic vesicle release model. *D*: distribution of correlation coefficients. Open diamonds show the correlation coefficients between the mean over 4 recordings and the corresponding model predictions for each one of the 16 neurons. The closed diamond is the mean correlation coefficient over all 16 neurons with its SE; closed square is the median with the interpolated 0.25 and 0.75 percentile. *E*: scatter plots comparing EPSC amplitudes of the same 2 neurons (i and ii) under various conditions. *Left*: the correlation between 2 single recordings of the same stimulus from the same cell, the scatter indicates the variation between the 2 trials. *Middle*: the correlation between data from a single trial (i.e., a single trace) and the corresponding model fit. The *x* axis plots the EPSC amplitudes recorded in voltage clamp, the *y* axis plots the amplitude computed by the model. The 2 scatter plots in the *right column* plot the comparison between the mean over 4 traces and the corresponding model prediction.

indicating that the model prediction was in the range of the naturally occurring amplitude variations. To quantify the quality of our predictions, we calculated the correlation coefficient between the predicted and corresponding measured amplitudes. Figure 1*D* shows the correlation coefficients of all 16 neurons that were tested in this way. The majority of cells show a correlation coefficient of >0.9, indicating a very high fit quality. The mean correlation coefficient over the 16 cells was 0.918 ± 0.017, the median was 0.94.

For two example cells (indicated by "i" and "ii" in Fig. 1*D*), the quality of fits is further illustrated with a set of correlation plots, shown in Fig. 1*E*. The two plots on the left show a comparison between two consecutive recordings of the same stimulation pattern for each one of the two neurons. For a perfect match, i.e., perfect repeatability, all points would fall on the black diagonal line. The deviations from this line demonstrate the degree of variability between individual trials. For each neuron in our sample, we compared the EPSC amplitudes from the four individual stimulus repetitions to each other (6 comparisons per neuron) and calculated the average correlation coefficient for each neuron (0.603 ± 0.012 to 0.961 ± 0.002, $n = 16$). The average correlation coefficient for all 16 neurons was 0.880 ± 0.019.

The two *middle plots* in Fig. 1*E* show the comparison between single EPSC traces and corresponding model prediction for the two sample neurons. The distribution of points is very similar to the *left plot.* Among our sample of neurons, the average correlation coefficient obtained by correlating data from each one of the four single traces with the corresponding model prediction was 0.884 ± 0.018 (4 comparisons per neuron, value for individual cells varied between 0.749 ± 0.012 and 0.955 ± 0.004, $n = 16$). These values are almost identical to the average correlation coefficient obtained by correlating single traces with each other, suggesting that the accuracy of predictions provided by our model was near maximal and that the remaining inaccuracies in the predictions were mainly due to biological noise. The two plots on the *right* compare the mean EPSCs calculated over four repetitions to the corresponding model predictions. The spread of points is smaller than in the other cases. As stated in the preceding text, the average correlation coefficient obtained by comparing model predictions to the average EPSC amplitude was 0.918 ±

0.017 and thus higher than in the cases described in the preceding text. Presumably, by averaging over four repetitions, the biological variability was reduced partially, with the result that the model predictions improved somewhat. The remaining prediction errors might be reduced even further with more repetitions. These data suggest that overall, the predictions obtained with our relatively simple model were quite good, and errors were almost within the range of biological variation. However, note that some of the graphs in Fig. 1*E* (*middle* and *right*) reveal a very slight S-shaped distribution of points in both the single trace as well as the average trace fits. This S-shape was seen for most of the recorded cells and indicates a (small) systematic prediction error of the model, with an underestimation of small and very large amplitudes and an overestimation of medium amplitudes.

Model variants

Although the simple vesicle release model already provided a very accurate description of synaptic short-term dynamics at the chronically active calyx of Held, some systematic deviations remained. This may not be surprising, as a large number of effects of short-term plasticity have been shown to influence synaptic strength. Some of them were incorporated in previous models, for example synaptic facilitation caused by an increase in calcium concentration (Varela et al. 1997), or postsynaptic receptor desensitization (Graham et al. 2004). The single-exponential time course for vesicle recovery that we assume in our basic model has long been replaced by a double-exponential recovery reflecting two populations of vesicles (Sakaba and Neher 2001; Wang and Kaczmarek 1998).

Therefore we wanted to investigate next how additional degrees of freedom introduced by new parameters improve the model predictions. We chose three extensions, namely a variant with a double-exponential recovery, one with added facilitation, and one which accounts for receptor desensitization (details see METHODS). Figure 2*A* shows a short clip of recorded EPSC amplitudes and corresponding predictions obtained with the different model variants. The experimental data, shown in black, is represented as the average of four repetitions of the same stimulus pattern recorded from a single cell. The predictions obtained with the basic model are shown in gray; the colored traces represent predictions obtained with the three model variants. Generally, the differences between the individual model predictions were rather small. To quantify these differences, we plotted the model predictions of the different variants against the experimentally measured values. Figure 2*B* shows these correlation graphs for the same cell as shown in *A*. A summary of the correlation coefficients between predictions and experimental data of all 16 neurons tested with various models is shown in *C*. The data suggest that the model improvements do not yield better predictions as the correlation coefficients obtained with the various models are almost the same. Also the shape of the correlation plots does not change in any obvious way. Finally we tested combinations of model improvements. For example, we tested a combination of receptor desensitization and double-exponential recovery, which neither resulted in higher correlation coefficients, nor an elimination of the systematic deviations shown in Fig. 1*E* (data not shown).

In all variants of the model, the parameters were not restricted to certain ranges, and all parameters were optimized to generate a model output with the smallest possible squared error as defined earlier. This strategy yielded parameters, which did not change significantly in the four different scenar-

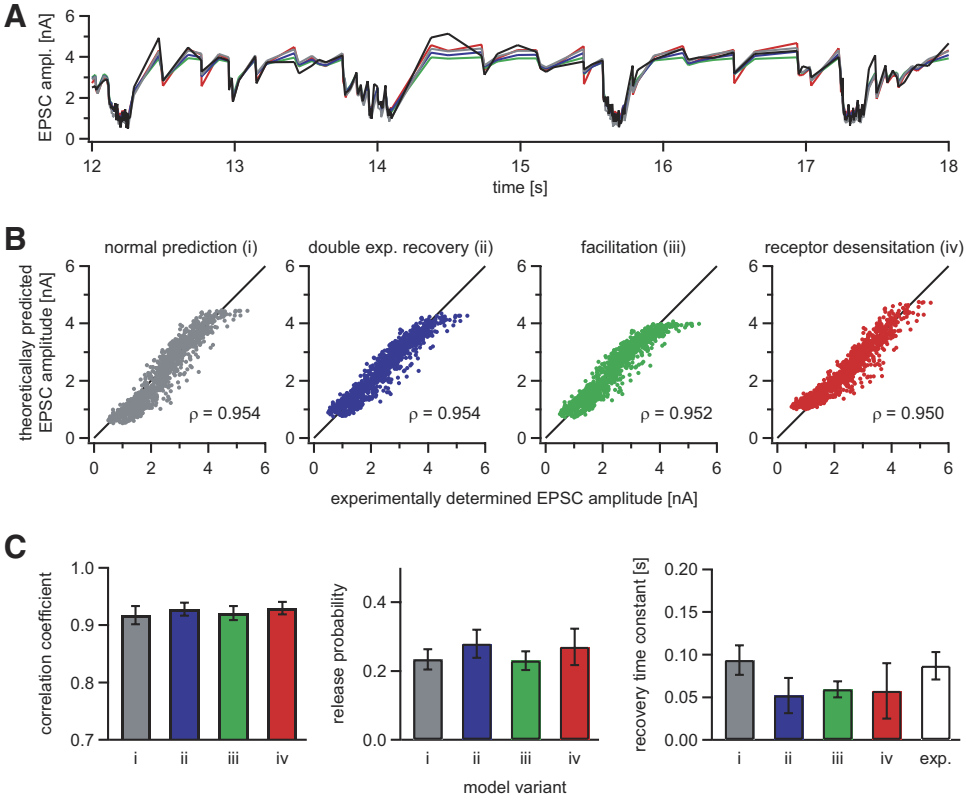

FIG. 2. *A*: a short clip of data showing the development of EPSC amplitudes over time. Black line indicates the mean amplitude measured over 4 repetitions. The different model variants are color coded as explained in *B*. *B*: scatter plots comparing predictions computed by the different model variants to actual recorded EPSC amplitudes. The correlation coefficients are noted in the bottom right corner of each graph. *C*: summary results for all 16 neurons. The first graph shows the average correlation coefficients achieved by each one of the 4 model variants, the color code is the same as above. The two other bargraphs compare the release probability and the recovery time constant, respectively. For the recovery time constant an independently determined value is added for comparison (□).

ios. Summary plots of these parameters, namely correlation coefficient, release probability, and recovery time constant are plotted in Fig. 2*C*. In case of the double-exponential recovery, the fast component of the recovery time course is plotted in Fig. 2*C* (*right*). The slow component is infinitely long in some cases ($>10^{10}$ s, 5 of 16 neurons) or has nearly the same value as the fast component (± 1 SD, 8 of 16 neurons). In the remaining 3/16 neurons, the slow component assumed independent values. However, in these cases the combination of slow and associated fast component yielded almost identical results as the fast component by itself in the corresponding model variant with single-exponential recovery. It appears that in these cases, the number of degrees of freedom in the data were smaller than the number of parameters in the fit and therefore one particular situation could be described by several parameter combinations. All three possibilities lead to the conclusion that the slow component of the recovery was not necessary for an accurate description of the experimental data set. One reason may be that values for the slow component are typically in the range of several seconds (von Gersdorff et al. 1997; Wang and Kaczmarek 1998; Wu and Borst 1999), while the largest interpulse intervals in all our stimulation protocols are in the sub second range. For the model with variable release probability (i.e., the model including synaptic facilitation), the minimal release probability is plotted in Fig. 2*C* (*middle*). In this model variant, either the parameter increasing the release probability is infinitely small or the recovery time course of the changing release probability is infinitely fast, depending on the seed values used (16 of 16 cells). Again, both possibilities lead to the conclusion that a variable release probability is not important for accurate predictions with our modeling approach. Receptor desensitization is a postsynaptic effect and is therefore not influencing the basic model parameters but rather altering the output of the basic model. The time courses describing the receptor desensitization for the neurons are either in a range similar to the single-exponential recovery from depression and thus cannot be distinguished from it (14 of 16 neurons) or infinitely short (2 of 16 neurons). All the results described in the preceding text suggest that none of the model extensions yielded useful results and that the parameter space of the basic model variant could capture the variability in our data set best.

Both release probability and recovery time constant, as determined by our model, are very similar to values that have been obtained from experimental data. The release probability has been measured, for example in the rat MNTB (Schneggenburger et al. 1999; Wu and Borst 1999), and determined to be ~0.2. The recovery time constant in the gerbil MNTB has been determined in our previous paper (Hermann et al. 2007) under similar experimental conditions and is plotted in Fig. 2*C* next to the modeling results for comparison. The close agreement of our modeling results with previous experimental results suggests that the parameters calculated by the model are the computational equivalents to the corresponding physiological phenomena.

Stimulation with trains consisting of regularly spaced intervals

One important feature of the firing pattern of auditory brain stem neurons is phase locking. For certain acoustic inputs, especially pure tones of low frequencies, cells fire with high temporal precision and phase lock to certain parts of the sound wave. This is especially true for MNTB neurons, which have a number of cellular specializations for temporal precision (Forsythe et al. 1998; Smith et al. 1998; Taschenberger and von Gersdorff 2000; Taschenberger et al. 2002; von Gersdorff and Borst 2002). Phase locking results in a very regular firing pattern not reflected by our Poisson distributed spike trains. Therefore we also tested the effects of regular spike trains with varying frequencies. Different frequencies were all tested in a single stimulus, which consisted of various segments with low and high frequencies. Each frequency segment consisted of 20 stimuli and was immediately followed by a segment of 20 stimuli at a different frequency (Fig. 3*A*). The different train frequencies were chosen to imitate sound stimuli at various frequencies. Within the train, each switch from a low to a high frequency was matched by a corresponding switch from a high to a low frequency. Note that the frequencies in Fig. 3*A* are plotted against stimulus number, not time. Figure 3*B* shows a short clip of the complete stimulus plotted against time (*top*), and a clip of the corresponding voltage-clamp trace from a sample cell (*B, bottom*). The segments marked by "i" and "ii" are shown at a magnified scale in Fig. 3, *C* and *D* (mean over 3 repetitions). Please note that Fig. 3*C* represents a high-frequency train (196 Hz), whereas *D* represents a low-frequency train (45 Hz) at a different time scale. For comparison, clips of the two trains plotted at the same time scale are shown in the gray insets of Fig. 3, *C* and *D*. To evaluate the data, the 20 EPSC amplitudes of each constant frequency period were extracted and plotted against time (Fig. 3, *C* and *D, bottom*). We then fitted the data points with a single-exponential function (solid line in *C* and *D, bottom*).

Besides mimicking phase-locked acoustic input, trains with regular stimulation patterns allow for the measurement of steady-state amplitudes and single-exponential time courses leading to these steady states. These two values are frequency dependent and characteristic for each synapse. In our case, predicting a neuron's response to a train with regularly spaced intervals with the vesicle release model allowed us to not only test the accuracy of the predicted EPSC amplitudes but also the accuracy of the predicted steady-state amplitudes as well as the dynamics of adjusting to it. We did this by obtaining a data set with Poisson trains as well as a data set with regularly spaced trains from each cell that was tested with this protocol. The Poisson data were used to fit the basic model and calculate the model parameters as described in the preceding text. Then the obtained parameters were used to calculate predictions for the steady-state amplitude I^* as well as for the time course of adaptation to this steady state characterized by the time constant τ_A. These two values were then compared with the parameters for the exponential fits of the experimental data. The steady-state amplitude I^* corresponds to the offset of the exponential fit, and the time constant τ_A corresponds to the characteristic time constant of the exponential fit. Figure 3*E* shows, for the same cell, the comparison of the steady-state amplitudes for various frequencies; the gray line corresponds to the model prediction, the black diamonds to the experimentally determined amplitudes. The time constants were plotted in a similar fashion in Fig. 3*F* for $\geq$150 Hz. For lower frequencies, time constants were not determined for the following reason: The experimental approach used exponential

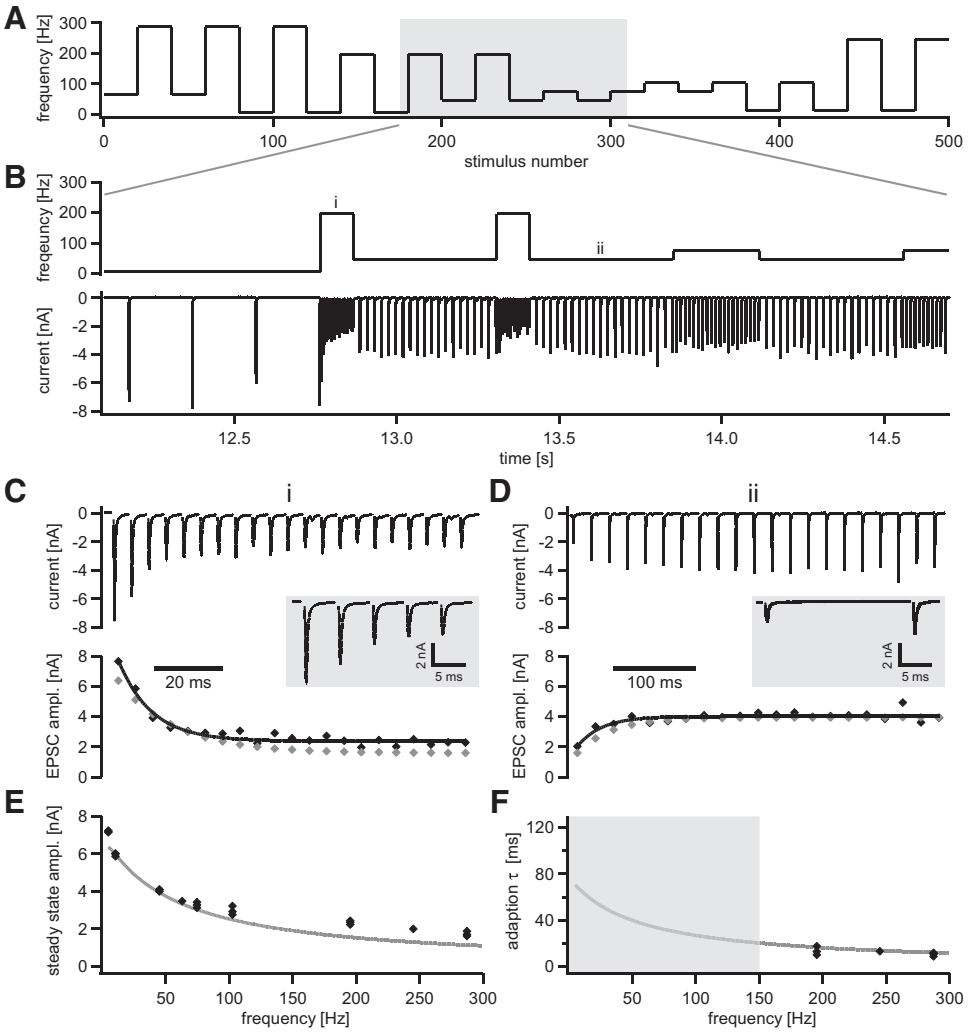

FIG. 3. *A*: time course of the 2nd stimulation protocol, plotted against stimulus number not time. Each period consists of 20 stimulations with constant interpulse intervals corresponding to the indicated frequency. Frequencies are randomly distributed and range from 5 up to 300 Hz. *B*: a short clip of the *top trace* plotted against time for comparison to the raw data trace below. The raw data are the mean over 3 repetitions of a voltage clamp recording. *C* and *D*: detailed views of 2 sample constant frequency periods. Note that the traces are plotted against different time axes; the gray insets compare the initial parts of the same trains on identical time scales. The graphs below show the extracted EPSCs plotted as black diamonds and the corresponding model predictions plotted as gray diamonds. The black lines represent single-exponential fits to the data shown by the black diamonds. *E*: summary of the steady-state amplitudes for all frequencies. The black diamonds represent the offset of the single-exponential fit shown in *C* and *D*. The gray line is the model prediction for the steady-state amplitude in dependency on the frequency. *F*: summary plot of the characteristic time constants of adaptation to the new steady state. As in *E*, black diamonds represent the time constant of the single-exponential fit; the gray line shows the model prediction. The low-frequency part has been blanked, see text for further information.

fits to determine the time constant, and thus the quality of the fit depended on a reasonable number of data points in the range of one time constant. The predicted time constants were very fast (<50 ms), therefore the transition to the new steady state happened for low frequencies within just a few events. Because of fluctuations in the measurements of EPSC amplitudes, the resulting error in the fitted time course was too large to allow any meaningful statements. To indicate this, time constants are not shown for frequencies <150 Hz (gray box in Fig. 3*F*).

The average differences between model predictions and measured EPSC amplitudes over our sample of five neurons are shown in Fig. 4. The absolute differences for the steady-state amplitude are plotted in Fig. 4*A*; deviations from zero indicate differences between calculated and measured EPSC amplitudes. Because steady-state amplitudes depend on the stimulation frequency and are larger for lower stimulation frequencies, absolute differences between measured and calculated amplitudes also tend to be larger for lower frequencies. Therefore we also calculated the normalized difference (Fig. 4*B,* solid square) and compared this difference to the coefficient of variation (CV) of the calculated steady-state amplitudes. The CV was calculated as the mean CV of the single cells, averaged over the sample of five neurons and is plotted in Fig. 4*B* (gray area). For all tested frequencies but one (196 Hz), the normalized difference between predicted and measured steady-state amplitude was smaller than one CV. Besides steady-state amplitudes, the model also predicted the neuron's time course for reaching the steady-state amplitude. This calculated time constant was compared with the measured time constant in five neurons; the differences between the two are plotted in Fig. 4*C*. For the considered frequencies the model provided very accurate predictions.

Natural stimuli

Finally, we tested the performance of our model on "natural" input, i.e., with spike trains that represent acoustic stimuli of biological relevance. We obtained these spike trains through in vivo recordings from single units in the MNTB of the anesthetized gerbil. The in vivo recording procedures were identical to the ones used in our previous study (Hermann et al. 2007). The presented stimuli were vocalizations of owls, typical gerbil predators (Lay 1974). The spectrogram of a 2-s sound sample is depicted in Fig. 5*A*.

Using this approach to mimic natural input in a brain slice preparation has two caveats. The first one is the variability of firing patterns between different MNTB cells in vivo, mainly caused by the differential tuning between cells. As information about the neuron's tuning is lost in a slice preparation, it is not possible to stimulate with one spike train associated with the

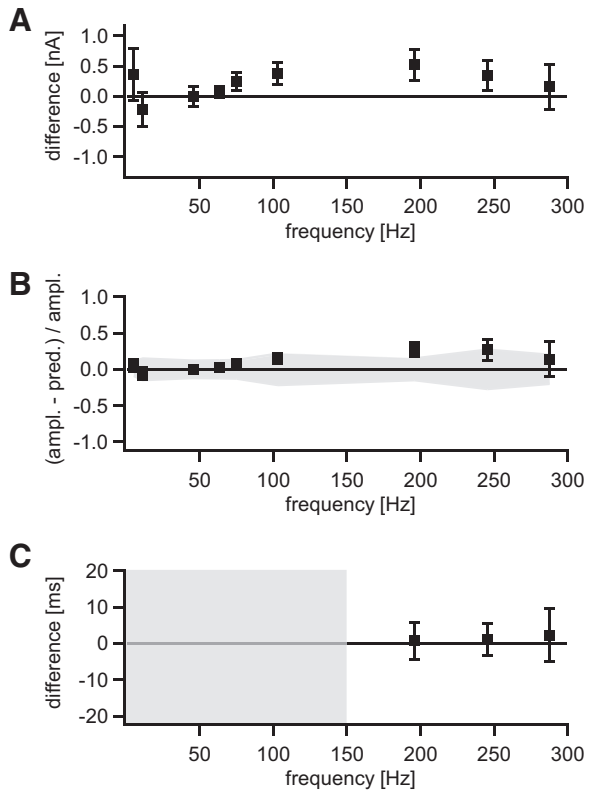

FIG. 4. Summary graphs showing the differences between experimental data and model prediction over 5 cells. *A*: difference between the offset of the single-exponential fit (i.e., measured steady-state amplitude) and predicted steady-state amplitude. *B*: the same difference as in *A* but normalized to the offset of the-exponential fit. Gray area is the coefficient of variation of the recorded EPSC amplitudes (for details see text). *C*: difference between the characteristic time constant of the exponential fit and the model prediction. Low frequencies were blanked; for details, see text.

"correct" frequency band. The second caveat arises from the fact that the in vivo recordings were conducted in the MNTB and not from globular bushy cells in the cochlear nucleus, which give rise to the calyx of Held. Also, we did not perform simultaneous pre- and postsynaptic recordings (Guinan and Li 1990; Kopp-Scheinpflug et al. 2003) and thus were unable to determine if our single units were calyces or postsynaptic principal neurons. With these caveats in mind, we stimulated calyceal input fibers with spike trains reflecting characteristics of natural sound evoked input. These spike trains have different characteristics than Poisson or regular stimulations and thereby present yet another class of stimulation pattern.

The spectrogram of the sample that we used to stimulate the cells in vivo is depicted in Fig. 5*A*. The barn owl call has pronounced temporal features with the main energy between 2 and 5 kHz. We chose data recorded from two in vivo units to stimulate cells in our slice preparation. The cells had best frequencies of 2,500 and 3,500 Hz, respectively, and showed a clear response to the stimulation. From each of these units, we recorded 10 repetitions of sound presentation and randomly chose three traces as stimuli for in vitro experiments (Fig. 5*B*). Thus a total of six spike trains were used to stimulate each neuron in vitro. An example of a voltage-clamp response recorded in vitro in response to the trace marked in Fig. 5*B* is shown in *C*. Similar to the other stimulation protocols, we extracted the EPSC amplitudes and compared them to the model prediction. The model was fitted using data from Poisson stimulations in the same cell, so the comparison between data and model prediction is based on parameters obtained with a different stimulation pattern. This was done to test if the model could also predict the synaptic strength in response to stimulation patterns not used for the parameter optimization. Figure 5*D* shows the comparison for the sample trace from *C;* the corresponding correlation coefficient is 0.94. The mean correlation coefficient over all stimulation patterns recorded in six neurons is 0.88 ± 0.03, slightly lower but statistically not different from the values obtained for the Poisson trains. Therefore we conclude that the model produced very good predictions for stimulation patterns based on naturally occurring input.

Model performance in rested synapses and during the transition period

The data presented in the preceding text suggest that a very simple vesicle release model is sufficient for describing the release dynamics at the calyx of Held. This result is inconsistent with findings of previous modeling studies, which have shown that simple models are not sufficient to accurately describe transmission at this synapse (Graham et al. 2004; Weis et al. 1999). However, one major difference between this and previous studies is that in our case synapses were tested only after they had been stimulated for prolonged periods of

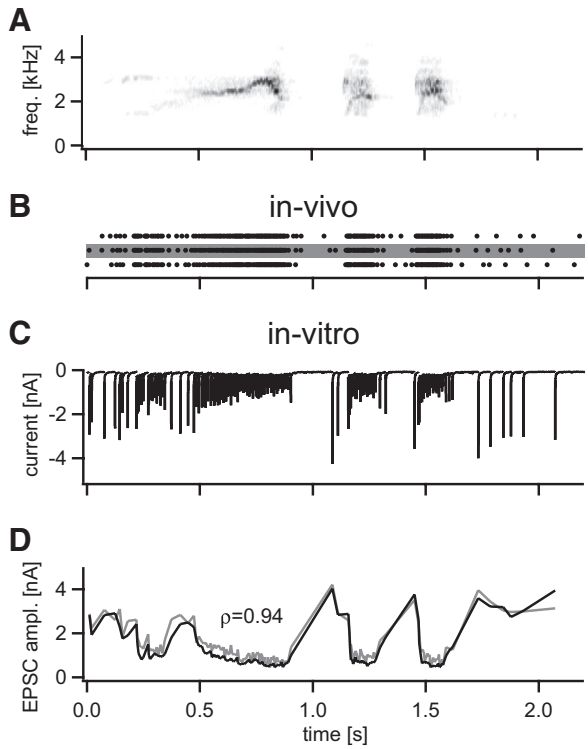

FIG. 5. *A*: spectrogram of a presented vocalization recorded from a barn owl (*Tyto alba*). *B*: raster plot of action potentials recorded during 3 presentations of the vocalization to a medial nucleus of the trapezoid body (MNTB) neuron in vivo. All 3 traces were used to stimulate neurons in vitro. *C*: voltage-clamp recording from a neuron during stimulation with the firing pattern indicated by the gray box in *B*. Similar to the previous protocols, the stimulation pattern was embedded in spontaneous activity. *D*: EPSC amplitudes extracted from the data trace. The gray trace indicates the experimental data shown in C, the black trace the corresponding model prediction.

time while previous studies tested and modeled the condition of rested synapses. To determine if and how key parameters of transmission might differ between the rested and active state, we analyzed synaptic responses during the conditioning period where neurons were shifted from a rested to a chronically active state. We determined changes in correlation coefficient, and the three model parameters (pool size, release probability, and recovery time constant) at the beginning of the conditioning period, i.e., when synapses were still rested, and during the following 2 min of conditioning with the 20-Hz Poisson train. This was done by fitting the parameters of the same simple release model to 10-s periods of Poisson responses, i.e., to analysis windows of on average 200 synaptic responses (gray box in Fig. 6*A*). Fitting the responses contained in one such analysis window to the model resulted in one set of numbers for the four parameters shown in Fig. 6, *B–E.* The analysis window was then shifted by 2 s such that the responses contained in the first 2 s of the previous analysis window were dropped and two seconds of new responses were added at the end of the new analysis window. A new set of numbers for the same four parameters was calculated by fitting the responses contained in the new analysis window and plotted in Fig. 6, *B–E.* Subsequently, this window was shifted again by 2 s, and the procedure was repeated until the analysis window reached the end of the 2-min conditioning period. This procedure of shifting an analysis window of a 10-s width in increments of 2 s was adopted to compromise between the need to fit the model to a sufficiently large number of synaptic responses to obtain accurate values for the computed parameters and the need for a high temporal resolution in this analysis. In some cases, the small number of points per analysis window leads to fluctuations in the parameters as for example in Fig. 6*B.* The periodic appearance of these slow changes can be attributed to the high overlap of adjacent analysis windows (8 s).

Figure 6, *B–E, left,* shows changes of the correlation coefficient and the three model parameters during the 120-s conditioning period that were obtained with the procedure described in the preceding text. Figure 6*B* indicates that correlation coefficients improved significantly during the 2-min conditioning period in the sample cell presented here as well as in almost all of the 11 neurons tested with this protocol. This result suggests that our simple vesicle release model performs well in capturing the dynamics of synaptic transmission in synapses that have been active for prolonged periods of time but performs significantly less well in rested synapses or synapses that have been driven with a only a small number of stimuli. Changes in pool size, release probability, and recovery time constant over the 2-min conditioning period are shown in Fig. 6, *C–E,* indicating that pool size decreased, release probability increased, and recovery time constant decreased consistently and significantly over the 2-min conditioning period.

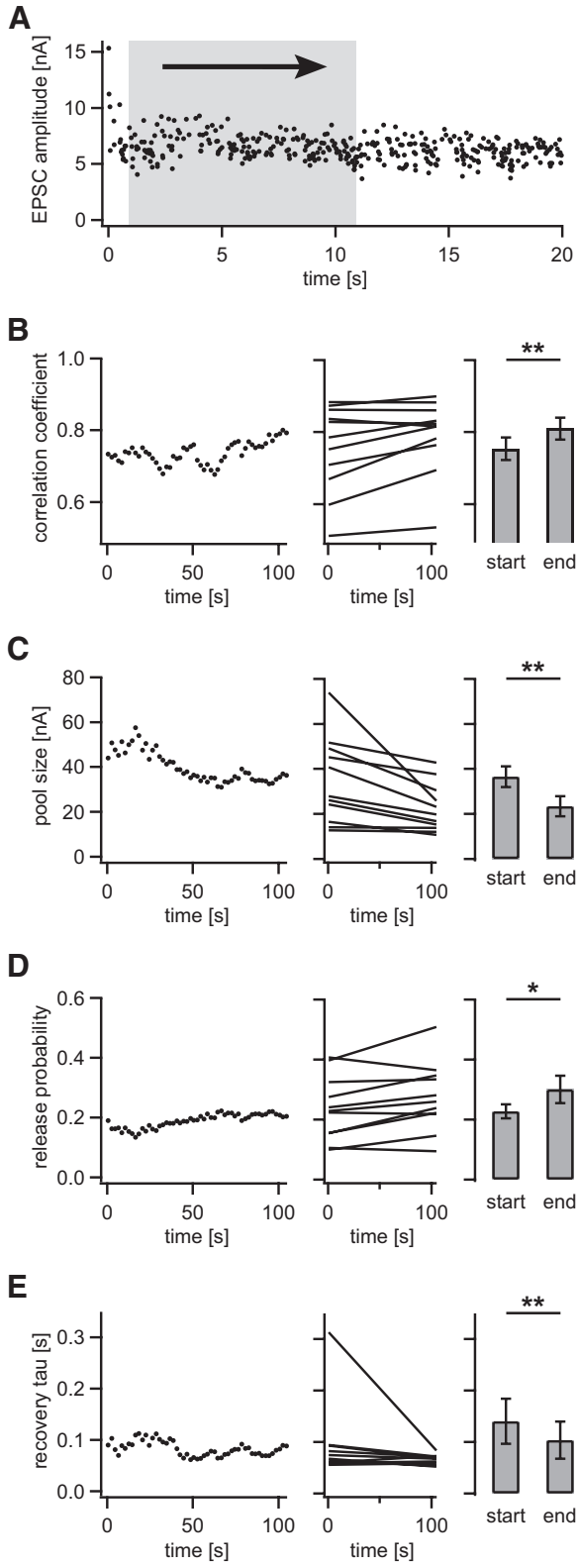

FIG. 6. Model performance during the transition from rested to active state. Model parameters were calculated for overlapping 10-s segments of the 2-min conditioning period. *A*: responses during a 10-s window of the conditioning period containing on average 200 Poisson-distributed stimuli were used to calculate 1 set of values for the model parameters. Subsequently the 10-s window was advanced by 2 s and a 2nd set of values was calculated, and the procedure repeated until the analysis window reached the end of the conditioning period. Responses to the 1st second of the conditioning period (i.e., the 1st 20 stimuli) were eliminated from this analysis as these values are dominated by the initial steep buildup of synaptic depression. *B–E*: values for the model parameters calculated with this method. *Left*: the continuous changes in parameters over the 120-s conditioning period for 1 sample neuron. *Middle*: the linear fits associated with the data traces of all 11 neurons tested with this procedure, and *right*: the average value of the first analysis window with the average value obtained with the last analysis window. Note that data from one neuron was omitted from the center graph of *E* to allow for better scaling. This neuron had an initial time constant of 560 ms, which decreased to 350 ms with conditioning.

These results suggest some functional differences between rested and active synapses. In summary, the data shown in Fig. 6 suggest that key parameters of synaptic transmission change during the transition from rested to active state and that the dynamics of rested synapses are not as well captured by the simple release model as the dynamics of chronically active synapses are.

DISCUSSION

The main question this study addresses is how well the response of the calyx of Held synapse to complex trains of continuous activity can be described using vesicle release models. We found that a very basic model including only a constant release probability and a single-exponential time course for vesicle replenishment can predict EPSC amplitudes already with very high accuracy. Two key features of the present study are the use of very long-lasting and statistically complex stimuli as well as the embedding of these into chronic "spontaneous" background activity.

Spontaneous activity is one of the hallmarks of auditory brain stem neurons in vivo but for methodological reasons is lost in slice preparations, such that auditory brain stem neurons in vitro are typically tested against a background of silence. Previous vesicle release models describing synaptic transmission at the calyx of Held (Graham et al. 2001, 2004; Weis et al. 1999) were based on electrophysiological data recorded from silent in vitro preparations (i.e., without the naturally present spontaneous activity), and thus only capture the dynamics of synaptic transmission under these conditions. However, previously we found that synaptic transmission at the calyx of Held in such silent slice preparations differs from transmission under natural activity levels in a number of key parameters such as synaptic amplitude, latency, synaptic depression during trains, recovery from depression, and fidelity of transmission (Hermann et al. 2007).

Therefore the central goals of this study were to model the transmission dynamics of chronically active calyces, compare results obtained with several extensions of the model, and test the performance of the model during complex trains of activity, including activity resulting from sound stimulation with natural and biologically relevant sound clips.

The surprising result is that already the most basic model including only a constant release probability and a single-exponential time course for vesicle replenishment performs exceptionally well in predicting EPSC amplitudes. Extending the model by increasing the number of parameters to account for additional biophysical effects such as receptor desensitization, two vesicle pools, or synaptic facilitation on a separate time course does not increase the prediction accuracy. Why does the most basic model perform so well although it disregards a number of physiological mechanisms that have clearly been shown to be present in the calyx of Held, albeit the rested calyx of Held in silent brain slices? It is unlikely that the stimulus trains used in the present study were too simplistic to capture the fine details of transmission dynamics. We note that the Poisson distributed activity, which was used to compute the model parameters, inherently includes a high degree of statistical complexity. Varying the mean frequency of the Poisson distribution over almost two levels of magnitude introduces additional complexity and ensures that the entire range of activity a MNTB neuron may encounter in the intact brain is covered by the stimulus train. We also tested trains with regular spaced inter spike intervals and stimulus trains derived from sound stimulation with natural sound clips, which increase the amount of statistical complexity even further. Therefore we assume that any model able to predict responses to the stimuli used in this study correctly should be able to predict responses to any naturally occurring sound situation equally well.

Species, age, and temperature differences may account for some of our findings. Most previous in vitro work on the calyx of Held has been performed in preparations from rat or mouse not gerbil. However, we previously found that synaptic transmission in the calyx of Held of the gerbil is very similar to that of other rodents in basic parameters. Receptor desensitization, while being very prominent in preparations from younger animals, plays a much smaller role in preparations from older animals such as the ones used in this study (Joshi and Wang 2002; Renden et al. 2005; Taschenberger et al. 2005). This finding may help explain why the model variation with added receptor desensitization did not yield higher correlation coefficients. EPSC amplitudes, or vesicle pools, are known to recover with double-exponential time courses, not single-exponential ones as used by our basic model (Sakaba and Neher 2001; Wang and Kaczmarek 1998). However, of the two associated time constants, one is very slow and on the order of seconds. Therefore interspike intervals on the order of seconds would be required to measure, or compute, this time constant properly. Due to spontaneous activity in the auditory brain stem, such long periods of silence are uncommon in vivo. Because the goal of our study was to capture the dynamics of synaptic transmission under conditions as closely as possible to those in the intact brain, our stimulus trains did not contain any interspike intervals long enough to properly measure the slow time constant. This might explain why the model variant with the double exponential did not yield higher correlation coefficients than the basic version of the model. It might also explain why the slow time constants were virtually eliminated from the computations during the parameter fitting process, either by assuming infinite values for the time constant or values that were virtually identical to those of the fast time constant.

We are uncertain why the model variant with added facilitation did not seem to yield improved predictions over the basic variant. Synaptic facilitation, i.e., an accumulation of calcium in the presynaptic terminal, must certainly be present during chronic stimulation at relatively high frequencies. It is possible that the introduction of chronic background activity into the slice preparations changes the dynamics of synaptic transmission such that the role of the various mechanisms of short-term plasticity are altered in comparison to the state of a rested synapse. Long-term stimulation of a slice preparation with thousands of stimuli might put calyces of Held into a functional state that is much less well understood than the functional state of rested calyces. Thus it cannot be ruled out that facilitation with an independent time scale, possibly also double-exponential recovery, might just not have a significant influence over EPSC dynamics during chronic long-term activity. It is also possible that the time courses of these are too similar to the basic features of the model such that the parameter optimization cannot extract them as separate parameters. In this case, the parameters computed by our model would represent a combination of physiological effects and the number of phys-

iologically relevant parameters is actually higher than estimated by the modeling process. On the other hand, the values for release probability and the fast recovery time constant as determined by our model are similar to values previously reported in the literature, suggesting that they correspond at least to a high degree to these physiological parameters rather than an abstract combination of several physiological effects. Nevertheless, the possibility that our model underestimates the number of physiological parameters relevant for transmission in active synapses cannot be ruled out completely.

An alternative explanation that can resolve the discrepancies between this study and older studies performed in rested synapses is that active synapses are in a different physiological state that can be described in mathematically simpler terms. This explanation implies that mechanisms of synaptic transmission known to influence transmission of rested synapses play a much smaller role in active synapses. Not much is known about the chronically active calyx of Held, and therefore more data are needed to verify or falsify this interpretation. Our own analysis of the transition between rested and active state revealed that model parameters change during the transition between rested and active states, suggesting that at least some biophysical parameters of synaptic transmission are affected by the chronic activity. More importantly, the same experiment revealed that our model performs significantly less well with data from rested synapses, suggesting that it is not an appropriate mathematical description of the rested state, supporting the interpretation of functional differences between rested and active states of the calyx of Held.

ACKNOWLEDGMENTS

We thank A. Loebel for help with the preparation of this manuscript, N. Lesica and C. Leibold for helpful comments on earlier versions, and F. Felmy for helpful discussions.

GRANTS

This work was funded by Deutsche Forschungsgemeinschaft (DFG) Grant KL 1842 to A. Klug.

REFERENCES

Abbott LF, Varela JA, Sen K, Nelson SB. Synaptic depression and cortical gain control. *Science* 275: 220–224, 1997.

Forsythe ID, Tsujimoto T, Barnes-Davies M, Cuttle MF, Takahashi T. Inactivation of presynaptic calcium current contributes to synaptic depression at a fast central synapse. *Neuron* 20: 797–807, 1998.

Graham BP, Wong AYC, Forsythe ID. A computational model of synaptic transmission at the calyx of Held. *Neurocomputing* 38: 37–42, 2001.

Graham BP, Wong AYC, Forsythe ID. A multi-component model of depression at the calyx of Held. *Neurocomputing* 58–60: 449–454, 2004.

Guinan JJ Jr, Li RY. Signal processing in brain stem auditory neurons which receive giant endings (calyces of Held) in the medial nucleus of the trapezoid body of the cat. *Hear Res* 49: 321–334, 1990.

Gundlfinger A, Leibold C, Gebert K, Moisel M, Schmitz D, Kempter R. Differential modulation of short-term synaptic dynamics by long-term potentiation at mouse hippocampal mossy fibre synapses. *J Physiol* 585: 853–865, 2007.

Hermann J, Pecka M, von Gersdorff H, Grothe B, Klug A. Synaptic transmission at the calyx of Held under in vivo like activity levels. *J Neurophysiol* 98: 807–820, 2007.

Irvine DRF. Physiology of the auditory brain stem. In: *The Mammalian Auditory Pathway: Neurophysiology,* edited by Popper AN, Fay RR. New York: Springer. 1992, p. 153–231.

Joshi I, Wang LY. Developmental profiles of glutamate receptors and synaptic transmission at a single synapse in the mouse auditory brain stem. *J Physiol* 540: 861–873, 2002.

Kadner A, Kulesza RJ Jr, Berrebi AS. Neurons in the medial nucleus of the trapezoid body and superior paraolivary nucleus of the rat may play a role in sound duration coding. *J Neurophysiol* 95: 1499–1508, 2006.

Kopp-Scheinpflug C, Lippe WR, Dorrscheidt GJ, Rubsamen R. The medial nucleus of the trapezoid body in the gerbil is more than a relay: comparison of pre- and postsynaptic activity. *J Assoc Res Otolaryngol* 4: 1–23, 2003.

Lay DM. Differential predation on gerbils (*Meriones*) by Little Owl, *Athene-Brahma. J Mammal* 55: 608–614, 1974.

Markram H, Tsodyks M. Redistribution of synaptic efficacy between neocortical pyramidal neurons. *Nature* 382: 807–810, 1996.

Nelder JA, Mead R. A simplex-method for function minimization. *Comput J* 7: 308–313, 1965.

Renden R, Taschenberger H, Puente N, Rusakov DA, Duvoisin R, Wang LY, Lehre KP, von Gersdorff H. Glutamate transporter studies reveal the pruning of metabotropic glutamate receptors and absence of AMPA receptor desensitization at mature calyx of held synapses. *J Neurosci* 25: 8482–8497, 2005.

Sakaba T, Neher E. Calmodulin mediates rapid recruitment of fast-releasing synaptic vesicles at a calyx-type synapse. *Neuron* 32: 1119–1131, 2001.

Schneggenburger R, Meyer AC, Neher E. Released fraction and total size of a pool of immediately available transmitter quanta at a calyx synapse. *Neuron* 23: 399–409, 1999.

Smith PH, Joris PX, Yin TC. Anatomy and physiology of principal cells of the medial nucleus of the trapezoid body (MNTB) of the cat. *J Neurophysiol* 79: 3127–3142, 1998.

Sommer I, Lingenhohl K, Friauf E. Principal cells of the rat medial nucleus of the trapezoid body—an intracellular in-vivo study of their physiology and morphology. *Exp Brain Res* 95: 223–239, 1993.

Taschenberger H, Leao RM, Rowland KC, Spirou GA, von Gersdorff H. Optimizing synaptic architecture and efficiency for high-frequency transmission. *Neuron* 36: 1127–1143, 2002.

Taschenberger H, Scheuss V, Neher E. Release kinetics, quantal parameters and their modulation during short-term depression at a developing synapse in the rat CNS. *J Physiol* 568: 513–537, 2005.

Taschenberger H, von Gersdorff H. Fine-tuning an auditory synapse for speed and fidelity: developmental changes in presynaptic waveform, EPSC kinetics, and synaptic plasticity. *J Neurosci* 20: 9162–9173, 2000.

Tsodyks MV, Markram H. The neural code between neocortical pyramidal neurons depends on neurotransmitter release probability. *Proc Natl Acad Sci USA* 94: 719–723, 1997.

Tsodyks M, Pawelzik K, Markram H. Neural networks with dynamic synapses. *Neural Comput* 10: 821–835, 1998.

Varela JA, Sen K, Gibson J, Fost J, Abbott LF, Nelson SB. A quantitative description of short-term plasticity at excitatory synapses in layer 2/3 of rat primary visual cortex. *J Neurosci* 17: 7926–7940, 1997.

von Gersdorff H, Borst JG. Short-term plasticity at the calyx of held. *Nat Rev Neurosci* 3: 53–64, 2002.

von Gersdorff H, Schneggenburger R, Weis S, Neher E. Presynaptic depression at a calyx synapse: the small contribution of metabotropic glutamate receptors. *J Neurosci* 17: 8137–8146, 1997.

Wang LY, Kaczmarek LK. High-frequency firing helps replenish the readily releasable pool of synaptic vesicles. *Nature* 394: 384–8, 1998.

Weis S, Schneggenburger R, Neher E. Properties of a model of Ca++-dependent vesicle pool dynamics and short term synaptic depression. *Biophys J* 77: 2418–2429, 1999.

Wu LG, Borst JGG. The reduced release probability of releasable vesicles during recovery from short-term synaptic depression. *Neuron* 23: 821–832, 1999.

Cover Image

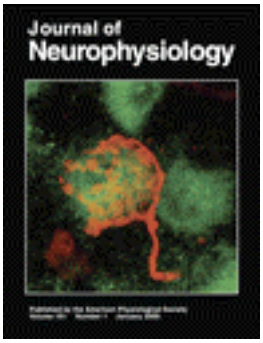

Cover: The image shows, in red, a single giant synapse, termed calyx of Held with a small part of its afferent axon. These giant synapses are located in the auditory brain stem, participate in sound localization pathway, and specialize in the processing of information with very high temporal fidelity. The calyx makes connection to a principal neuron of the medial nucleus of the trapezoid body (MNTB), shown directly under the calyx in green. Other principal neurons are labeled as well. The calyx was visualized via rhodamine-dextrane tracing, and postsynaptic neurons were labeled with a fluorescent Nissl stain. Labeling and confocal image by Josh Pfeiffer. For more information, see Hermann J, Grothe B, and Klug A. Modeling Short-Term Synaptic Plasticity at the Calyx of Held Using In Vivo-Like Stimulation Patterns. J Neurophysiol 101: 20–30, 2009. First published October 29, 2008: doi:10.1152/jn.90243.2008.

J Neurophysiol 98: 577–578, 2007.
First published June 20, 2007; doi:10.1152/jn.00641.2007.

Short-Term Plasticity Turns Plastic. Focus on "Synaptic Transmission at the Calyx of Held Under In Vivo-Like Activity Levels"

Erwin Neher
Max-Plank-Institute for Biophysical Chemistry, Gottingen, Germany

Short-term plasticity (STP) is a use-dependent change in synaptic strength on the time scale of millisecond to seconds and is observed in almost every synapse of the CNS. Each type of synapse has its own "personality" with respect to this property. When stimulated a few times within a second, some synapses show facilitation, others depression or else complex sequences of facilitatory and depressing changes (Dittman et al. 2000). It has been shown that terminals at two axonal branches of the same neuron can express very different forms of STP (Reyes et al. 1998; Rozov et al. 2001) and that STP serves important aspects of signal processing in the nervous system. In this issue of the *Journal of Neurophysiology* (p. 807–820), Hermann et al. (2007) ask the question whether the way we usually characterize STP of a given synapse actually reports that personality, which is relevant for its physiological function. The answer, not surprisingly, is no!

The object of their study is the Calyx of Held, a glutamatergic presynaptic terminal in the auditory pathway. It came to fame by the fact that it is large enough so that it can be voltage clamped (Borst et al. 1995; Forsythe 1994). Furthermore, the terminal contacts the soma of a large, compact postsynaptic neuron, so that voltage clamp can be applied simultaneously to both the pre- and the postsynapse (Borst et al. 1995; Takahashi et al. 1996). This offers unique possibilities for a detailed biophysical analysis of synaptic transmission. The synapse, when studied the usual way, displays pronounced short-term depression, very similar to other glutamatergic synapses (Dittman et al. 2000). The "usual way" means that a short burst of stimuli is applied after a long period of rest. However, unlike many central synapses, for which coding is relatively sparse, the task of the Calyx of Held—as a synapse in the afferent sensory information flow—is to fire on average 10–100 times per second, even in complete silence (Kopp-Scheinpflug et al. 2003). Tone bursts cause short episodes of firing in the auditory nerve of 100–500 action potentials per second. The basic question of the Hermann et al. paper is exactly what type of STP is observed, when firing rate changes from an average of ~40 to a high frequency of several hundred Hertz. They find, first of all, that the synapse is partially depressed after conditioning by a 40-Hz Poisson train. This is expected from previous work on calyces of other species, which had shown that the steady-state excitatory postsynaptic current (EPSC) amplitude during ≈40-Hz stimulation is ~30–40% of that of a rested synapse. A second finding is more surprising: The relative depression during the high-frequency train is much less than that of a 100- or 300-Hz train applied to a resting synapse. In fact, Hermann et al. observe that switching from a 40-Hz Poisson train to a 100-Hz tetanus decreases steady-state EPSC size only by ~20%. Furthermore, they find that recovery from such depression occurs very rapidly, on the 50- to 100-ms time scale, quite unlike recovery to resting levels, which takes seconds.

Two important questions emerge from this study: what is the mechanism of this activity-dependent alteration of STP, and what is it good for in the context of auditory signal processing?

Hermann et al. discuss the latter question but only give a few clues regarding the mechanisms. This is why I will speculate about the latter issue in the following text.

PHYSIOLOGICAL SIGNIFICANCE

Hermann et al. point out that synaptic failures are observed during deep depression at several hundred Hertz. Thus it is quite clear that the Calyx of Held is not the fail-safe relay, which it had been assumed to be in many previous studies. On the other hand, they do point out that first responses to a burst stimulus are transmitted quite safely, even after 60-Hz long-term conditioning. Thus the information, which is most important for sound localization (about the wave-front of sound events) is preserved. Given that there are failures, the synapse contributes to the overall short-term depression (STD) of the auditory pathway and given the importance of STD for information processing [see for example the influence of STD in another type of auditory system; (Cook et al. 2003)] any realistic model of sound processing should consider the STD data after appropriate conditioning and not those of a rested synapse. In that sense, the plasticity of STD needs detailed attention.

MECHANISMS

Why does a synapse depress only little during a transition from a 40-Hz Poisson train to a 100-Hz tetanus, while it depresses by ~2/3, when the same tetanus is applied to a rested synapse? Given that the tetanus starts from a state of partial depression, we may ask whether this is a sufficient explanation in the light of past work on STD.

The major mechanism of STD at this synapse is the depletion of release-ready vesicles (Schneggenburger et al. 2002). Any *simple* model of depletion and recruitment of vesicles predicts that transmission at steady-state should decline with the inverse of frequency beyond a certain characteristic frequency. The transition from conditioning to burst stimulation is a 2.5-fold increase in average frequency, and we would expect to observe additional depression by about that factor, but we observe only a 20% change!

Part of the answer to this discrepancy is that the Calyx of Held, like many other types of synapses, does not conform to the "simple" model of depression. When one uses rested synapses and plots the level of steady-state depression during

Address reprint requests and other correspondence to E. Neher (E-mail: eneher@gwdg.de).

high-frequency trains against stimulation frequency, invariably a two-component curve is obtained: depression develops already at very low stimulation frequencies and EPSCs reach a level of ~40–50% of the initial value at frequencies as low as 5–10 Hz (Taschenberger et al. 2005; Weis et al. 1999). Beyond that point the curve becomes shallower with a further half-decline only at 200 Hz and beyond. Therefore actually only very little additional depression is expected when switching from 40 to 100 Hz—as observed by Herman et al. Several studies have been performed to explain the deviation of the depression-versus-frequency curve from a 1/*f* relationship (Dittman and Regehr 1998; Kusano and Landau 1975). Promising, from the current point of view, are mechanisms that assume an acceleration of vesicle recruitment beyond the "breakpoint" of the relationship at ~10–20 Hz (Taschenberger et al. 2005; Weis et al. 1999). Alternatively, presynaptic Ca^{2+}-current inactivation may explain part of the decline at low frequencies (Takahashi et al. 2000). The first explanation goes along nicely with the finding of Hermann et al. that vesicle recruitment is fast after "conditioning" of the synapse. The question remains: why is recruitment accelerated by conditioning? A likely explanation is the finding at many synapses (Dittman and Regehr 1998; Stevens and Wesseling 1998) including the Calyx of Held (Sakaba and Neher 2001; Wang and Kaczmarek 1998) that elevated [Ca^{2+}] speeds up vesicle recruitment.

In conclusion, we are left with the message that STD is plastic, which means that its properties are influenced by "physiological" levels of background activity. The work of Hermann et al. shows that this has functional significance. On the basis of this work, it may well be worthwhile to study the mechanistic basis of vesicle recruitment (Wadel et al. 2007), its modulation by activity and by second messengers, and its precise influence on STD.

REFERENCES

Borst JG, Helmchen F, Sakmann B. Pre- and postsynaptic whole-cell recordings in the medial nucleus of the trapezoid body of the rat. *J Physiol* 489: 825–840, 1995.

Cook DL, Schwindt PC, Grande LA, Spain WJ. Synaptic depression in the localization of sound. *Nature* 421: 66–70, 2003.

Dittman JS, Kreitzer AC, Regehr WG. Interplay between facilitation, depression, and residual calcium at three presynaptic terminals. *J Neurosci* 20: 1374–1385, 2000.

Dittman JS, Regehr WG. Calcium dependence and recovery kinetics of presynaptic depression at the climbing fiber to Purkinje cell synapse. *J Neurosci* 18: 6147–6162, 1998.

Forsythe ID. Direct patch recording from identified presynaptic terminals mediating glutamatergic EPSCs in the rat CNS in vitro. *J Physiol* 479: 381–387, 1994.

Hermann J, Pecka M, von Gersdorff H, Grothe B, Klug A. Synaptic transmission at the calyx of Held under in vivo-like activity levels. *J Neurophysiol* 98: 807–820, 2007.

Kopp-Scheinpflug C, Lippe WR, Dorrscheidt GJ, Rubsamen R. The medial nucleus of the trapezoid body in the gerbil is more than a delay: comparison of pre- and postsynaptic activity. *J Assoc Res Otolaryngol* 4: 1–23, 2003.

Kusano K, Landau EM. Depression and recovery of transmission at the squid giant synapse. *J Physiol* 245: 13–22, 1975.

Reyes A, Lujan R, Rozov A, Burnashev N, Somogyi P, Sakmann B. Target-cell-specific facilitation and depression in neocortical circuits. *Nat Neurosci* 1: 279–285, 1998.

Rozov A, Burnashev N, Sakmann B, Neher E. Transmitter release modulation by intracellular Ca^{++} buffers in facilitating and depressing nerve terminals of pyramidal cells in layer 2/3 of the rat neocortex indicates a target cell specific difference in presynaptic calcium dynamics. *J Physiol* 531: 807–826, 2001.

Sakaba T, Neher E. Calmoudlin mediates rapid recruitment of fast-releasing synaptic vesicles at a calyx-type synapse. *Neuron* 32: 1119–1131, 2001.

Schneggenburger R, Sakaba T, Neher E. Vesicle pools and short-term synaptic depression: lessons from a large synapse. *Trends Neurosci* 25: 206–212, 2002.

Stevens CF, Wesseling JF. Activity-dependent modulation of the rate at which synaptic vesicles become available to undergo exocytosis. *Neuron* 21: 415–424, 1998.

Takahashi T, Forsythe ID, Tsujimoto T, Barnes-Davies M, Onodera K. Presynaptic calcium current modulation by a metabotropic glutamate receptor. *Science* 274: 594–597, 1996.

Takahashi T, Hori T, Kajikawa Y, Tsujimoto T. The role of GTP-binding protein activity in fast central synaptic transmission. *Science* 289: 460–463, 2000.

Taschenberger H, Scheuss V, Neher E. Release kinetics, quantal parameters and their modulation during short-term depression at a developing synapse in the rat CNS. *J Physiol* 568: 513–537, 2005.

Wadel A, Neher E, Sakaba T. The coupling between synaptic vesicles and Ca(2+) channels determines fast neurotransmitter release. *Neuron* 53. 563–75, 2007.

Wang LY, Kaczmarek LK. High-frequency firing helps replenish the readily releasable pool of synaptic vesicles. *Nature* 394: 384–388, 1998.

Weis A, Schneggenburger R, Neher E. Properties of a model of Ca^{++}-dependent vesicle pool dynamics and short term synaptic depression. *Biophys J* 77: 2418–2429, 1999.

J Neurophysiol 98: 807–820, 2007.
First published May 16, 2007; doi:10.1152/jn.00355.2007.

Synaptic Transmission at the Calyx of Held Under In Vivo–Like Activity Levels

Joachim Hermann,[1] Michael Pecka,[1] Henrique von Gersdorff,[1,2] Benedikt Grothe,[1] and Achim Klug[1]
[1]*Ludwig-Maximilians-University, Munich, Germany; and* [2]*The Vollum Institute, Oregon Health and Science University, Portland, Oregon*

Submitted 29 March 2007; accepted in final form 13 May 2007

Hermann J, Pecka M, von Gersdorff H, Grothe B, Klug A. Synaptic transmission at the calyx of Held under in vivo–like activity levels. *J Neurophysiol* 98: 807–820, 2007. First published May 16, 2007; doi:10.1152/jn.00355.2007. One of the hallmarks of auditory neurons in vivo is spontaneous activity that occurs even in the absence of any sensory stimuli. Sound-evoked bursts of discharges are thus embedded within this background of random firing. The calyx of Held synapse in the medial nucleus of the trapezoid body (MNTB) has been characterized in vitro as a fast relay that reliably fires at high stimulus frequencies (≤800 Hz). However, inherently due to the preparation method, spontaneous activity is absent in studies using brain stem slices. Here we first determine in vivo spontaneous firing rates of MNTB principal cells from Mongolian gerbils and then reintroduce this random firing to in vitro gerbil brain stem synapses at near-physiological temperature. After conditioning synapses with afferent fiber stimulation for 2 min at Poisson averaged rates of 20, 40, and 60 Hz, we observed a number of differences in the properties of synaptic transmission between conditioned and unconditioned synapses. Foremost, we observed reduced steady-state EPSC amplitudes that depressed even further during an embedded short-stimulation train of 100, 300, or 600 Hz (a protocol that thus simulates in vitro what probably occurs at the in vivo MNTB after a short sound stimulus in a silent background). Accordingly, current-clamp, dynamic-clamp, and loose-patch recordings revealed a number of action potential failures at the postsynaptic cell during high-frequency–stimulation trains, although the initial onset of evoked activity was still transmitted with higher fidelity. We thus propose that some in vivo auditory synapses are in a tonic state of reduced EPSC amplitudes as a consequence of high spontaneous spiking and this in vivo–like conditioning has important consequences for the encoding of signals throughout the auditory pathway.

INTRODUCTION

The calyx of Held is a large synaptic terminal innervating principal neurons of the medial nucleus of the trapezoid body (MNTB) (Forsythe 1994; Held 1893; Kuwabara et al. 1991; Smith et al. 1991). MNTB neurons sign-invert calyceal excitation into glycinergic inhibition to various nuclei in the auditory brain stem (Banks and Smith 1992; Bledsoe et al. 1990; Moore and Caspary 1983; Spangler et al. 1985; Thompson and Schofield 2000). In vitro, the signal derived from the calyx generates large excitatory postsynaptic currents (EPSCs) with a short synaptic delay (Barnes-Davies and Forsythe 1995; Borst and Sakmann 1996; Sakaba and Neher 2001; Taschenberger et al. 2002). Speed and fidelity of synaptic transmission are considered very reliable up to several hundred Hertz in mature animals (Futai et al. 2001; Joshi et al. 2004; Taschenberger and von Gersdorff 2000; Wu and Kelly 1993), leading to a view of the calyx of Held as a very reliable relay synapse.

All the in vitro work mentioned earlier was performed in brain slices. Inherently, auditory brain slice preparations differ from intact brains in various parameters, including spontaneous activity. In vivo, neurons of the auditory brain stem fire spontaneously at frequencies that vary from >1 to ≥100 Hz, a property that results mainly from the dynamics of the transduction channels in the cochlear hair cells (Geisler et al. 1985; Hudspeth 1997; Kiang 1965; Liberman 1978; Roberts et al. 1988), resulting in spontaneous firing of the auditory nerve (Geisler et al. 1985; Liberman 1978). Spontaneous firing can also be observed in many brain stem nuclei including the cochlear nucleus (Brownell 1975; Goldberg and Brownell 1973; Joris et al. 1994; Schwarz and Puil 1997; Spirou et al. 1990, 2005) and MNTB (Kadner et al. 2006; Kopp-Scheinpflug et al. 2003; Smith et al. 1998; Sommer et al. 1993).

In an intact brain, MNTB neurons fire spontaneously at levels, which might be suitable to chronically induce some forms of short-term plasticity, such as synaptic depression or facilitation (Schneggenburger et al. 2002; von Gersdorff and Borst 2002). Sound stimuli, i.e., streams of high-frequency activity embedded in this spontaneous firing (Klyachko and Stevens 2006), would then be processed by the synapse on the background of chronic depression and/or facilitation (Fig. 1*A*). Because of the nature of the brain slice preparation, spontaneous activity and its potential effects on short-term plasticity might be lost in standard in vitro recordings (Fig. 1*B*). If that were the case, properties of synaptic transmission in the calyx of Held under in vivo conditions may be different from those commonly observed in vitro.

This study investigates synaptic transmission in the calyx of Held under in vivo–like spontaneous activity levels. We first measured the rates and statistical properties of spontaneous firing in the MNTB of Mongolian gerbils (*Meriones unguiculatus*) in vivo. Subsequently, we stimulated the afferent fibers that give rise to calyceal inputs in gerbil MNTB brain slices at physiological temperature for prolonged periods of time with stimuli that mimicked the random spontaneous activity as closely as possible (Fig. 1*C*). We assessed changes in synaptic transmission resulting from this long-term stimulation, such as synaptic currents, the degree of depression, recovery from depression, and finally the spiking properties of "spontaneously active" neurons.

Address for reprint requests and other correspondence: A. Klug, Neurobiology Group, Dept. Biology II, Grosshaderner Strasse 2, 82152 Martinsried, Germany (E-mail: achim.klug@lmu.de).

The costs of publication of this article were defrayed in part by the payment of page charges. The article must therefore be hereby marked "*advertisement*" in accordance with 18 U.S.C. Section 1734 solely to indicate this fact.

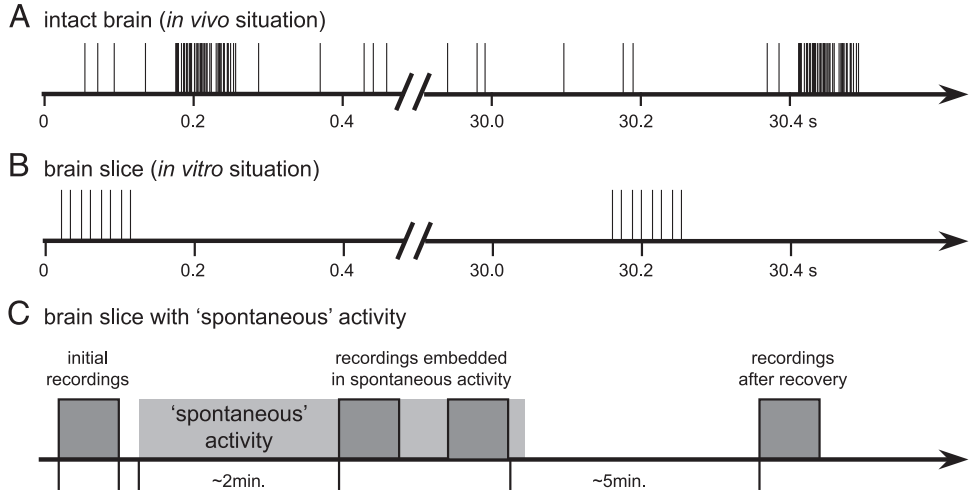

FIG. 1. *A*: illustration of in vivo activity in the medial nucleus of the trapezoid body (MNTB). In the intact brain, MNTB neurons are chronically spontaneously active. Responses to sound stimuli, indicated by high-frequency bursts, are embedded in the background activity. *B*: in a typical slice preparation, the background activity is not present, such that trains of high-frequency stimuli used to imitate responses to sound are embedded in periods of complete silence. *C*: our experimental approach attempted to bring the spontaneous activity back into slice preparations. Responses to simulated sound stimuli were tested to obtain a baseline of synaptic properties, then spontaneous activity was simulated for several minutes, then the same "sound stimuli" were tested again while they were embedded in background activity. At the end of data collection, the cell was allowed to recover and the same set of simulated sound stimuli was tested again to assess the level of recovery.

METHODS

In vivo recordings

Auditory responses from 36 single neurons were recorded in 16 Mongolian gerbils (*Meriones unguiculatus*) of both sexes, aged between 21 and 60 days. We found no systematic differences in aurality, firing frequency, threshold, characteristic frequency, or other response parameters of neurons, which depended on the age of the animal (data not shown), and thus the data from all 36 neurons were pooled. In our sample there was also no covariation between spontaneous activity and auditory threshold or between spontaneous activity and a neuron's characteristic frequency (regression analyses; data not shown). For experimental reasons, the reported in vivo data were recorded from MNTB postsynaptic neurons, not calyces of Held or globular bushy cells in the anteroventral cochlear nucleus. The underlying assumption is that the spontaneous activity in the MNTB is not high enough to induce synaptic failures at the calyx of Held synapse, such that the presynaptic spike frequency is identical to the postsynaptic activity.

Data were collected simultaneously for this study and a different project involving MNTB response properties (data not shown). All experiments complied with institutional guidelines and were approved by the appropriate government authorities (Reg. Oberbayern AZ 55.2-1-54-2531-57-05).

SURGICAL PROCEDURES. Before surgery, animals were anesthetized by an initial intraperitoneal injection (0.5 ml/100 g body weight) of ketamine (20%) and xylazine (2%, both in physiological NaCl). During surgery and recordings, a dose of 0.05 ml of the same mixture was applied subcutaneously in scheduled intervals that were based on the animal's body weight. Constant body temperature was maintained using a thermostatically controlled heating blanket.

Skin and tissue covering the upper part of the skull were removed and a small metal rod was mounted to the frontal part of the skull using UV-sensitive dental-restorative material (Charisma, Heraeus Kulzer, Hanau, Germany). Custom-made earphone holders were attached to the gerbil head, allowing for the safe insertion of earphones or probe tube microphones into the ear canal. The animal was then transferred to a sound-attenuated chamber and mounted in a custom-made stereotaxic instrument (Schuller et al. 1986). The animal's position in the recording chamber was standardized with reference to stereotaxic landmarks on the skull (Loskota et al. 1974). For electrode penetrations to the MNTB, a small hole of approximately 1 mm^2 was cut into the skull lateral to the lambdoid suture. Micromanipulators were used to position the recording electrode according to landmarks on the brain surface and a reference point, which was used for all penetrations. The meninges overlying the cortex were removed and saline was applied to the opening to prevent dehydration of the brain.

Typical recording sessions lasted 10–14 h. After successful recordings, the animal was killed by injection of an overdose of chloral hydrate (Sigma–Aldrich Chemie, Munich, Germany). The last electrode position was then marked with a current-induced lesion (20 μA for 80–120 s). The head was fixated in 4% paraformaldehyde and prepared for anatomical processing. Transverse sections were cut and Nissl-stained to verify the recording sites. An example of an anatomical verification is shown in Supplemental Fig. 1*C*.[1] The lesion site can be clearly seen in the center of the left MNTB.

RECORDINGS OF NEURAL ACTIVITY. Single-unit responses were recorded extracellularly using 10-MΩ glass electrodes filled with 1 M NaCl. The recording electrode was advanced under remote control, using a piezodrive (Inchworm controller 8200, EXFO Burleigh Products Group, Victor, NY). Extracellular action potentials were recorded by an electrometer (npi electronics, Tamm, Germany or Electro 705, WPI, Berlin, Germany), a 50/60-Hz noise eliminator (Humbug, Quest Scientific Instruments, North Vancouver, BC, Canada), a band-pass filter (VBF/3, Bortolin Kemo, Porcia, Italy), and an amplifier (model 7607, Toellner Electronic Instrumente, Herdecke, Germany) and subsequently fed into the computer by an A/D-converter [RP2-1, Tucker-Davis Technologies (TDT), Alachua, FL]. Clear isolation of action potentials from a single neuron (signal-to-noise ratio >5) was achieved by visual inspection on a spike-triggered oscilloscope and by off-line spike-cluster analysis (Brainware, TDT). Two examples of recorded single-cell spike waveforms are shown in Supplemental Fig. 1, *A* and *B*. The unit in supplemental Fig. 1*A* is an example of a neuron with a low spontaneous rate (10 Hz), whereas supplemental Fig. 1*B* shows an example of a neuron with a very high spontaneous rate (107 Hz). Both units were recorded from the same animal; histological verification of the recording site is shown in Supplemental Fig. 1*C*.

STIMULUS PRESENTATION AND RECORDING PROTOCOLS. Stimuli were generated at a 50-kHz sampling rate using TDT System III.

[1] The online version of this article contains supplemental data.

Digitally generated stimuli were converted to analog signals (DA3-2/RP2-1, TDT), attenuated (PA5, TDT), and delivered to earphones (MDR-EX70LP, Sony, Berlin, Germany).

The standard stimulus was a 200-ms toneburst with a rise/fall time of 5 ms, presented at a repetition rate of 2 Hz. Stimulus presentation was randomized. To search for acoustically evoked responses, noise stimuli were delivered binaurally. When an auditory neuron was encountered, we first determined its best frequency (BF) and absolute threshold audiovisually to set stimulus parameters subsequently controlled by the computer. The frequency that elicited responses at the lowest sound intensity was defined as BF, the lowest sound intensity evoking a noticeable response at BF as threshold. These properties were confirmed by off-line analysis of the frequency versus level response areas. Monaural pure tones to each ear and binaural pure tones without interaural intensity or time differences were presented to define the aurality of the neuron. MNTB neurons responded to stimulation of the contralateral ear only, with a tonic/primary-like firing pattern, and were not affected by stimulation of the ipsilateral ear.

Spontaneous activity of a neuron was determined by recording action potentials in several 5-s-long intervals without sound stimulation and averaging the measured firing rate. All quantifications in this study are based on off-line analysis with the software packages Brainware (TDT), Matlab (The MathWorks, Natick, MA), and IGOR (WaveMetrics, Lake Oswego, OR).

In vitro recordings

Slices of brain stem were prepared from Mongolian gerbils (*Meriones uniguiculatus*) aged 14 to 19 days (posthearing animals). Data from these different ages were pooled because no age-dependent variations in synaptic amplitudes, degree of depression, response to conditioning, or firing probability were observed (data not shown).

SLICE PREPARATION. Animals were briefly anesthesized by isoflurane inhalation (Isofluran Curamed, Curamed Pharma, Karlsruhe, Germany) and decapitated. The brain stem was dissected out under ice-cold dissection ringer (125 mM NaCl, 2.5 mM KCl, 1 mM $MgCl_2$, 0.1 mM $CaCl_2$, 25 mM glucose, 1.25 mM NaH_2PO_4, 25 mM $NaHCO_3$, 0.4 mM ascorbic acid, 3 mM myoinositol, 2 mM pyruvic acid; all chemicals from Sigma–Aldrich). Sections (200–250 μm) were cut with a vibratome (VT1000S, Leica, Wetzlar, Germany). Slices were transferred to an incubation chamber containing extracellular solution (ECS) (125 mM NaCl, 2.5 mM KCl, 1 mM $MgCl_2$, 2 mM $CaCl_2$, 25 mM glucose, 1.25 mM NaH_2PO_4, 25 mM $NaHCO_3$, 0.4 mM ascorbic acid, 3 mM myoinositol, 2 mM pyruvic acid; all chemicals from Sigma–Aldrich) and bubbled with 5% CO_2-95% O_2. Slices were incubated for 1 h at 37°C, after which the chamber was brought to room temperature. Recordings were obtained within 4–5 h of slicing.

WHOLE CELL RECORDINGS. All recordings were performed at 36–37°C. After incubation, slices were transferred to a recording chamber and continuously superfused with ECS at 3–4 ml/min through a gravity-fed perfusion system. MNTB neurons were viewed through a Zeiss Axioskop 2 FS microscope equipped with DIC optics and a ×40 water-immersion objective (Zeiss, Oberkochen, Germany). Whole cell recordings were made with an EPC 10 double amplifier (HEKA Instruments, Lambrecht/Pfalz, Germany). Signals were filtered at 5–10 kHz and subsequently digitized at 20–100 kHz using Patchmaster Version 2.02 software (HEKA). Uncompensated series resistance, between 5.5 and 15 MΩ, was compensated to values between 2.1 and 5.8 MΩ with a lag time of 10 μs. Potential changes in series resistance were monitored throughout the recordings and data collection was discontinued whenever series resistance changed by >2 MΩ. All voltages are corrected for a −12-mV junction potential.

Patch pipettes were pulled from 1.2-mm borosilicate glass (WPI) or 1.5-mm borosilicate glass (Harvard Instruments, Kent, UK) using a Sutter P-97 electrode puller (Sutter Instrument, Novato, CA) or a DMZ Universal Puller (Zeitz Instruments, Munich, Germany). Pipettes were filled with potassium gluconate–based internal solution for current-clamp recordings (120 mM K-gluconate, 4 mM $MgCl_2$, 10 mM HEPES, 5 mM EGTA, 10 mM tris-phosphocreatine, 4 mM Na_2-ATP, 0.3 mM tris-GTP, 0.5 mM $CaCl_2$; all chemicals from Sigma–Aldrich) or cesium methanesulfonate–based solution for voltage-clamp recordings (125 mM $CsMeSO_3$, 4.5 mM $MgCl_2$, 9 mM HEPES, 5 mM EGTA, 14 mM tris-phosphocreatine, 4 mM Na_2-ATP, 0.3 mM tris-GTP, 1.5 mM $CaCl_2$, all chemicals from Sigma–Aldrich).

During all recordings, 500 nM strychnine hydrochloride (Sigma–Aldrich) and 20 μM SR95531 were added to the bath to block glycinergic and $GABA_A$-ergic inhibition, respectively. During voltage-clamp recordings, 5 mM QX-314 (Alomone Labs, Jerusalem, Israel) was added to the pipette fill to eliminate sodium currents.

STIMULATION OF SYNAPTIC INPUTS. Synaptic currents were elicited by midline stimulation of the calyceal input fiber bundle with a 5-MΩ bipolar stimulation electrode (matrix electrodes with 270-μm distance; FHC, Bowdoinham, ME). Stimuli were 100-μs-long square pulses of 10 to 40 V delivered with an STG 2004 computer-controlled four-channel stimulator (Multi Channel Systems, Reutlingen, Germany) and a stimulation isolation unit (Iso-flex, AMPI, Jerusalem, Israel). The stimulator permitted completely independent uploading and operation of the four channels, allowing the seamless integration and thus true embedding of simulated auditory signals (i.e., high-frequency bursts) in the simulated spontaneous activity. Spontaneous activity was simulated by using 20-, 40-, and 60-Hz Poisson-distributed stimulus trains (see Figs. 1 and 2, *C* and *E*). Sound-evoked activity was simulated by short trains consisting of 20 stimuli at 100, 300, or 600 Hz.

CONDUCTANCE-CLAMP EXPERIMENTS. Excitatory conductances were simulated with an SM-1 amplifier (Cambridge Conductance, Cambridge, UK). The 10–90% rise of the current output in response to a voltage change for this amplifier was 290 ns. Reversal potentials were set to 0 mV for the excitatory postsynaptic conductances (EPSGs). The conductance waveforms used were previously recorded as EPSCs in voltage-clamp mode. After extrapolating the artifacts, EPSGs were normalized. All conductance values correspond to peak conductances. In experiments in which background leak was added, a constant step command was fed from the computer into the conductance-clamp amplifier by a separate channel and the reversal potential for this channel was set to −60 mV. The separately calculated output of both channels was added together and fed to the HEKA amplifier.

STATISTICAL ANALYSIS. Data were analyzed in IGOR 5 (WaveMetrics), MS Excel 2004 (Microsoft, Redmond, WA), and Matlab 7 (The MathWorks). Unless otherwise noted, all errors are reported as standard error. Statistical significance was tested with a Student's *t*-test, unless otherwise noted. Significant differences are marked with a single asterisk for values of $P < 0.05$ and with a double asterisk for $P < 0.01$.

RESULTS

In vivo spontaneous firing rates of MNTB cells

The first goal was to determine the spontaneous firing rates of MNTB neurons in the intact brain of Mongolian gerbils (*Meriones unguiculatus*). Neural activity was recorded in vivo from single cells in the MNTB with standard extracellular recording techniques. When a neuron was encountered and isolated, its basic response features such as aurality, auditory threshold, and frequency tuning were assessed. Among the 36 neurons from which activity was recorded, thresholds for sound stimulation ranged from 0 to 60 dB SPL (mean = 32 ±

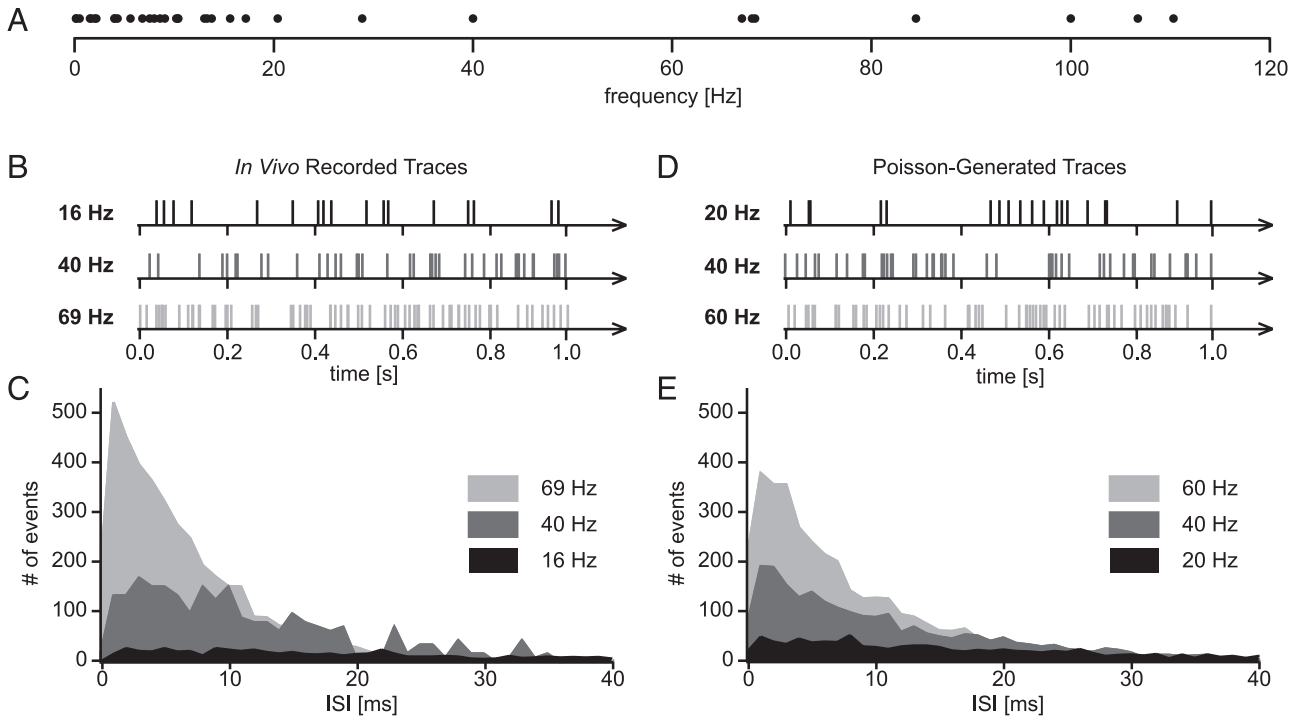

FIG. 2. *A*: distribution of spontaneous firing rates measured among our sample of 36 neurons. Each dot represents the average spontaneous firing rate of one neuron. Mean spontaneous firing rate among the 36 neurons was 24.9 ± 5.5 Hz. *B* and *C*: in vivo recordings of spontaneous activity from 3 MNTB neurons; clips of original trace (*B*); interspike interval (ISI) distribution (*C*). Although the spontaneous firing rates differed between the neurons and were 16, 40, and 69 Hz, the ISI distribution could be described by a single-exponential curve, and thus was near-Poisson-distributed in each case. *D* and *E*: based on the results from *B* and *C*, 3 stimulation protocols of simulating spontaneous activity in brain slices at 20, 40, and 60 Hz were created. ISI distribution was designed to be near-Poisson.

2.8 dB SPL) and characteristic frequencies were between 486 Hz and 16.8 kHz. Consistent with known input patterns to the MNTB, all neurons could be excited when sound was presented to the ear contralateral to the recording site. None of the neurons showed any effects of ipsilateral stimulation.

After a neuron's basic response properties to auditory stimulation were assessed, its spontaneous firing rate in the absence of sound stimulation was measured over ≥50 s and average discharge rates were calculated and defined as the neuron's spontaneous firing rate. Among the 36 neurons, spontaneous firing rates ranged from 0.15 to 110 Hz (Fig. 2*A*). The mean spontaneous rate was 24.9 ± 5.5 Hz. Short clips of spike trains are shown in Fig. 2*B*. The spontaneous rates of these neurons were 16, 40, and 69 Hz, respectively. An analysis of the interspike intervals (ISIs) revealed that the spikes are near-Poisson distributed with the exception that very short ISIs (<1 ms) are underrepresented (three ISI histograms in Fig. 2*C*).

Introducing spontaneous rates into slice preparations of the MNTB

Based on these in vivo data, three representative frequencies of spontaneous rates were chosen for stimulation of the in vitro brain slice preparations: 20, 40, and 60 Hz (Fig. 2*D*). Distribution of the spike events in each one of these trains was chosen to be near-Poisson, to imitate the in vivo spontaneous activity as closely as possible (Fig. 2*E*). MNTB calyceal input fibers were stimulated with these spike trains for prolonged periods of time (≥2 min) and voltage-clamp recordings were performed from MNTB principal neurons. During the 2-min conditioning, 7,200 Poisson-distributed stimuli were presented in case of the 60-Hz train, 4,800 stimuli in the case of the 40-Hz train, and 2,400 stimuli in the case of the 20-Hz conditioning train.

Effects of "spontaneous" firing on excitatory synaptic currents in the calyx of Held

At the beginning of each experiment, a synapse was "rested" or completely recovered, i.e., no stimuli had been given to the input fibers for ≥5 min. During the 2-min conditioning period with Poisson-distributed activity, EPSCs depressed substantially with at least two exponential components. The three graphs in Fig. 3, *A–C* show EPSC amplitudes of three different neurons in response to 2-min conditioning stimuli at 20, 40, and 60 Hz (Fig. 3, *A*, *B*, and *C*, respectively). Each dot in the graphs represents the amplitude of one EPSC and the solid lines represent double-exponential fits.

The initial EPSC amplitudes in the three examples were between about 5 and 9 nA, fairly typical values of rested calyx of Held/MNTB recordings in animals of this age group (e.g., Taschenberger and von Gersdorff 2000; von Gersdorff and Borst 2002). We term this value the "initial amplitude" or "A_0." The synaptic current then depressed substantially during the first few events of the stimulus train (*insets* in Fig. 3, *A–C*, initial steep declines of amplitudes), then declined much slower (later shallow decline of amplitudes), and then stabilized during the second half of the 2-min train to values between about 2 and 3 nA.

We were interested in these steady-state values measured during the second half of the conditioning period because

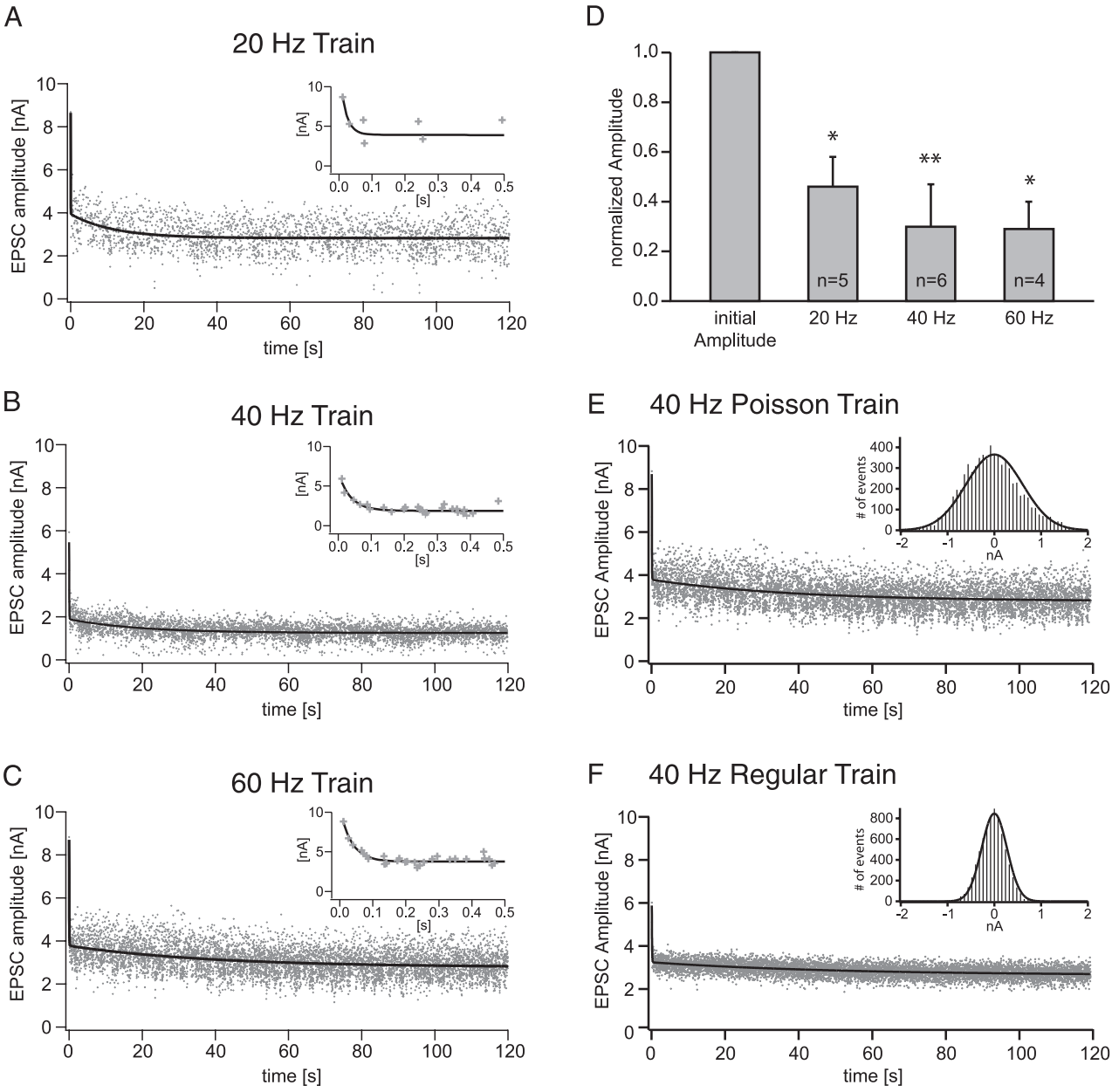

FIG. 3. *A–C*: excitatory postsynaptic current (EPSC) amplitudes of 3 representative neurons that were stimulated with 20, 40, and 60 Hz "spontaneous" Poisson-distributed activity, respectively. Graphs show the changes of EPSC amplitudes during the 2-min conditioning period. Each dot represents the amplitude of one EPSC. *Insets*: magnification of events during the first 0.5 s of conditioning. Solid lines represent double-exponential fits with the following time constants: 20 Hz: τ_{fast} = 18.3 ms, τ_{slow} = 11.7 s; 40 Hz: τ_{fast} = 36.5 ms, τ_{slow} = 19.1 s; 60 Hz: τ_{fast} = 35.6 ms, τ_{slow} = 39.3 s. *D*: comparison of initial EPSC amplitudes, termed "rested A_0 values," and EPSC amplitudes after the 2-min conditioning protocol with Poisson-distributed activity for our sample of neurons. For the 20-Hz conditioning protocol, the in vivo A_0 value was 46% of the rested A_0, for the 40-Hz conditioning it was 30%, and for the 60-Hz conditioning it was 29%. An asterisk next to a bar indicates a significantly different mean compared with the control (unconditioned) situation (Student's *t*-test). Average initial, rested A_0 values of EPSC amplitudes for the 3 groups were: 20-Hz group: 7.17 ± 0.82 nA; 40-Hz group: 6.76 ± 0,74 nA; 60-Hz group: 6,41 ± 0,66 nA; these values were not significantly different from each other (ANOVA). *E* and *F*: comparison of EPSC variability for one neuron in response to a Poisson-distributed 40-Hz stimulus train (*B*) and a regular 40-Hz stimulus train (*C*). In both cases, synaptic current amplitudes converge to the same value, although the variability in response to the Poisson-distributed stimuli are about twice the variability in response to regularly spaced stimuli of the same frequency.

we hypothesize that these values represent the normal state of the "rested" synapse in vivo. The reason is that an in vivo gerbil calyx of Held presumably would fire spontaneously at frequencies similar to the conditioning frequencies used in this experiment and thus synaptic currents, even in the absence of any sound input, would be chronically depressed to values similar to those measured during the steady-state period of the conditioning phase. Therefore we term these steady-state current values the "in vivo initial amplitude" or "in vivo A_0."

Figure 3*D* compares "rested A_0" values to "in vivo A_0" values for our sample of neurons, suggesting that typical synaptic amplitudes in the calyx of Held might be much smaller in vivo than those observed in standard in vitro experiments.

To assess the effects of the Poisson distribution, five neurons were tested with trains composed of Poisson-distributed stimuli

versus trains with regularly spaced stimuli of identical frequencies. The type of stimulus train did not affect the time course of synaptic depression or the value of the observed in vivo A_0 (Fig. 3, *E* and *F*). The difference of A_0 values within each pair was not statistically different (*t*-test, $P = 0.74$). However, the variability of synaptic currents was much larger in the case of Poisson-distributed stimuli compared with evenly spaced stimuli (Fig. 3, *E* and *F*, Gaussian curve *insets*). On average, the standard deviation of synaptic currents was 0.04 when stimuli with regularly spaced intervals were used. Presumably, one physiological basis of this variability is the stochastic nature of vesicle release. In contrast, the SD of current amplitudes was 0.08 when stimuli were Poisson distributed. Most likely, the reason for this larger variability is the additional effect of changing interspike intervals, which is added to the variability caused by stochastic release. However, note that the type of stimulus train used does not appear to affect the final observed in vivo A_0.

Effects of simulated tone bursts on "rested" versus "spontaneously" active synapses

Our next goal was to determine the effects of the "spontaneous" activity on the processing of high-frequency trains by the calyx of Held synapse. The high-frequency trains attempt to simulate simple sound-evoked activity, such as short tones. We tested trains of 20 pulses at 100, 300, and 600 Hz, which simulated pure tones of 200-, 67-, and 33-ms duration, respectively. Effects of each stimulus train were tested before the conditioning period, i.e., on the "rested" synapse, and then after the conditioning period while the simulated tone activity was embedded in the "spontaneous activity," and a third time ≥5 min after the "spontaneous" stimulation was stopped. Figure 4*A* (*black trace*) shows an EPSC train recorded in response to a 300-Hz, 20-pulse-stimulus train from a "rested" neuron. The synaptic current measured in response to the first event was about 6.9 nA. Subsequently, the synaptic current depressed during the stimulus train, such that the current measured in response to stimulus number 20 was depressed to 1.6 nA, i.e., the EPSC was now only 23% of the initial current.

After the synapse had been conditioned with "spontaneous" activity of 60 Hz, the synaptic current in response to the first stimulus of the same 300-Hz train was about 2.1 nA and thus substantially lower than that in the "rested" condition (Fig. 4*B*, first event). More interestingly, the relative depression induced by the 300-Hz train was substantially less than it was under control conditions, such that the synaptic current at stimulus number 20 was still about 1.1 nA. Therefore in the preconditioned synapse, the current was depressed to only 54% of the value of the first stimulus in the train, suggesting that the degree of relative synaptic depression under in vivo conditions might be substantially smaller than that measured by in vitro recordings from "rested" synapses.

Afterward the cell was allowed to recover for 5 min (i.e., it received no stimulation) and the synaptic amplitudes and depression ratios recovered to preconditioning values (Fig. 4*A*, *gray trace*), suggesting that the observed effects shown in Fig. 4*B* are reversible and specific and cannot be attributed to synaptic rundown or other damaging effects of the intense stimulation protocol.

Synaptic amplitudes in response to the first and last events of the various 20-pulse-test trains are shown in Fig. 4*C*. For each group of bars, the amplitude of the first event (dark gray bar) is compared with the amplitude of the 20th event after a 100-,

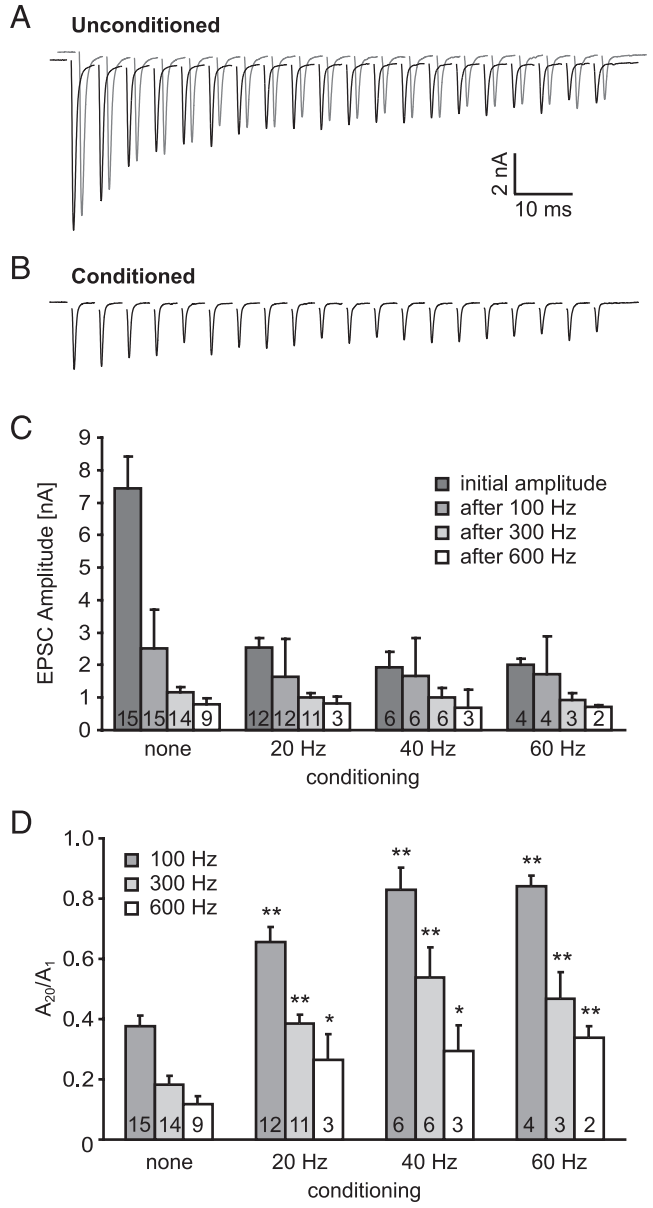

FIG. 4. *A* and *B*: responses of one neuron to the same 300-Hz, 20-pulse stimulus train before conditioning with spontaneous activity (*A*, black line), whereas the 300-Hz train was embedded in 60-Hz spontaneous activity (*B*), and about 5 min after the "spontaneous" activity was ended (*A*, gray line). *C*: absolute EPSC amplitudes with various conditioning and test frequencies. Trains of 100, 300, and 600 Hz were tested with 20 stimuli in the trains in each case. Dark bars labeled "initial amplitude" refer to the EPSC amplitude of the first event of a train (similar for 100-, 300-, and 600-Hz stimulus trains), whereas the bars labeled "after 100/300/600 Hz" refer to the amplitude of the 20th event in the train of the respective frequency. Numbers in the bars indicate sample size. *D*: ratios of synaptic current amplitudes in response to the last stimulus over the current of the synaptic response to the first stimulus of the 20-pulse trains. Low ratios indicate substantial relative depression during the 20-pulse-stimulus trains, whereas high ratios indicate low relative synaptic depression. Numbers in the bars indicate sample size. An asterisk next to a bar indicates a significantly different mean compared with the respective control (= unconditioned) condition, which is shown by the same color bar in the group "none" (Student's *t*-test).

300-, and 600-Hz stimulus train. Note that the difference in amplitudes between event 1 and event 20 is greatest in unconditioned synapses and smallest in synapses that have been conditioned with 60 Hz of Poisson activity.

Figure 4*D* shows the amount of relative synaptic depression induced by the various 20-pulse trains. The bars represent the ratio of the 20th over the first postsynaptic current amplitude of the train; i.e., small values indicate that at event 20 only a small portion of the initial synaptic current was measured and therefore synaptic depression caused by the train was substantial. High values indicate that the high-frequency trains induced a much smaller amount of relative depression because the current measured at event 20 of the train was more similar to the initial current.

Overall, the 100-Hz trains induced the lowest amount of synaptic depression (dark gray bars) and the 600-Hz trains the highest amount (white bars). More interestingly, the same high-frequency train induced a much smaller amount of relative depression when the synapse was previously conditioned with spontaneous activity. In all cases the high-frequency trains induced a significantly smaller amount of relative synaptic depression when the synapses were previously conditioned with "spontaneous activity."

Recovery of firing is very fast under in vivo–like conditions

Our next goal was to determine the recovery from synaptic depression in "spontaneously active" synapses. Recovery from depression is a critical property, especially in highly active auditory brain stem synapses, because the speed of recovery determines how well the neuron can respond to acoustic events that occur shortly after the first event. We first measured the recovery of firing patterns of MNTB neurons in vivo (Fig. 5*A*). Two identical tone bursts of 200-ms duration were presented to single MNTB units with a variable pause between them. The first tone burst elicited a certain firing rate and firing pattern in the neuron. When the second, identical tone burst was presented after only a very short pause, it elicited a lower response rate in the neuron, which was most apparent during the onset portion of the response (Fig. 5*A*, *top*). As the pause between the two tones was increased, neural responses to the second tone recovered progressively and at some point resembled the responses measured to the first tone (Fig. 5*A*, *bottom*). The in vivo recovery time course of six MNTB neurons is plotted in Fig. 5*B*. Among these six neurons, the average in vivo recovery time constant was 82 ± 23 ms, suggesting that recovery of neural responses in the MNTB to acoustic stimuli in vivo is typically very short.

This finding raises a dilemma because recovery from synaptic depression has been measured in the calyx of Held in vitro, with very different results. In these experiments, the presynaptic vesicle pool was depleted, either with a depleting high-frequency stimulus or by voltage clamping the presynaptic terminal to a positive potential. After this pool depletion, test stimuli were given at distinct time intervals to assess the degree of recovery. These experiments typically found recovery time constants at the order of several seconds, not milliseconds (e.g., von Gersdorff et al. 1997; Wang and Kaczmarek 1998).

The in vivo data and the in vitro data are not directly comparable because of additional recoveries at the level of the hair cells, auditory nerve (e.g., Spassova et al. 2004), and cochlear nucleus, as well as potential effects of inhibition. However, the in vivo recovery shown in Fig. 5*B* has to present an upper limit for the vesicular recovery at the level of the calyx of Held because the calyx of Held is one element of the network tested with the in vivo experiment. Therefore the in vivo data suggest that recovery from synaptic depression at the calyx of Held should occur with time constants of no longer than about 80 ms.

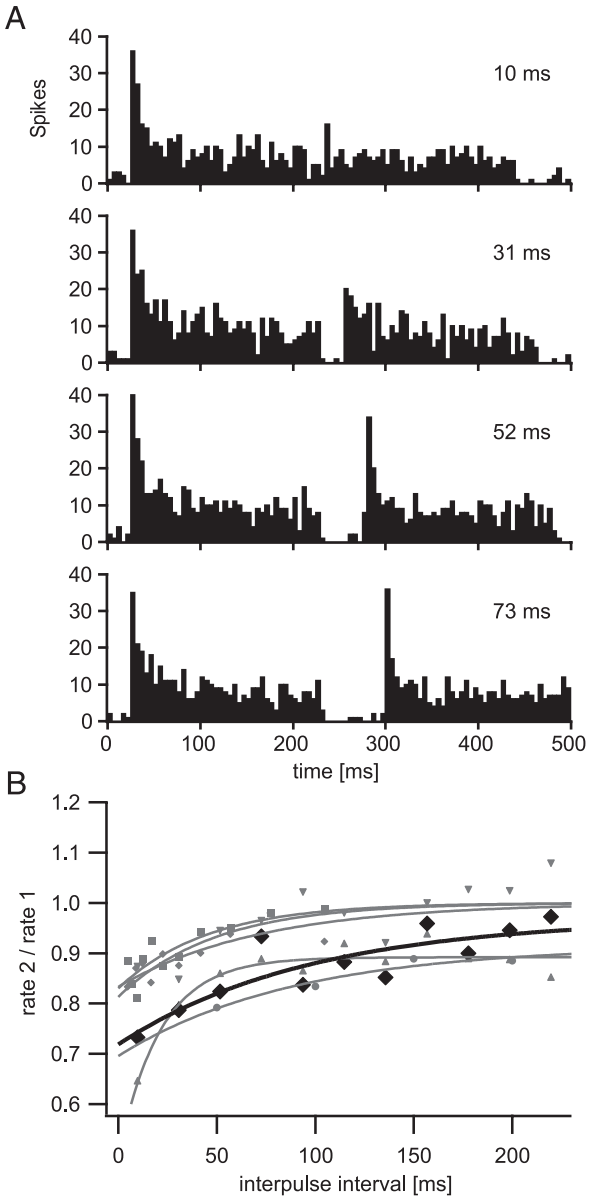

FIG. 5. *A*: poststimulus time histograms of a single MNTB neuron's in vivo responses to 2 identical best frequency (BF) tone bursts of 200-ms duration with varying ISIs. As the ISI was increased, the neuron's responses to the second tone recovered back to a point where the responses to the second tone were comparable to the neuron's firing pattern in response to the first tone. Tones were presented at 1,200 Hz and 30 dB above threshold. Firing frequencies in response to the first tone were about 260 Hz for the onset response only (= first 15 ms) and about 80 Hz for the sustained part of the response. For the second tone, the onset response varied between 90 and 260 Hz (10- and 73-ms ISI, respectively), whereas the sustained part varied between 52 and 72 Hz (10- and 73-ms ISI, respectively). *B*: time constants of in vivo recovery of firing of 6 single MNTB units. Neuron presented in *A* is indicated by the bold black line.

Recovery from depression is very fast in spontaneously active synapses

To test this, we measured recovery from depression in vitro. Recovery time constants were determined initially in unconditioned neurons by depleting the vesicle pool with a high-frequency train, then allowing the synapse to recover for a specified amount of time, and finally measuring the relative amplitude of a test EPSC. An example of a synapse in which the time course of recovery was determined with this method is shown in Fig. 6, *A* and *B*. Figure 6*A* shows data points on a magnified time axis, following a recovery time course that was best described with an exponential that had a time constant of 72 ms. The average fast time constant of our sample of neurons was 87 ± 16 ms. However, the fast time constant accounted for only about half of the recovery. Complete recovery to the rested A_0 value could best be described with double-exponential fits (Fig. 6*B*). The slow time constant of the same synapse shown in Fig. 6*A* was 1.84 s (Fig. 6*B*), whereas the average slow time constant of our sample of neurons was 1.59 ± 0.17 s. In each case tested, the two time constants together could account for the complete amplitude of the rested A_0 value.

Because of the nature of the experimental protocol, recovery from depression could not be measured in conditioned synapses with the same method as used earlier because the required time intervals (up to several seconds) would be far longer than the amount of time that a neuron is nonactive during "spontaneous activity". Therefore the time course of recovery in conditioned neurons was measured by fitting an exponential function to the time course of EPSC amplitude recovery as a function of the preceding interpulse interval. The various interpulse intervals, which inherently occur during a Poisson-distribution of spikes, yield a suitable range of time periods to measure the fast recovery time constant. When this was done, we found fast time constants very similar to those found in unconditioned synapses. Figure 6*C* shows an example of a cell in which recovery from depression was measured with the described method. For events where the test stimulus followed shortly after a previous stimulus, the EPSC amplitude of the test EPSC was small. As the time interval before the test stimulus increased, the amplitude of the EPSC progressively increased, presumably as a result of recovery from depression. For this synapse, the time constant of recovery from depression was 74 ms. The average recovery time constant for our sample of neurons was 90 ± 15 ms. As for the unconditioned synapse, the relative contribution of the fast time constant to overall recovery accounted for about half of the rested A_0 amplitude. Therefore we assume that the (missing) slow component of recovery in conditioned synapses might be similar to that of unconditioned synapses, although we were unable to measure this parameter for the reason described earlier.

The fast recovery time constants of both unconditioned and conditioned synapses are very similar to the recovery time constants measured in vivo shown in Fig. 5, suggesting that recovery from activity in the calyx of Held occurs at a time course similar to that of the recovery of other components of the circuit. Although we also found a slow component of recovery that was in a range similar to that described previously by other groups, our in vivo data suggest that the

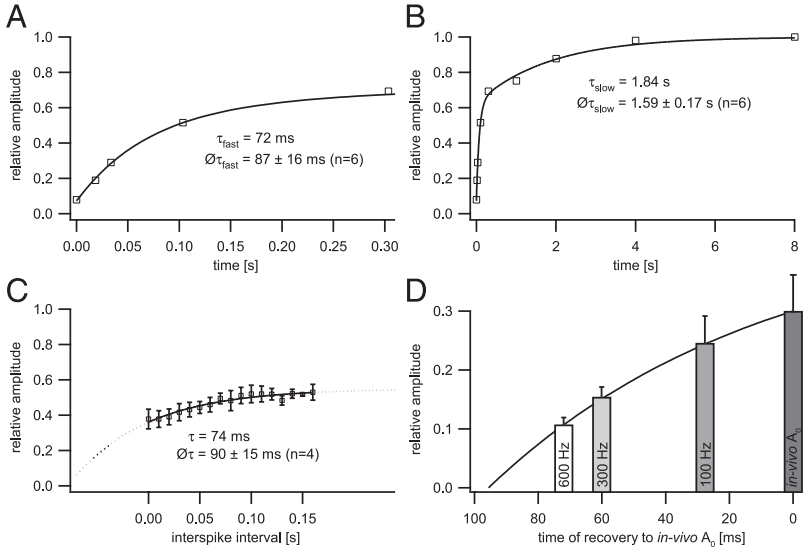

FIG. 6. *A* and *B*: recovery from depression in unconditioned synapses. Data were obtained with a protocol that depletes the vesicle pool with a 300-Hz, 20-pulse-stimulus train, followed by a pause of variable time to allow for pool refilling, followed by a test stimulus. Amplitudes plotted in graphs refer to the amplitudes measured in response to the test stimulus. Recovery could be best described with double-exponential fits that had fast time constants of 87 ± 16 ms and slow time constants of 1.59 ± 0.17 s. *C*: recovery from depression in conditioned synapses. In contrast to *A* and *B*, recovery was assessed by analyzing the variable ISIs inherently contained in the Poisson-distributed trains. Only the fast component was measured here and was found to be very similar to the fast component of unconditioned synapses. *D*: illustration of recovery from depression in active synapses, which happens within milliseconds. In vivo A_0 point is indicated at *time = 0*; the amplitude of the bar is based on data in Fig. 3*D*. This amplitude represents the state of a synapse after it has been conditioned with a 60-Hz Poisson train for several minutes, but has not received a high-frequency stimulation. Presumably, this situation compares to the state of a synapse in an intact brain, while the animal is not receiving sound stimulation. Typical values for synaptic currents after 100-, 300-, and 600-Hz 20-pulse stimulus trains are presented in the graph. These amplitudes presumably compare to the state of a synapse after a short tone burst has just been played to the animal. Naturally, synaptic amplitudes are lower than those in the in vivo A_0 state, as a result of the recent high-frequency activity. Position of the bars along the *x*-axis is chosen such that the respective amplitudes correspond to the value of the exponential curve at the same time. Time of recovery indicates the time it would take for the synapse to recover in vivo from one of the mentioned 20-pulse-stimulus trains back to the in vivo A_0 point. Time constant of exponential = 90 ms, corresponding to the average value presented in Fig. 6*C*; values of bars correspond to last group of bars in Fig. 4*C*.

short time constant might be the dominant one for in vivo recovery.

This point is further illustrated in Fig. 6*D*. The general idea of this cartoon is that recovery in vivo does not proceed up to the point of a completely full pool, i.e., the rested A_0 seen in silenced synapses in brain slices. Rather, in vivo, recovery of the calyx progresses up to the in vivo A_0, the value of synaptic current that is typically available to a spontaneously active and thus chronically depressed synapse for the processing of high-frequency sound stimuli. The graph in Fig. 6*D* plots a typical exponential time course of recovery with a time constant of 90 ms, as determined earlier. The typical "in vivo A_0" point of a synapse, which is spontaneously active at 60 Hz without acoustic input, is marked at *time 0* (value = 29% of the rested A_0; see Fig. 3*D*). When the synapse now processes a tone burst of 20 pulses at 100, 300, or 600 Hz, the synaptic amplitude depresses even further, typically to the values indicated by the respective bars (values of amplitudes based on data from Fig. 4*D*). At the end of the tone burst, the synapse recovers back to the in vivo A_0 value, which takes longer or less long, depending on the frequency of the tested stimulus and the resulting depression. In this example, which assumes an exponential time course of 90 ms for vesicle pool refilling, the recovery of the synapse back to the in vivo A_0 point would take between 25 and 74 ms. In other words, a spontaneously active synapse might need only 25–74 ms to recover from a high-frequency sound input because the synapse is chronically depressed by the spontaneous activity and thus recovers only partially back to the steady-state level.

Reduced synaptic reliability in active calyces

The data presented so far suggest that synaptic currents produced by the calyx of Held under simulated in vivo conditions are considerably smaller than those typically measured in vitro in "rested" or silent brain slices. The very large synaptic currents produced by rested calyces in older animals are known to bring postsynaptic neurons well above threshold for firing and thus allow for secure synaptic transmission (e.g., Taschenberger and von Gersdorff 2000). In light of the synaptic currents seen under the simulated in vivo conditions, presented earlier, we next asked the question whether these reduced currents are still suitable for fail-safe synaptic transmission.

This question was addressed with three different techniques. First, current-clamp data were obtained from MNTB neurons, whereas the calyceal fiber bundle was stimulated, with stimulation protocols equivalent to those used for the voltage-clamp experiments shown earlier. Figure 7*A* shows the firing pattern of a representative neuron in response to a 300-Hz, 20-pulse-stimulus train. Consistent with previous reports, the neuron responded faithfully to the 300-Hz train—i.e., it fired one action potential in response to each synaptic event—when the slice was rested. However, after the neuron was conditioned with 60 Hz of "spontaneous activity" as described earlier, the same 300-Hz stimulus train elicited a substantial number of synaptic failures (Fig. 7*B*). For those events where the neuron failed to fire an action potential, a small excitatory postsynaptic potential (EPSP) could be observed in the voltage trace, suggesting that the calyx of Held fired an action potential and produced a synaptic current in response to the stimulus. However, the synaptic current appears to have been subthreshold. The probability of a failure to occur increased with the number of the event in the 20-pulse train. Events early in the train were less likely to fail than events in the latter part of the stimulus train.

Among our sample of neurons tested with this method, we observed some variability in the number of failures as well as other response characteristics. For example, some neurons showed fewer failures, whereas others showed a higher number. Also, in some neurons stimulation of the fiber pathway with 300 Hz resulted in a small plateau from which action potentials to the stimuli were fired (Fig. 7*A*), whereas the plateau was absent in other neurons. Also, we observed some variation in the height of the action potential. Differences in channel complement or best frequency to which the neuron was tuned might account for this variability.

For our sample of neurons, the probability of a postsynaptic spike was tested as a function of the position of the event in the train. Firing probability was defined as the number of spikes fired in response to a given stimulus in the train over the number of repetitions presented. In the unconditioned synapse, the firing probability was almost 100% throughout the 300-Hz stimulus train; very few failures occurred toward the end of the stimulus train (Fig. 7*H*, black dotted line and open circles, $n = 5$). However, when synapses were conditioned with 60 Hz of spontaneous activity, the number of failures during the 300-Hz train increased (Fig. 7*H*, black solid line and closed circles, $n = 5$). In most cases, postsynaptic neurons still answered reliably during the initial three or four events of the train, although the reliability declined afterward.

The reliability of synaptic transmission was also tested with conductance-clamp recordings. The advantage of conductance clamp was twofold: First, this method does not rely on the presynaptic axons and the calyx to follow the intense stimulation protocol. Therefore synaptic failures arising from axonal failures can be ruled out more reliably than with the technique presented earlier. Second, conductance clamp offers the possibility of combining simulated synaptic currents with added background leaks to reduce the neuron's input resistance (see following text). In our recordings, EPSG waveforms derived from 300-Hz EPSC trains were used to simulate calyceal synaptic currents in response to a 300-Hz stimulus train. Two waveforms were used in these experiments: a 300-Hz, 20-pulse EPSG waveform that simulated synaptic currents of a rested calyx (Fig. 7*C*, *bottom*) and an EPSG waveform that simulated the response of a calyx to the same stimulus train embedded in spontaneous activity (Fig. 7*D*, *bottom*). Both waveforms were previously recorded as EPSC waveforms from an MNTB neuron under voltage-clamp conditions, while electrically stimulating the input fibers to the calyx. The waveforms were chosen to reflect the observation that peak EPSC currents are larger in rested than in conditioned synapses (Fig. 3*D*) and that synaptic depression within a high-frequency train is reduced in active synapses (Fig. 4, *A* and *B*). Conductance-clamp recordings with these two waveforms were performed on seven MNTB neurons. The neurons reliably fired action potentials when excitatory synaptic currents typical for a rested calyx were injected (Fig. 7*C*, *top*). In the rare case that failures could be observed, they occurred toward the end of the train (Fig. 7*H*, red dotted line and open squares, $n = 7$). However, when currents typical for a spontaneously active synapse were used, failures in the neuron's response to the 300-Hz, 20-pulse EPSG

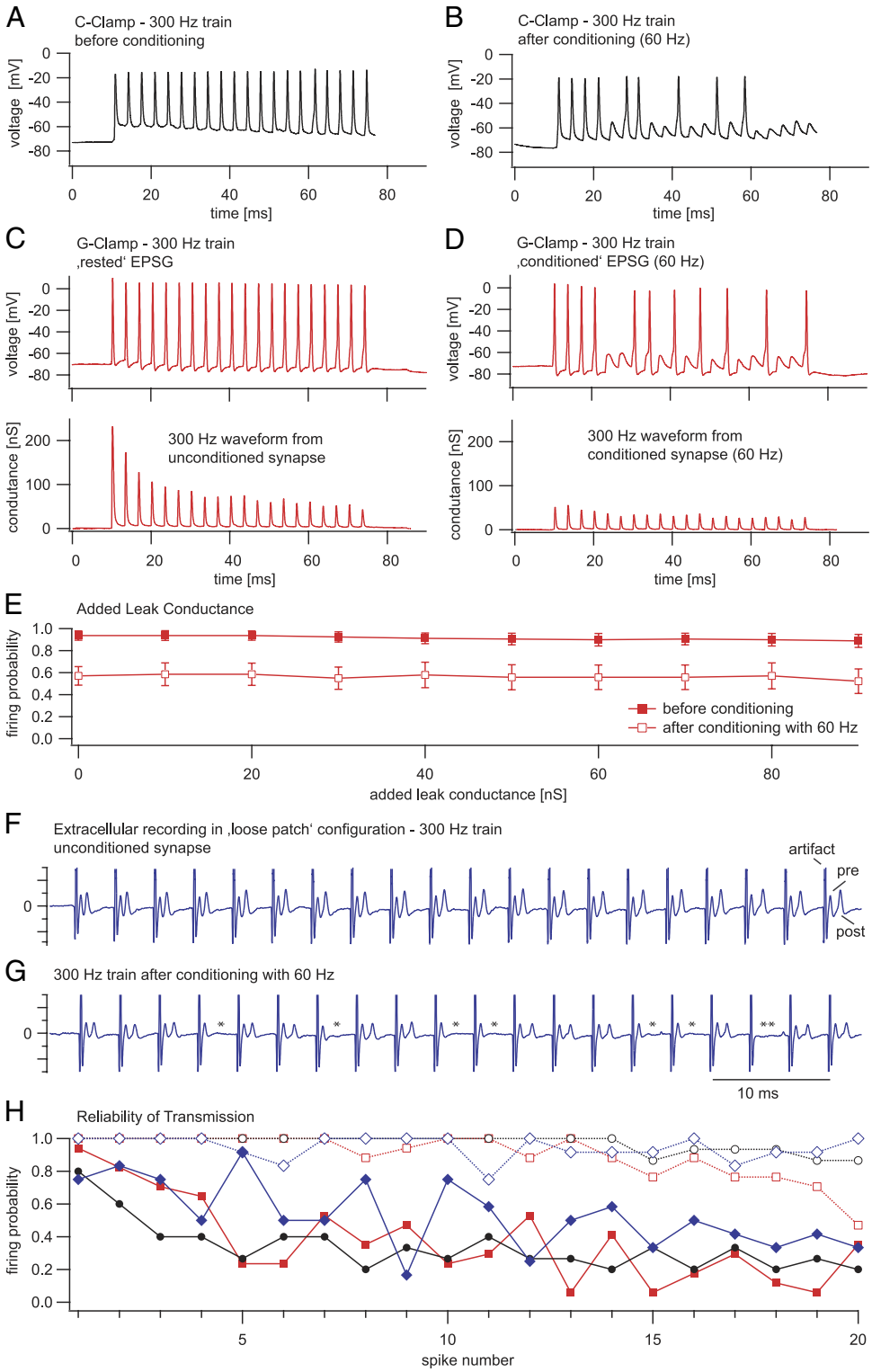

FIG. 7. Reliability of synaptic transmission in spontaneously active synapses. *A*: current-clamp recording of MNTB neuron while the calyceal input fibers were stimulated with a 300-Hz, 20-pulse train; the neuron responded to each stimulation with one action potential. *B*: after the slice was conditioned with 60 Hz of spontaneous activity, a number of failures could be observed during the same 300-Hz train. For each failure, an excitatory postsynaptic potential can be observed in the place of the missing action potential, suggesting that the failure was postsynaptic. *C*, *top*: responses of MNTB neuron when a 300-Hz conductance waveform was used to simulate currents of a rested synapse; the neuron responded to each event with one action potential, similar to that observed when the calyceal fibers were stimulated. Conductance waveform is shown in the *bottom panel*. Peak conductance was 232 nS. *D*, *top*: responses of MNTB neuron when a 300-Hz conductance waveform was used to simulate currents of a synapse that was conditioned with 60 Hz of spontaneous activity; the neuron failed to respond to a number of events. Corresponding conductance waveform is shown in the *bottom panel*. Peak conductance was 56 nS. *E*: various levels of background leak were added to the EPSG waveforms under conductance-clamp conditions, effectively reducing the input resistance of the neurons to values that are closer to input resistances observed in neurons under in vivo conditions. *F* and *G*: example of a loose-patch recording of a MNTB neuron while calyceal input fibers were

train could be observed (Fig. 7*D*, *top*). These failures tended to occur more frequently toward the end of the EPSG waveform, but could sometimes also be observed early in the train (Fig. 7*H*, red solid line and closed squares, $n = 7$).

Interestingly, the firing probabilities and frequencies for conditioned synapses shown in Fig. 7*E* closely match those observed in vivo. For both current-clamp and conductance-clamp experiments, the firing probability of the first few events in the train was 0.7 to 1.0, based on the calculation method described earlier. For a train frequency of 300 Hz, this corresponds to a firing frequency of about 200 to 300 Hz. The onset portion of the in vivo spike trains shown in Fig. 5*A* had a firing frequency of about 260 Hz (considered is the response to first tone of the pair only). The average firing frequency of the neuron in response to the latter part of the 200-ms tone was about 80 Hz. This corresponds well to the in vitro data shown in Fig. 7*E*, where the firing probability of the neuron to the latter portion of the train is about 1/3, i.e., about 100 Hz.

A number of studies have observed that a neuron's input resistance is substantially higher in brain slices than in the intact brain (e.g., Bernander et al. 1991; Paré et al. 1998). The main reason for this observation is probably that neurons in the intact brain receive a large number and variety of synaptic inputs. When these inputs are activated at different points in time, postsynaptic receptors open and thus decrease the neuron's input resistance. In brain slices, many of these inputs are silent and/or cut, with the result that the neuron's input resistance increases. It is unknown whether and how much the input resistance of an MNTB neuron differs in brain slices compared with the intact brain because the projection pattern to MNTB neurons is much simpler than in the case of, say, cortical neurons. However, prominent glycinergic inhibition to MNTB has been described in vitro (Awatramani et al. 2004). These inputs, when activated, will decrease the input resistance of postsynaptic neurons. An artificially high-input resistance in neurons of MNTB brain slices would facilitate the neuron's responses to synaptic events. In this case, the synaptic failures shown in Fig. 7, *A–E* would be an underestimate of the true in vivo failure rates. We attempted to address this issue by adding a background leak to MNTB neurons during presentation of the EPSG waveforms. The background leak had a constant amplitude of 10–90 nS with a reversal potential of −60 mV and effectively reduced the input resistance of the postsynaptic neuron up to fivefold. Figure 7*F* shows the overall firing probability of six MNTB neurons, when EPSG waveforms of 300-Hz trains plus various amounts of background leak were tested. As expected, the firing probability decreased with increasing background leak, although the effect was minor.

The last approach to test the reliability of synaptic transmission was to use "loose-patch" extracellular recordings. For these experiments, an MNTB neuron in a brain slice was only loosely patched without obtaining a gigaseal and no break-in into the neuron was performed, such that the recordings were effectively extracellular. In some recordings, action potentials of both the calyx of Held (termed "prepotential") and the postsynaptic principal neuron could be observed. An example is shown in Fig. 7, *F* and *G*. In this recording, stimulation of the calyceal input fibers produced three peaks in response to each event. The first one was the stimulation artifact (labeled "artifact"), followed by the prepotential (labeled "pre"), and then followed by the postsynaptic action potential (labeled "post"). The advantage of this method is that the interior environment of the postsynaptic cell is left undisturbed. For whole cell recordings, a common concern is that the perfusion of the neuron with artificial intracellular fluid might change the firing properties of the neuron, which would result in inaccurate measurements of failure rates. However, even when the postsynaptic neuron was left intact, transmission failures could be observed in the calyx of Held synapse when the slice was driven at in vivo–type activity levels. Figure 7*F* shows a loose-patch recording of a rested brain slice. Consistent with the data shown earlier, the synapse was appreciably fail-safe when a 300-Hz, 20-pulse train was tested, i.e., each prepotential was followed by a postsynaptic action potential (Fig. 7*F*). However, when the slice was conditioned with 60-Hz spontaneous activity, a substantial amount of failures could be observed in response to the same 300-Hz test train (Fig. 7*G*; postsynaptic failures are indicated by single asterisks). In one case, neither a prepotential nor a postpotential could be observed (marked by a double asterisk), suggesting that for this event, the failure must have occurred in the calyceal input fiber. The blue lines in Fig. 7*H* show the average reliability of transmission measured with this technique (blue dotted line and open diamonds: unconditioned synapses, $n = 6$; blue solid line and closed diamonds: conditioned synapses, $n = 6$).

Furthermore, the latency of synaptic transmission was increased when synapses were spontaneously active (Fig. 7, *F* and *G*). In this cell, the synaptic latency increased by 0.19 ms when the synapse was conditioned. For all 11 neurons from which spike-latency data were available, the average latency increase was 0.4 ± 0.13 ms. This discrepancy matches well with the discrepancy between published values for in vitro synaptic latency (Taschenberger et al. 2002; von Gersdorff and Borst 2002) versus in vivo latency (Guinan and Li 1990; Kopp-Scheinpflug et al. 2003) at the calyx of Held. These data suggest that highly active calyces have a longer synaptic latency than previously reported in vitro, but also that our conditioning protocol might be suited to transform calyces into a functional state that more closely resembles the functional state of an active in vivo calyx of Held.

In summary, the data presented in Fig. 7 suggest that the calyx of Held synapse shows a substantial amount of synaptic

stimulated. In loose patch recordings, no gigaseal is formed and no break-in into the cell is performed. Because the recording is effectively extracellular, the internal environment of the postsynaptic cell is undisturbed. Even under these conditions, MNTB neurons exhibited a substantial number of failures in response to a 300-Hz train, when the slice was conditioned with 60 Hz of spontaneous activity. Artifact = stimulation artifact; pre = prepotential = presynaptic action potential; post = postsynaptic action potential. Postsynaptic failures are indicated by a single asterisk. For one event, neither a prepotential nor a postpotential could be observed (double asterisk), suggesting an axonal failure for that event. *H*: firing probability as a function of the number of the event in the 20-pulse train. Black graphs with circular symbols represent data from 5 neurons tested with current clamp as described in *A* and *B*. Red graphs with squared symbols represent data from 7 neurons tested under conductance clamp conditions, as described in *C* and *D*. Blue graphs with diamond symbols represent data from 6 neurons tested with extracellular, loose-patch recordings. For all experimental methods, few failures could be observed under conditions that correspond to a rested synapse, and occurred toward the end of the 20-pulse train (open symbols and dotted lines). However, for situations that correspond to a spontaneously active synapse, the same 300-Hz trains elicited a substantial number of failures (solid symbols and solid lines). Firing probability of a given neuron was defined as the ratio of number of action potentials per 3 stimulations. Presented in graph are average firing probabilities of 5–7 neurons per method, as described earlier.

failures, after cells were stimulated for several minutes with Poisson-distributed activity. One possible interpretation of these results is that in vivo, the MNTB might not be the simple and reliable relay that is commonly observed under standard in vitro conditions.

DISCUSSION

The main question addressed in this study is the question of how synaptic transmission in the calyx of Held synapse changes when synapses are stimulated for prolonged periods of time with Poisson-distributed activity, which, we hypothesize, imitates naturally occurring spontaneous activity. There are four main findings. First, the introduction of "spontaneous" activity into in vitro preparations of the calyx of Held considerably depresses synaptic currents, even at relatively low spontaneous frequencies of 20 Hz. Second, in these "spontaneously active" synapses, the degree of additional depression induced by high-frequency trains (i.e., simulated sound inputs) is reduced considerably. Third, recovery from synaptic depression is very fast. Data from corresponding in vivo extracellular recordings also show fast recovery of firing and are consistent with these in vitro findings. Fourth, in chronically active synapses with reduced synaptic currents, the reliability of transmission is reduced during high-frequency bursts of afferent input.

Background firing in MNTB neurons

Spontaneous activity in the lower auditory system is a widespread phenomenon. It is assumed that this activity is explained by the probabilistic behavior of the transduction channels of the inner hair cells and the resulting chronic transmitter release at the hair cell synapse. The spontaneous activity is still present at the level of the cochlear nucleus (Brownell 1975; Goldberg and Brownell 1973; Joris et al. 1994; Schwarz and Puil 1997; Spirou et al. 1990, 2005) and most auditory brain stem nuclei, such as MSO in bats (Grothe 1994), MNTB in cats (Smith et al. 1998), MNTB in gerbils (Kopp-Scheinpflug et al. 2003), and MNTB in rats (Sommer et al. 1993). Consistent with our data presented here, studies of spontaneous activity in the lower auditory system typically report a large variability of rates among neurons, even within the same species or the same nucleus. One possible explanation for this large variability is that different neurons receive inputs from different classes of auditory nerve fibers with low, medium, or high spontaneous rates (Liberman 1978), which would give rise to auditory brain stem neurons with very diverse spontaneous firing rates.

For the experiments presented here, three frequencies of Poisson-distributed activity were chosen for stimulation of brain slices: 20, 40, and 60 Hz. Although the mean spontaneous firing rate in our sample of neurons was 24.9 Hz and thus closer to the lowest of these frequencies, the three frequencies chosen for stimulation successfully cover the spectrum of observed in vivo spontaneous rates (see Fig. 2*A*; see also Kopp-Scheinpflug et al. 2003). However, because of the nature of the brain slice preparation, the original in vivo spontaneous firing rate of a given neuron is unknown. Therefore it is possible or even likely that an originally low spontaneously active neuron was stimulated with a high-frequency stimulus train and vice versa. However, all neurons in our in vitro sample responded stereotypically and in a very similar fashion to our various stimulus protocols and no responses were observed that could be explained by the use of an inappropriate background stimulation rate.

Measurements of spontaneous activity presented in this study were performed under anesthesia. As with almost every type of anesthesia, the ketamine–xylazine mixture used in this study might have depressed the neurons' spontaneous activity to a certain degree (Destexhe et al. 2003). Therefore the actual spontaneous firing rates in MNTB neurons of behaving gerbils might be higher than those shown in this study. On the other hand, the values for spontaneous activity determined here match closely with findings of other studies using various species and various types of anesthesia or, in some cases, no anesthesia at all (e.g., Irvine 1992; Kiang 1965; Ryan and Miller 1978). We therefore conclude that the values presented here are representative or, at worst, a conservative lower limit of the true effects induced by spontaneous activity.

We also note that double-walled sound-attenuated rooms by themselves create the biologically unnatural situation of complete absence of sound. Natural auditory environments always contain a certain level of background noise, which contributes to the background activity of auditory neurons. Therefore the effects of chronic activity on synaptic transmission in behaving animals might be even larger, but are not likely to be smaller than presented here.

Prolonged spontaneous spiking changes properties of synaptic transmission

Our data show that prolonged stimulation even at a frequency of 20 Hz decreases synaptic currents to less than half of the original value, whereas stimulation with frequencies of 60 Hz reduces currents to about one third. It might be surprising to find that such low frequencies cause such a high degree of depression because all brain slices were prepared from animals well past the onset of hearing and recordings were performed at physiological temperature. α-Amino-3-hydroxy-5-methyl-4-isoxazolepropionic acid (AMPA) receptor desensitization as well as *N*-methyl-D-aspartate (NMDA) currents, although playing a substantial role in preparations from young animals (Neher and Sakaba 2001; Sakaba and Neher 2001), play only a very minor role in animals past the age of hearing onset (Futai et al. 2001; Renden et al. 2005; Taschenberger et al. 2005). Under these conditions, MNTB neurons can follow stimulation frequencies of ≥600 Hz for at least short periods (Futai et al. 2001; Taschenberger and von Gersdorff 2000; Wu and Kelly 1993). The depression we observed in response to long-term stimulation progressed with at least two time constants: an initial, fast time constant, which can be seen during the first few stimulus pulses, and a much slower time constant. The mechanisms for the slow time constant are unclear, but are likely to be multiple and will be studied in the future. When the processing of high-frequency trains was tested in rested versus spontaneously active synapses, the observed relative degree of synaptic depression caused by the high-frequency train was much larger in the rested than in the active synapse. This might have important functional implications at the calyx of Held, which sustains high levels of activity.

Our findings also suggest that recovery from synaptic depression is very fast under biologically relevant activity levels. These time constants of about 90 ms are an order of magnitude shorter than previously reported values for rested synapses, which are in the range of several seconds (e.g., von Gersdorff et al. 1997: 4.2 s; see also Ishikawa and Takahashi 2001; Schneggenburger et al. 2002; Wang and Kaczmarek 1998; Wu and Borst 1999). Age, temperature, and species differences might account for some of this discrepancy. However, there is strong evidence suggesting that calcium accumulation in the presynaptic terminal through high-frequency firing may play a role in speeding up the recovery from depression (Wang and Kaczmarek 1998). It appears that this faster recovery plays a dominant role in active synapses.

Reliability of synaptic transmission

In vitro studies of the calyx of Held in animals past hearing onset have reported very reliable synaptic transmission and a number of cellular specializations to increase synaptic reliability. Our data are consistent with the view that "rested" calyces produce large synaptic currents and have a high transmission reliability. However, we show that in chronically active synapses, the synaptic currents are much smaller. Our current-clamp, conductance-clamp, and extracellular action potential recordings all suggest that spontaneously active synapses may show synaptic failures during periods of high-frequency activity. Therefore the calyx of Held may not always show the reliable 1:1 transmission postulated from in vitro experiments in rested synapses. This finding is consistent with previous in vivo results from the MNTB. Among the in vivo studies performed in the MNTB only those where both presynaptic and postsynaptic activity have been recorded simultaneously can address the question of transmission failures at the calyx of Held synapse. To our knowledge, two studies report simultaneous pre- and postsynaptic recordings at the MNTB and both agree on the occurrence of postsynaptic failures (Guinan and Li 1990; Kopp-Scheinpflug et al. 2003) in vivo. However, the two studies differ in the number of failures observed. Guinan and Li (1990) found failures mainly with prolonged high-frequency stimulation of the afferent fiber bundle and only occasionally with sound stimulation, whereas Kopp-Scheinpflug et al. (2003) found a substantial number of failures with sound stimulation. Species differences might account for some of this discrepancy, but note that these recordings were performed with intact synaptic inhibition and under anesthesia. Because MNTB neurons are known to receive a substantial amount of glycinergic inhibition (Awatramani et al. 2004), it is possible that some of these failures are the result of spike suppression by inhibition and that some of the difference observed in the two studies arises from differential recruitment of synaptic inhibition. Nevertheless, the presence of synaptic inhibition alone also questions the interpretation of the calyx of Held as a fail-safe "relay" synapse. This view has been formed by previous in vitro studies performed in slices from animals past hearing onset, where EPSCs well above action potential threshold have been measured even in response to stimulus frequencies of several hundred Hertz. However, these stimulus trains typically consisted of no more than 20–50 stimuli, with considerable recovery time of several seconds between trials. Our experimental setup avoided these periods of silence because they do not occur under in vivo conditions. Presumably the lack of prolonged periods of recovery keeps calyces in a chronic state of synaptic depression and causes transmission to fail during periods of embedded high-frequency activity.

In conclusion, the aim of this study was to perform a first description of the effects of prolonged "spontaneous activity" on synaptic transmission at the calyx of Held synapse. We conclude from our data that synaptic transmission in the calyx of Held differs in a number of significant ways when synapses are stimulated with a Poisson-distributed stimulus train for prolonged periods of time. Future studies will determine the specific contribution of multiple modulators, receptors, or channel types in the calyx of Held synapse to the "rested" or the "spontaneously active" synaptic state.

ACKNOWLEDGMENTS

We thank F. Felmy, G. Pollak, L. Trussell, and J. Gittelman for critical comments on the manuscript.

GRANTS

H. von Gersdorff was funded by a "Mercator Professor" award from Deutsche Forschungsgemeinschaft (DFG) and National Institute on Deafness and Other Communication Disorders Grant R01 DC-04274. The research was funded by DFG Grant KL-1842 to A. Klug.

REFERENCES

Awatramani GB, Turecek R, Trussell LO. Inhibitory control at a synaptic relay. *J Neurosci* 24: 2643–2647, 2004.

Banks MI, Smith PH. Intracellular recordings from neurobiotin-labeled cells in brain slices of the rat medial nucleus of the trapezoid body. *J Neurosci* 12: 2819–2837, 1992.

Barnes-Davies M, Forsythe ID. Pre- and postsynaptic glutamate receptors at a giant excitatory synapse in rat auditory brainstem slices. *J Physiol* 488: 387–406, 1995.

Bernander O, Douglas RJ, Martin KA, Koch C. Synaptic background activity influences spatiotemporal integration in single pyramidal cells. *Proc Natl Acad Sci USA* 88: 11569–11573, 1991.

Bledsoe SC Jr, Snead CR, Helfert RH, Prasad V, Wenthold RJ, Altschuler RA. Immunocytochemical and lesion studies support the hypothesis that the projection from the medial nucleus of the trapezoid body to the lateral superior olive is glycinergic. *Brain Res* 517: 189–194, 1990.

Borst JG, Sakmann B. Calcium influx and transmitter release in a fast CNS synapse. *Nature* 383: 431–434, 1996.

Brownell WE. Organization of the cat trapezoid body and the discharge characteristics of its fibers. *Brain Res* 94: 413–433, 1975.

Destexhe A, Rudolph M, Paré D. The high-conductance state of neocortical neurons in vivo. *Nat Rev Neurosci* 4: 739–751, 2003.

Forsythe ID. Direct patch recording from identified presynaptic terminals mediating glutamatergic EPSCs in the rat CNS, in vitro. *J Physiol* 479: 381–387, 1994.

Futai K, Okada M, Matsuyama K, Takahashi T. High-fidelity transmission acquired via a developmental decrease in NMDA receptor expression at an auditory synapse. *J Neurosci* 21: 3342–3349, 2001.

Geisler CD, Deng L, Greenberg SR. Thresholds for primary auditory fibers using statistically defined criteria. *J Acoust Soc Am* 77: 1102–1109, 1985.

Goldberg JM, Brownell WE. Discharge characteristics of neurons in anteroventral and dorsal cochlear nuclei of cat. *Brain Res* 64: 35–54, 1973.

Grothe B. Interaction of excitation and inhibition in processing of pure tone and amplitude-modulated stimuli in the medial superior olive of the mustached bat. *J Neurophysiol* 71: 706–721, 1994.

Guinan JJ Jr, Li RY. Signal processing in brainstem auditory neurons which receive giant endings (calyces of Held) in the medial nucleus of the trapezoid body of the cat. *Hear Res* 49: 321–334, 1990.

Held H. Die centrale Gehörleitung. *Archiv Anat Physiol Anat Abteil* 1893: 201–247, 1893.

Hudspeth AJ. How hearing happens. *Neuron* 19: 947–950, 1997.

Irvine DRF. Physiology of the auditory brainstem. In: *The Mammalian Auditory Pathway: Neurophysiology*, edited by Popper AN, Fay RR. New York: Springer-Verlag, 1992, p. 153–231.

Ishikawa T, Takahashi T. Mechanisms underlying presynaptic facilitatory effect of cyclothiazide at the calyx of Held of juvenile rats. *J Physiol* 533: 423–431, 2001.

Joris PX, Carney LH, Smith PH, Yin TC. Enhancement of neural synchronization in the anteroventral cochlear nucleus. I. Responses to tones at the characteristic frequency. *J Neurophysiol* 71: 1022–1036, 1994.

Joshi I, Shokralla S, Titis P, Wang LY. The role of AMPA receptor gating in the development of high-fidelity neurotransmission at the calyx of Held synapse. *J Neurosci* 24: 183–196, 2004.

Kadner A, Kulesza RJ Jr, Berrebi AS. Neurons in the medial nucleus of the trapezoid body and superior paraolivary nucleus of the rat may play a role in sound duration coding. *J Neurophysiol* 95: 1499–1508, 2006.

Kiang NY-S. *Discharge Patterns of Single Fibers in the Cat's Auditory Nerve.* Cambridge, MA: MIT Press, 1965.

Klyachko VA, Stevens CF. Excitatory and feed-forward inhibitory hippocampal synapses work synergistically as an adaptive filter of natural spike trains. *PLoS Biol* 4: e207, 2006.

Kopp-Scheinpflug C, Lippe WR, Dorrscheidt GJ, Rubsamen R. The medial nucleus of the trapezoid body in the gerbil is more than a relay: comparison of pre- and postsynaptic activity. *J Assoc Res Otolaryngol* 4: 1–23, 2003.

Kuwabara N, DiCaprio RA, Zook JM. Afferents to the medial nucleus of the trapezoid body and their collateral projections. *J Comp Neurol* 314: 684–706, 1991.

Liberman MC. Auditory-nerve response from cats raised in a low-noise chamber. *J Acoust Soc Am* 63: 442–455, 1978.

Loskota W, Lomax P, Verity M. *A Stereotaxic Atlas of the Mongolian Gerbil Brain.* Ann Arbor, MI: Ann Arbor Science, 1974.

Moore MJ, Caspary DM. Strychnine blocks binaural inhibition in lateral superior olivary neurons. *J Neurosci* 3: 237–242, 1983.

Neher E, Sakaba T. Combining deconvolution and noise analysis for the estimation of transmitter release rates at the calyx of Held. *J Neurosci* 21: 444–461, 2001.

Paré D, Shink E, Gaudreau H, Destexhe A, Lang EJ. Impact of spontaneous synaptic activity on the resting properties of cat neocortical pyramidal neurons in vivo. *J Neurophysiol* 79: 1450–1460, 1998.

Renden R, Taschenberger H, Puente N, Rusakov DA, Duvoisin R, Wang LY, Lehre KP, von Gersdorff H. Glutamate transporter studies reveal the pruning of metabotropic glutamate receptors and absence of AMPA receptor desensitization at mature calyx of held synapses. *J Neurosci* 25: 8482–8497, 2005.

Roberts WM, Howard J, Hudspeth AJ. Hair cells: transduction, tuning, and transmission in the inner ear. *Annu Rev Cell Biol* 4: 63–92, 1988.

Ryan A, Miller J. Single unit responses in the inferior colliculus of the awake and performing rhesus monkey. *Exp Brain Res* 32: 389–407, 1978.

Sakaba T, Neher E. Quantitative relationship between transmitter release and calcium current at the calyx of Held synapse. *J Neurosci* 21: 462–476, 2001.

Schneggenburger R, Sakaba T, Neher E. Vesicle pools and short-term synaptic depression: lessons from a large synapse. *Trends Neurosci* 25: 206–212, 2002.

Schuller G, Radtke-Schuller S, Betz M. A stereotaxic method for small animals using experimentally determined reference profiles. *J Neurosci Methods* 18: 339–350, 1986.

Schwarz DW, Puil E. Firing properties of spherical bushy cells in the anteroventral cochlear nucleus of the gerbil. *Hear Res* 114: 127–138, 1997.

Smith PH, Joris PX, Carney LH, Yin TC. Projections of physiologically characterized globular bushy cell axons from the cochlear nucleus of the cat. *J Comp Neurol* 304: 387–407, 1991.

Smith PH, Joris PX, Yin TC. Anatomy and physiology of principal cells of the medial nucleus of the trapezoid body (MNTB) of the cat. *J Neurophysiol* 79: 3127–3142, 1998.

Sommer I, Lingenhohl K, Friauf E. Principal cells of the rat medial nucleus of the trapezoid body: an intracellular in vivo study of their physiology and morphology. *Exp Brain Res* 95: 223–239, 1993.

Spangler KM, Warr WB, Henkel CK. The projections of principal cells of the medial nucleus of the trapezoid body in the cat. *J Comp Neurol* 238: 249–262, 1985.

Spassova MA, Avissar M, Furman AC, Crumling MA, Saunders JC, Parsons TD. Evidence that rapid vesicle replenishment of the synaptic ribbon mediates recovery from short-term adaptation at the hair cell afferent synapse. *J Assoc Res Otolaryngol* 5: 376–390, 2004.

Spirou GA, Brownell WE, Zidanic M. Recordings from cat trapezoid body and HRP labeling of globular bushy cell axons. *J Neurophysiol* 63: 1169–1190, 1990.

Spirou GA, Rager J, Manis PB. Convergence of auditory-nerve fiber projections onto globular bushy cells. *Neuroscience* 136: 843–863, 2005.

Taschenberger H, Leao RM, Rowland KC, Spirou GA, von Gersdorff H. Optimizing synaptic architecture and efficiency for high-frequency transmission. *Neuron* 36: 1127–1143, 2002.

Taschenberger H, Scheuss V, Neher E. Release kinetics, quantal parameters and their modulation during short-term depression at a developing synapse in the rat CNS. *J Physiol* 568: 513–537, 2005.

Taschenberger H, von Gersdorff H. Fine-tuning an auditory synapse for speed and fidelity: developmental changes in presynaptic waveform, EPSC kinetics, and synaptic plasticity. *J Neurosci* 20: 9162–9173, 2000.

Thompson AM, Schofield BR. Afferent projections of the superior olivary complex. *Microsc Res Tech* 51: 330–354, 2000.

von Gersdorff H, Borst JG. Short-term plasticity at the calyx of Held. *Nat Rev Neurosci* 3: 53–64, 2002.

von Gersdorff H, Schneggenburger R, Weis S, Neher E. Presynaptic depression at a calyx synapse: the small contribution of metabotropic glutamate receptors. *J Neurosci* 17: 8137–8146, 1997.

Wang LY, Kaczmarek LK. High-frequency firing helps replenish the readily releasable pool of synaptic vesicles. *Nature* 394: 384–388, 1998.

Wu LG, Borst JG. The reduced release probability of releasable vesicles during recovery from short-term synaptic depression. *Neuron* 23: 821–832, 1999.

Wu SH, Kelly JB. Response of neurons in the lateral superior olive and medial nucleus of the trapezoid body to repetitive stimulation: intracellular and extracellular recordings from mouse brain slice. *Hear Res* 68: 189–201, 1993.

Cover

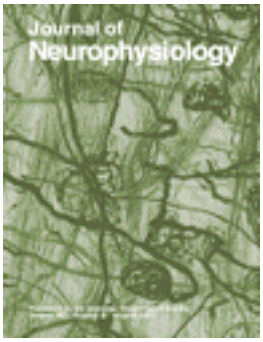

Shown are giant synapses, termed calyces of Held, and afferent axons in the medial nucleus of the trapezoid body (MNTB) of the gerbil. Clearly visible are several calyces, which synapse directly onto postsynaptic MNTB cell bodies. Rhodamine-dextrane staining and confocal image by Marc Ford. For more information see Hermann J, Pecka M, von Gersdorff H, Grothe B, and Klug A. Synaptic Transmission at the Calyx of Held Under In Vivo-Like Activity Levels. *J Neurophysiol* 98: 807–820, 2007. First published May 16, 2007; doi:10.1152/jn.00355.2007.